Biochemical and Functional Analysis of the PREP1 Interactor: p160 Myb Binding Protein 1

Thesis

Silvia Mori

Open University Personal Identifier : Y7046930
Universita' Vita-Salute San Raffaele Personal Identifier: 002105

BIOCHEMICAL AND FUNCTIONAL ANALYSIS OF THE PREP1 INTERACTOR: p160 MYB BINDING PROTEIN 1

Degree of Doctor of Philosophy (PhD)
in Molecular and Cellular Biology

November 2010

DIBIT
Department of Molecular Genetics
Università Vita-Salute San Raffaele
Milan – Italy

Director of Studies
Francesco Blasi

Second Supervisor
Jesper Svejstrup

DATE OF SUBMISSION: 20 SEPT 2010
DATE OF AWARD: 3 DEC 2010

ProQuest LLC.
789 East Eisenhower Parkway
P.O. Box 1346
Ann Arbor, MI 48106 – 1346

TABLE OF CONTENTS

DECLARATION

This PhD Thesis has been written by myself and has not been used in any previous application for a degree. All the results presented are original data and were obtained in the laboratory of Molecular Genetics (DIBIT - San Raffaele Scientific Institute, Milan), under the guidance of Professor Francesco Blasi. For scientific completeness, some data, obtained in collaboration with other laboratories, are presented and they are clearly identified at the end of the pertaining result chapter. Some of the work showed in this Thesis has been published and the relative reference is reported at the end of the relative result chapter.

ABSTRACT

p160 myb binding protein 1a (p160) is a nucleolar protein the function of which is poorly understood. To date, only a few interactors, mainly transcription factors (e.g. Myb, Jun), have been characterized. One of these is Prep1, an homeodomain transcription factor essential for embryonic development, involved, in particular, in haemopoiesis, angiogenesis, and oculogenesis, as well as in apoptosis and tumorigenesis. In this thesis work I show that p160 is capable of binding Prep1 through the same region as another Prep1 interactor, Pbx, and that such binding inhibits Prep1 action on the HoxB enhancer. I demonstrate that the two proteins, Prep1 and p160, interact mainly in the nucleoplasm and hence only under conditions that favor p160 translocation from the nucleolus to the nucleoplasm (e.g. after treatment with Actinomycin D).

Moreover I studied p160 during cell-cycle, since during mitosis p160 assumes a para-chromosomal localization. In HeLa cells, depletion of p160 by siRNA transfection decreases the proliferation rate and increases cell-death, mostly via apoptosis. p160-depleted HeLa cells accumulate in the G2/M phases of the cell-cycle and show a variety of mitotic defects: extended division time and structural alterations of the metaphasic plate. All these data suggest that p160 is essential for proper cell division. This phenotype is also in agreement with my observations that p160 down-regulated NIH 3T3 cells are more sensitive to transformation by Ras and Myc and undergo spontaneous neoplastic transformation even in the absence of oncogenes.

INTRODUCTION

In my thesis work I studied the interaction between the nucleolar protein p160 and the homeodomain transcription factor Prep1, trying to elucidate p160 function. In this first section I will describe these two interactors and the main cellular process involved: the cell-cycle.

1. The nucleolar protein p160 myb binding protein 1a

1.1 The nucleolus

The nucleolus is an extremely organized sub-nuclear compartment whose main functions are rRNA synthesis and ribosome assembly. It is an almost spherical structure surrounded by a layer of condensed chromatin and not by a membrane. The nucleolus is composed of three layers (Alberts B. et al., 1994) (Fig. 1):

- the Fibrillar Center (FC), which is made up of a network of fine fibrils and does not contain actively transcribed DNA;
- the Dense Fibrillar Component (DFC), surrounding the FC, is the site of rDNA genes transcription and pre-rRNAs modification;
- the Granular Component (GC), surrounding the fibrillar complexes at the border with the chromatin and nucleoplasm, is the site of ribosome subunits assembly.

Nucleoli originate from the nucleolar organizing region (NOR), that contains rDNA genes arranged in head-to-tail tandem repeats located on acrocentric chromosomes [11]. The dimension and the number of nucleoli vary from cell to cell but, in general, they are bigger in actively proliferating cells, as they need active protein synthesis.

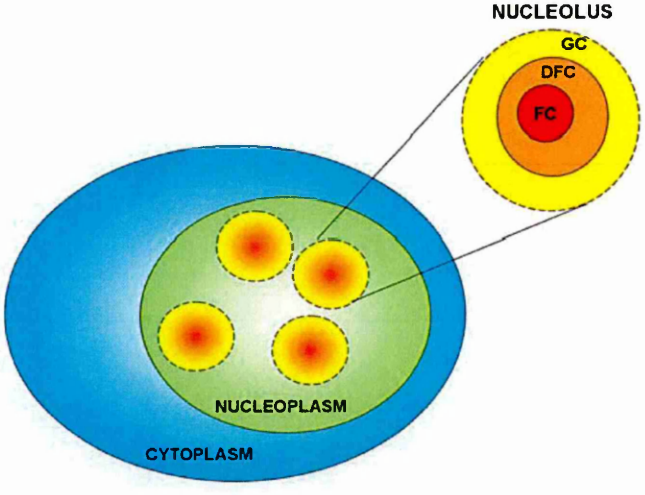

Fig. 1 Nucleolar organization. Schematic representation of the nucleolus: Fibrillar Component (FC), Dense Fibrillar Component (DFC) and Granular Component (GC) are indicated.

Nucleoli undergo cycles of disassembly and reassembly each time the cell undergoes mitosis. In fact, there are no visible nucleoli during metaphase [11]. During prophase the complex cyclin B1-cyclin dependent kinase 1 (CDK1) hyper-phosphorylates the nucleolar RNA polymerase I initiation complex and this determines nucleolar disassembly and this event takes place in concomitance with nuclear envelope disassembly [73]. Some nucleolar proteins remain attached to the surface of condensed chromosomes, in a region called Perichromosomal Region (PR), while others are

released in the nucleoplasm [39]. In the PR there are rRNA processing components: ribonucleoproteins (RNPs), small nucleolar RNA U3 (U3 snoRNA), pre-RNA and fibrillarin [25]. The function of the PR is still not clear, but it might serve to isolate chromosomes from cytoplasm or function as a binding site for chromosomal passenger proteins or favour an equal distribution of nucleolar components in the two daughter cells [48]. In anaphase, nucleolar proteins remain either attached to the chromosomes or in Nucleolar Derived Foci (NDF) in the cytoplasm. At the onset of telophase there is a reduction of the cyclin B1/CDK1 complex that determines the reactivation of the rRNA transcription and the reassembly of the nucleolus. NDF disassemble and the nucleolar proteins are transferred to fibrogranular structures on the surface of chromosomes (pre-nucleolar bodies, PNBs) and on nucleolar organizing regions. As soon as nucleoli reassemble PNBs transfer their content to nucleoli [115] (Fig. 2).

The main nucleolar function is ribosome biogenesis. The first step of this activity consists in the transcription of rDNA by RNA polymerase I at the border between FC and DFC. The 45S rRNA precursor is produced and cleaved into 28S, 18S and 5,8S rRNAs that are post-transcriptionally modified at the level of DFC. These products interact with small nucleolar ribonucleoproteins (snoRNPs) and are subsequently assembled with other ribosomal proteins. The last step is the interaction with the export machinery in the nucleolar GC region and the transport to the cytoplasm [31,126] (Fig. 3).

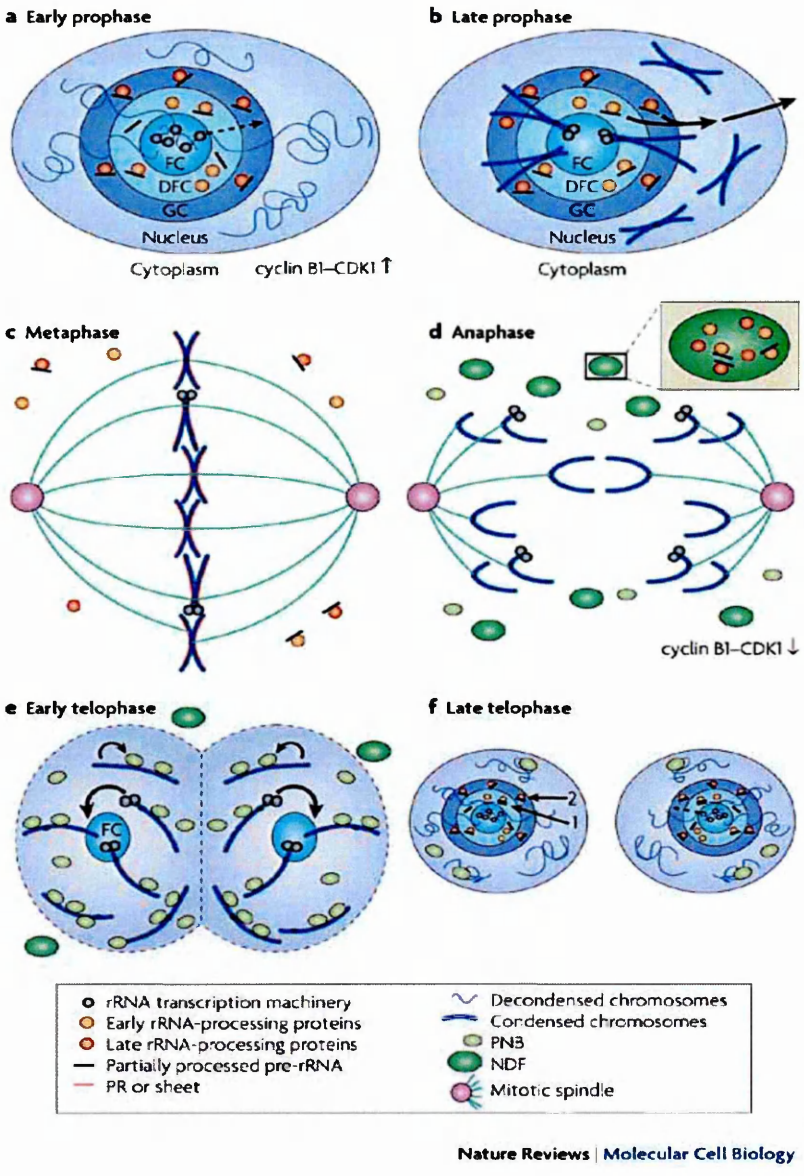

Fig. 2 Nucleolar assembly and disassembly in mitosis. Schematic representation of the nucleolar components during the different mitotic phases [11].

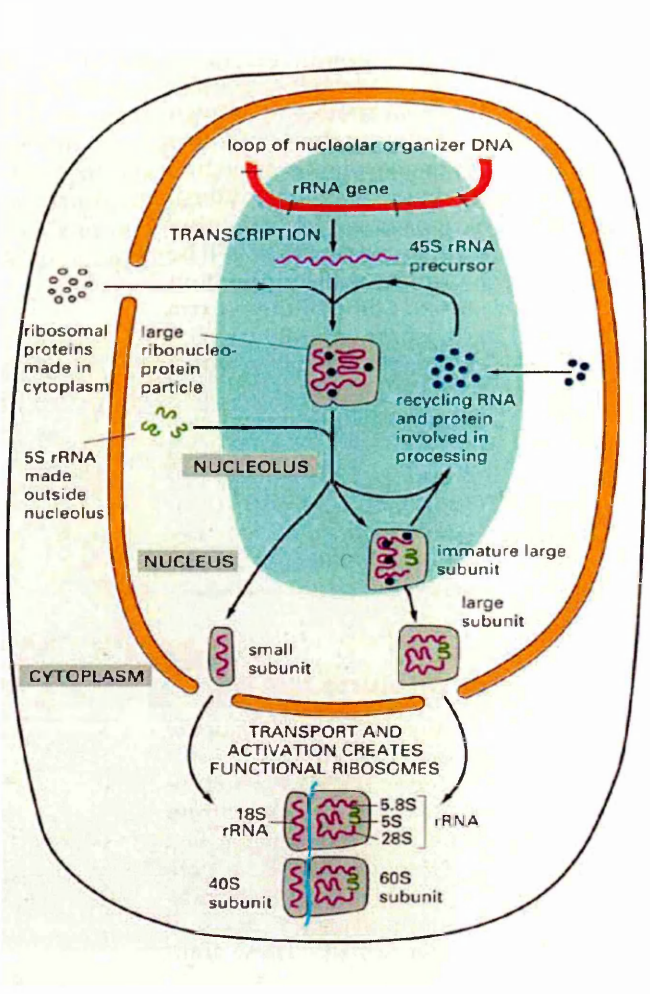

Fig. 3 The assembly of ribosomes. Schematic representation of ribosomes generation: transcription, association with ribonucleoproteins, maturation and transport into the cytoplasm (Alberts B. et al., 1994).

The nucleolus participates in other cellular processes as well: cell-cycle control, stress response and coordination of the biogenesis of other classes of RNPs. In particular, several nucleolar proteins are involved in cell-cycle regulation or are fundamental for cell division. Nucleophosmin is essential for chromosomes congression, mitotic spindle, centrosomes formation and proper kinetocore-microtubules attachment [2,43]. RNA methyltransferase Misu (NSun2) is a substrate for Aurora B kinase and during mitosis is

required for proper spindle assembly and chromosome segregation [53,113]. SENP5, a SUMO protease, prevents inhibition of cell proliferation and its absence causes defects in nuclear morphology and problems in cytokinesis [21]. The nucleolus is also a sensor for cellular stress, stabilizing p53 through the sequestration of HDM2 (E3 ubiquitin ligase) in the nucleolus by p14ARF [132].

The nucleolus is also involved in many diseases in which proteins are sequestered in nucleoli (Werner syndrome, Bloom syndrome [84]) or in which there is an altered ribosomes biogenesis for mutations in ribosomal proteins (Diamond-Blackfan anemia, dyskeratosis [19,47]). It may also be involved in viral infections since some viruses target nucleoli and alter their function. Moreover, alterations in the level of nucleolar proteins can determine cell transformation: NPM, if present at low levels, determines genomic instability which favours cell transformation [43]. In addition nucleoli are currently used as a prognostic marker for tumor progression: the bigger the nucleoli, the faster will be the tumor progression [20].

1.2 p160

p160 Myb binding protein 1a was identified as an interactor of Myb [32]. In particular, p160 binds a leucine-zipper motif of the negative regulatory domain (NDR) of Myb that is essential because it mediates DNA binding, transactivation and transformation [27,51,59,108]. p160 binds but does not inhibit Myb function. p160 is ubiquitously expressed, in particular in fetal liver cells that are highly proliferating and this might be indicative of a role in proliferation [124]. It was also found a shorter form of p160, named p67, that derives from proteolitic cleavage of the protein and it is present in a

small subset of cells, in particular in some immature myeloid cells. p67 represents the N-terminal part of p160 and can bind Myb through the same NDR, but, differently from the whole-length protein, it is also capable of inhibiting Myb's transactivating function [32,124].

The p160 gene is located on chromosome 11 in mouse and on chromosome 17p13.3 in human [61]. The p160 human gene has an interesting localization because this region is frequently affected (50-80%) in loss of heterozygosity in different malignancies like: sporadic breast and ovarian cancer, medulloblastomas, astrocytomas, osteosarcomas, and leukemia, etc. [103,114,121,123].

p160 is highly conserved across species [61] and also has an homolog in yeast: POL5, which is the fifth essential DNA polymerase in *Saccharomyces cerevisiae*. POL5 is a nucleolar protein with low polymerase activity, that is essential for cell growth because it plays a poorly understood role in rRNA synthesis, binding near or at the enhancer region of rDNA repeating units [119]. POL5 has a high degree of similarity with the N-terminal and middle part of p160 [135] (Fig. 4, red lines).

The p160 structure presents a central acidic domain whose function is unknown, two putative leucine zipper-like motifs (starting at amino acids 307 and 900) and several Leucine Charged Domains (LCD), important for protein-protein interaction, probably essential for the binding of p160 to c-Myb and c-Jun. There are also seven short basic amino acid sequences embedded in a proline-serine-rich region at the C-terminus that are required for the nuclear and nucleolar localization (Fig. 4) [62]. p160 can bind importin α through this region and can be imported into the nucleus by way of the importin α/β heterodimer. p160 is predominantly found in the nucleolus and only a small

fraction in the nucleoplasm [124]. P160 can also translocate to the cytoplasm via the leucine-rich motifs (LCD and leucine zipper-like domains) that can function as export signals as they are recognized by the nuclear export receptor CRM1 [62].

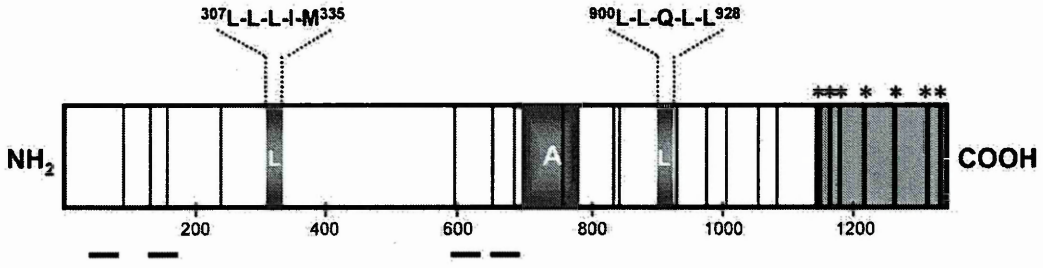

Fig. 4 p160 structure. Schematic representation of p160; L, leucine zipper-like domain; A, acidic domain; *, basic amino acid repeat motifs; solid lines, LCD (LXXLL motif) [62]; horizontal lines represent the POL5 homology regions.

Yamauchi et al., demonstrated that after ribosomal stress (e.g. treatment with Actinomycin D) p160 is processed into two shorter forms: p67 and p140 that lacking the nucleolar localization signal, translocate to the nucleoplasm [134]. They also identified two p160 containing complexes that might be important for its function. The small complex contains p140, p67, Nucleolin, Nucleophosmin (NPM) and EBP1, while the large complex contains p140, Nucleolin and NPM, and in addition Topoisomerase I, Nucleostemin, Histone H1x and ribosomal subunit proteins. The latter complex is interesting because Nucleolin, NPM and Nucleostemin are known to stimulate ribosome biogenesis through their involvement in rRNA transcription, ribosome maturation and assembly and transport of ribosomes [44,91]. This might be indicative of an involvement of this complex and consequently of p160, in ribosome biogenesis, and is supported by

the high degree of similarity the p160 shares with yeast POL5, which in turn is essential for rRNA synthesis [119]. They also hypothesized that the translocation of the small complex (containing p67 and p140) to the nucleoplasm allows the interaction of p67 with transcription factors, such as c-Myb, and consequently regulates cell-cycle progression, proliferation and apoptosis.

Finally, upon proteasome inhibition, p160 was detected among the endogenous sumoylated proteins and this post-translational modification may be important in defining p160 function and/or fate (Appendix I, [85]).

Another hint on p160 function is its particular localization during mitosis. In fact a proteomic analysis of the chromosome scaffold fraction revealed that p160 was located on chromosome arms [38].

1.3 p160 interactors

Although the function of p160 is still not clear, several interactors were characterized. It was originally identified as an interactor of c-Myb, a transcription factor that plays an essential role in controlling proliferation and differentiation of hematopoietic cells, where p160 might act as a co-regulator [124].

P160 can also interact with the leucine-zipper domain of another transcription factor, c-Jun, but the function of this interaction is not clear [32].

Another interactor is the transcription factor PPAR gamma co-activator 1α (PGC1α), a key regulator of mammalian energy metabolism. P160 binds the negative regulatory domain of PGC1α and inhibits its transcriptional activity. When p38 MAPK

phosphorylates PGC1α, the binding of p160 is inhibited and the transcription factor can exert its function [30].

p160 binds also to the acidic activation domain of the aromatic hydrocarbon receptor (AhR, a bHLH/Per-Arnt-Sim transcription factor, together with its partner Arnt) and increases transcriptional activation [57].

Another p160 interactor is RelA/p65, a member of the NF-kB family of inducible transcription factors that regulates cell-cycle, proliferation and apoptosis. p160 binds the transcription activation domain of RelA/p65 and represses its activity by competing with the binding of the transcription co-activator p300 [97].

The last interactor found is Prep1 (see below). The lack of this interaction in Prep1 hypomorphic mice ($Prep1^{i/i}$) renders their skeletal muscle more sensitive to insulin and the mice are protected from diabetes. Indeed Prep1 seems to protect p160 from degradation; thus a decrease in Prep1 levels causes a decrease of p160 levels. Since p160 is also a repressor of PGC1α, its decrease increases the activity of PGC1α and activates glucose uptake [96].

2. The Homeodomain transcription factor Prep1

2.1 Homeodomain class of transcription factors

Transcription factors are characterized by the presence of at least two domains: a DNA-binding domain and a trans-activating domain [72]. They are grouped in families according to the structure of their DNA-binding motif (Alberts B. et al., Molecular

biology of the cell, 1994), one of which is the Helix-Turn-Helix (HTH) class, characterized by two α-helices connected with a small amino acidic chain. Homeodomain proteins, which are required for the development of every single area of the organism and are coded by the Hox gene cluster, belong to this class [90]. The term homeodomain originates from a homeotic mutation of *Drosophila* melanogaster gene Antennapedia (Antp) that determines the switch of one body segment to another, inducing the development of legs in the place of antennae [82,83,90]. The homeodomain proteins are characterized by a conserved 60 amino acids DNA-binding motif (coded by 180 nucleotides homeobox), known as the homeodomain (HD). X-ray crystallography and Nuclear Magnetic Resonance (NMR) studies indicate that the HD has a HTH structure with three distinct α-helices. The recognition helix, at the Carboxyl-terminus (C-terminal) of the motif, contacts DNA in the major groove and makes specific base pair contacts, whereas the Amino-terminus (N-terminal) moiety makes contact with the minor groove [40,41]. The association of homeobox proteins between themselves increases their DNA-binding specificity. Based on the similarities in the motifs outside the HD, Homeodomains proteins are classified as follow:

- *Hexapeptide class*, includes the Hox family, in which all proteins have an N-terminal 6 amino acids protein interaction domain [40].
- *TALE (Three Amino acid Loop Extension) class*, which includes Pbx and Meis/Prep proteins with an atypical HD [14,90].
- *POU class*, which includes the Octamer family and contains the N-terminal POU bipartite DNA-binding domain. It consists of two highly conserved

regions connected by a variable linker, in addition to the homeodomain [40,117].

- *LIM class*, which, in addition to the homeodomain, contains an N-terminal LIM metal binding protein-protein interaction domain [40,58].

2.1.1 Hox Family

The main function of Hox genes products is to pattern the anterior-posterior body axis of embryos [69,76]. These proteins share a short tryptofan-containing hexapeptide motif with the consensus IYPWMK or ANW, located N-terminal of the HD that is required to bind specifically the TALE motif (see below) [16,18,66,102,104]. Hox proteins have a weak DNA-binding capacity, hence in order to bind and regulate their target genes, they need such co-factors as the TALE proteins [81,90].

2.1.2 TALE family

The TALE family of proteins is divided into 2 classes:

- the *PBC* proteins which comprise Pbx (preB cell homeobox) in mammals, Exd (Extradenticle) in Drosophila, Lzr (Lazarus) in Zebrafish and CEH-20 in Caenorhabditis Elegans;
- the *MEINOX* proteins with Prep (Pbx-regulating protein) and Meis (Myeloid ecotropic viral integration site) in mammals, Hth (Homothorax) in Drosophila and UNC-62 in Caenorhabditis Elegans.

In Fig. 5 is shown the schematic structure of PBC and MEINOX members. All TALE members show a divergent HD containing a proline (P) – tyrosine (Y) – proline (P) motif in position 24-26 between the first and the second α-helix, through which they contact the hexapeptide motif of Hox proteins increasing their affinity for DNA [14,15]. Pbx proteins contain an additional DNA binding α-helix located C-terminally to the HD (α4-HCM) [104]. N-terminally to the HD, the PBC proteins have two conserved domains: PBC-A and PBC-B, the first of which mediates the interaction with MEINOX proteins [15,112]. Also MEINOX proteins have two conserved domains: HM1 or HR1 (Homology Region 1) and HM2 or HR2 (Homology Region 2) that are conserved in the two Prep and Meis subclasses and make contacts with Pbx proteins [15,90]. Moreover several Hox genes can interact directly with Meis proteins through the C-terminal region (CTD) of Meis that includes the HD [130].

PBC proteins are considered Hox cofactors because they interact directly with Hox proteins increasing their affinity for DNA and determining the DNA binding specificity and selectivity [90]. PBC proteins can heterodimerize with Hox proteins only in the presence of DNA and are able to bind the sequence TGATNNAT [22,105].

MEINOX proteins act by modifying the PBC-Hox complex binding activity, extending its potential regulatory role.

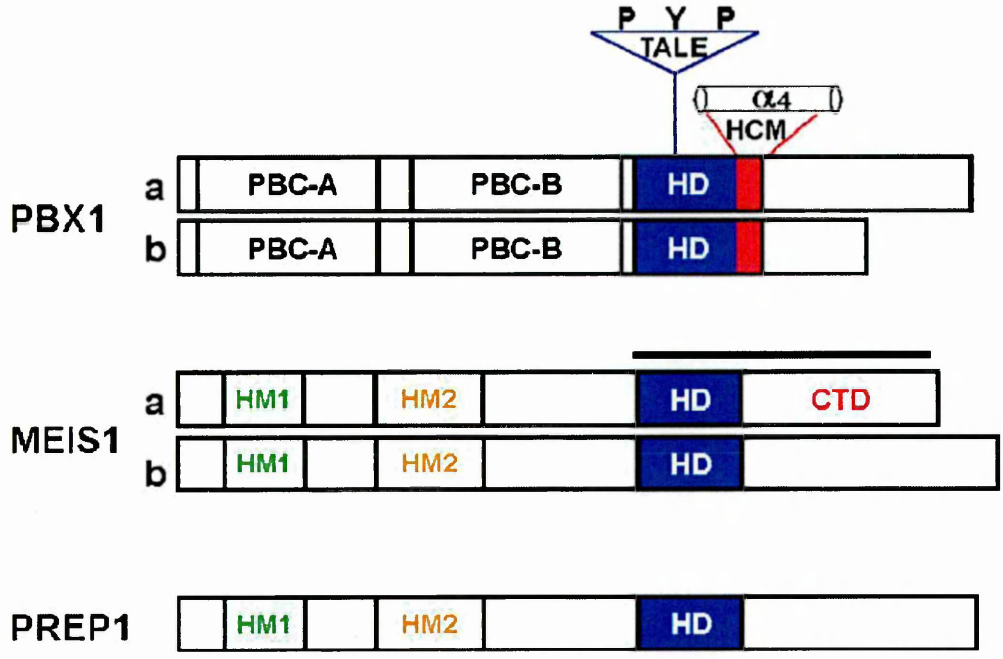

Fig. 5 Structure of TALE homeodomain proteins. Pbx1 is a member of PBC proteins while Meis1 and Prep1 are members of MEINOX proteins. a,b refer to splice variants of Pbx1 and Meis1 proteins. PBC-A, B, HM-1, 2 domains are shown. HD is the homeodomain, CTD the C-terminal domain and HCM is the fourth α-helix domain [90].

2.2 Prep1

Prep 1 is a member of the MEINOX class of homeodomain transcription factors. It was identified as a component of the human transcription factor UEF3, important for the regulation of the urokynase-type Plasminogen Activator (uPA) enhancer [7]. The human Prep1 gene (PKNOX1) is located on chromosome 21 and encodes a 436 amino acids protein, while the murine gene is on chromosome 17 and codes for a 435 amino acids protein that shares 97% identity with its human counterpart [8]. Prep1 has a high degree of similarity with the Meinox protein Meis1, especially in the DNA recognition helix

and, like Meis1, it shows a binding preference, but low affinity, for TGACAG and TGATNNAT elements [10]. Prep1 and the PBC class proteins Pbx1/2 associate through their N-terminal sequence and, thus, the dimer acquires a higher affinity for DNA and enhancing Hox dependent transactivation. Indeed Prep1, Pbx and HoxB1 can form a transcriptionally active ternary complex on DNA (Fig. 6; [9]). Prep1, like Meis1, binds Pbx in a DNA-independent way forming dimeric DNA-binding factors [17,67].

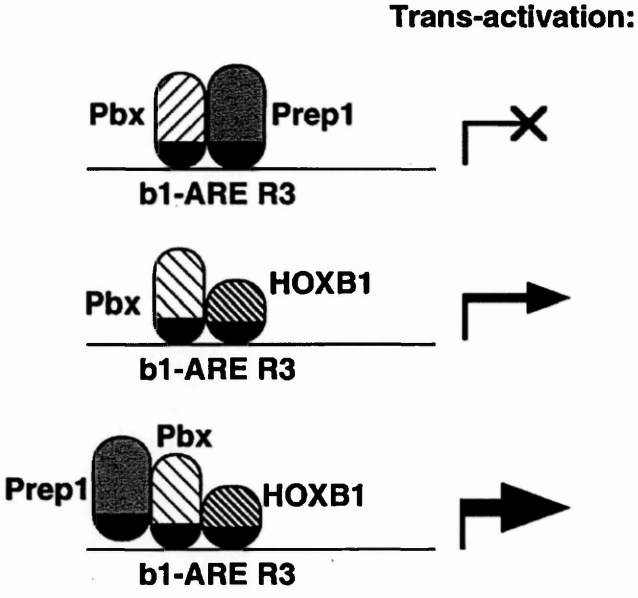

Fig. 6 Prep/Pbx/Hox transactivation. Schematic representation of the Prep/Pbx/Hox interaction: (top) Prep and Pbx alone cannot transactivate the b1-ARE enhancer R3 site of the Hox gene; (middle) Pbx and HoxB1 can activate transcription; (bottom) Prep1/Pbx/HoxB1 complex determine the strongest transactivation [9].

Prep1 is ubiquitously expressed in embryonic and adult mouse tissue, that is particularly strong in the thymus and testes, and is uniformly expressed during embryogenesis from the fertilized oocyte to 17.5 d.p.c. [36]. Prep1 lacks a nuclear localization signal (NLS), but can translocate to the nucleus when it heterodimerizes with Pbx. Pbx is localized in

the nucleus but, as shown in *Drosophila* Schneider cells, is exported to the cytoplasm. When Prep1/Pbx are complexed in the nucleus Pbx is no longer exported in the cytoplasm because Prep1 (or Meis) inhibits this process (Fig. 7, [6]). It is also interesting that Prep1 controls the level of Pbx, protecting it from degradation by favoring its entry into the nucleus. In fact excess Prep1 increases the cellular level of Pbx and consequently the DNA binding activity of the Prep1/Pbx complex. Therefore, the balance between Prep1 and Pbx and the rate of synthesis of Prep1 is functionally important in determining the Pbx nuclear localization and activity [74]. This observation was also made in *Drosophila* and *Zebrafish* were Hth or Meis overexpression stabilize Exd and Pbx [70,129].

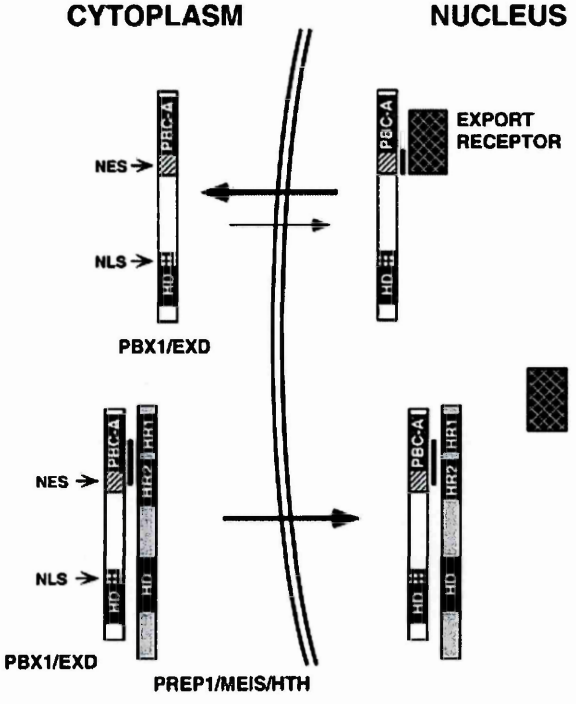

Fig. 7 Prep/Pbx localization. Schematic representation of the regulation of the subcellular localization of Pbx/Exd with or without Prep1/Meis/Hth in Drosophila Shneider cells. NES, Nuclear Export Signal; NLS, Nuclear Localization Signal [6].

Prep1 KO mice, like the Pbx and Meis KO mice, show an embryonic lethal phenotype [3,26,50,63,80,118]. In particular, Prep1 embryos die at 7.5 d.p.c. [33]. An hypomorphic mutation ($Prep1^{i/i}$), which determines the expression of only 3-10% of the protein, is lethal in 75% of the embryos between E17.5 and P0. 25% of the embryos survive, but have anomalies in T-cell development [100]. $Prep1^{i/i}$ embryos show organ hypoplasia, eye malformation and anomalies in erythropoiesis and angiogenesis [37]. Prep1 can also regulate the apoptotic potential of the cell, acting at the level of the Bcl-XL promoter. In fact $Prep1^{i/i}$ Mouse Embryonic Fibroblast (MEF) show increased apoptosis [86]. However, Prep1 overexpressing cells also show a high degree of p53-dependent apoptosis, since p53 is a direct transcriptional target of Prep1. In human, since Prep1 is located on chromosome 21, it is overexpressed in Down Syndrome patient cells (as the cause of this disease is the presence of three copies of chromosome 21). In this case the increase in apoptosis maybe is responsible for the neurodegenerative phenotype and for immune defects [87].

Recently, it has been demonstrated that Prep1 is a tumor suppressor since it is down-regulated in 70% of human tumors and since $Prep1^{i/i}$ mice develop spontaneous tumors [75].

2.2.1 Prep1 cooperates with other transcription factors

Prep1, in complex with Pbx, regulates the activity of a variety of proteins, such as: Pdx, Pax6, Oct1, MyoD and Smad 2,3,4:

- Pdx is an orphan homeodomain protein that regulates somatostatin. When Prep1 associates with the Pdx/Pbx heterodimer increases the activation of the somatostatin promoter [42].
- Pax6 is an homeodomain protein fundamental for pancreas organogenesis. In non-pancreatic cells Prep/Pbx heterodimers can bind a G3B region on the glucagon gene enhancer and repress its transcription, while in pancreatic islets Pax6 can bind to the enhancer with its homeodomain, thus inhibiting the binding of the dimer and favoring glucagon expression [49].
- Oct1 is a POU homeodomain protein that is fundamental for the transcription of the gonadotropin releasing hormone (GnRH). The Prep/Pbx heterodimer can bind the regulatory region of the GnRH gene and, together with Oct1, is essential for gene expression in hypothalamic neurons [109].
- MyoD is part of the bHLH proteins and is involved in myogenin expression. MyoD together with E2a binds DNA and regulates gene expression. The binding of a Pbx/Meis-Prep1 dimer predisposes several muscle-specific genes to the transcriptional activity of MyoD-E2a [65].
- Smad proteins bind the responsive elements of Activin and activate transcription of the Follicle-Stimulating Hormone (FSH) gene. Pbx/Prep can form a complex with Smad proteins modulating Activin function [4].

2.2.2 Prep1 interactors

In addition to Pbx and Smad proteins, another direct interactor of Prep1 has been recognized: 4EHP (eukaryotic translation initiation factor 4E homolog protein). 4EHP

can heterodimerize with Prep1 in the cytosol and regulate HoxB4 mRNA translation; this interaction is important for mammalian female germ cells development [128].

Thus only a few direct Prep1 interactors are known. In order to find new Prep1 interactors, a Tandem Affinity Purification (TAP) protocol was developed in our laboratory. TAP allowed us to identify macromolecular complexes under native conditions [23]. For this experiment a Prep-TAP construct was prepared and shown to be fully active in vivo: in the presence of Pbx1, Prep1-TAP was transported into the nucleus of the cell, indicating that Prep-TAP interacts with Pbx. Prep1-TAP was transcriptionally active and the TAP-tag did not interfere with DNA binding. This allowed to use two consecutive non-denaturing affinity purification steps [106,111], resolve the eluates by SDS-PAGE, and analyze them by MALDI-TOF Mass Spectrometry. In two independent experiments, as expected, Pbx1b and Pbx2 were found as specific interactors thus providing an internal control for the experiment. However, a new interactor was also identified (Fig. 8): the nucleolar protein p160 myb binding protein 1a (p160, MYBBP1A), based on the sequences obtained from 9 and 8 different peptides, purified only from the nuclear fraction. From the nuclear fraction also non-muscle myosin heavy chain II A (NMMHCIIA), an actin associated motor protein, and β-actin were isolated. The specificity of these interactions has been characterized elsewhere.

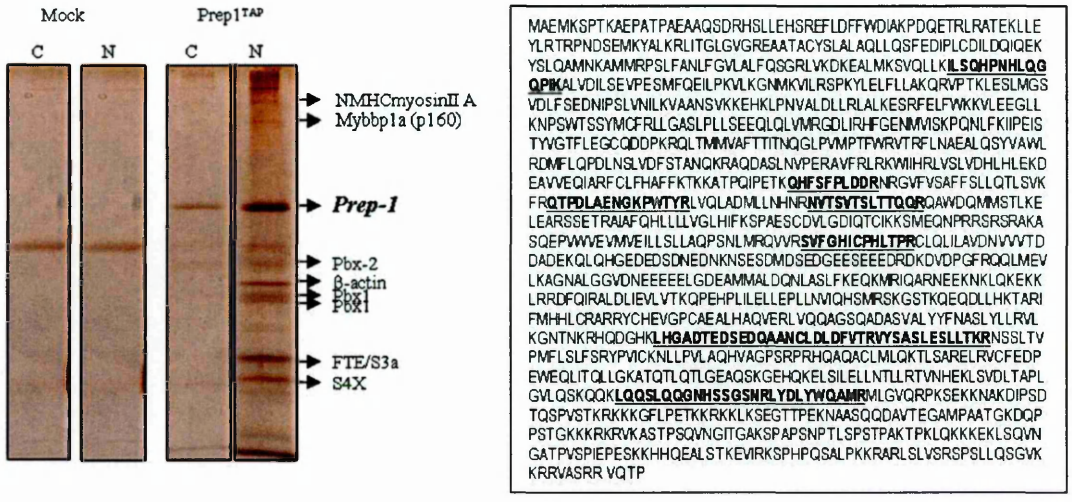

Fig. 8 Tandem Affinity Purification of the Prep1 interactome. On the left is shown the silver stained gel after TAP. C, cytoplasmic fraction; N, nuclear fraction for both mock (untreated cells) and Prep1^{TAP} expressing cells; on the right of the gel are indicated the proteins identified. The right panel shows p160 protein sequence with in bold the peptides identified; adapted from [23].

3. Cell-Cycle regulation

3.1 Cell-cycle

The cell-cycle is an ordered series of events leading to cell replication. During cell-cycle a cell duplicates its DNA content and subcellular organelles and divides into two, in general identical, daughter cells with a very regulated and organized process.

The cell-cycle is divided in the M-phase (mitosis), i.e. the process that determines cell division, and interphase that is the period between two consecutives mitotic divisions

and allows the cell to grow and replicate its content. Interphase is subdivided (as shown in Fig. 9) in G1, S and G2 phases:

- *G1* (Gap 1), is the period from the end of the previous M-phase (mitosis) to the onset of DNA synthesis (S-phase, see below). This is a "growth phase" during which there is a high biosynthetic activity. In particular, various enzymes required for DNA replication in the following S-phase are synthesized (Lodish H. et al., 2008).
- *S* (Synthesis phase), starts with DNA synthesis. At the beginning of the S-phase each chromosome is composed of one chromatid that is replicated by DNA polymerase; the two chromatids are then joined at centromere. During mitosis, a protein complex called kinetocore, fundamental for chromosomes segregation, is assembled on the centromere. The centrosome is another important structure for cell division. In fact it is an organelle that serves as main microtubules organizing center. It is composed of two orthogonally arranged centrioles surrounded by pericentriolar material, made up mainly of Tubulin and Pericentrin. During this phase, centrosomes are also duplicated [110,122]. RNA transcription and protein synthesis are very low during this phase, only histone production takes place [93].
- *G2* (Gap 2), starts immediately after the S-phase and lasts until the cell enters mitosis. During this phase there is again a significant increase in protein synthesis, mainly focused to the production of microtubules that are required for the mitotic process.

After G2, the cell enters in mitosis and following cell division each daughter cell begins the interphase of a new cell-cycle. However, some cells in G1 enter a resting state (G0 phase): they stop dividing and become quiescent or senescent. During quiescence the cell stops proliferation for a short or long period of time, sometimes indefinitely. This state is common for cells that are fully differentiated (e.g. neurons). Senescence occurs in cells that have DNA damage and are not able to repair it. A standard cell-cycle lasts approximately 24 hours but only one hour is dedicated to mitosis, the rest is the time that the cell needs to replicate its content.

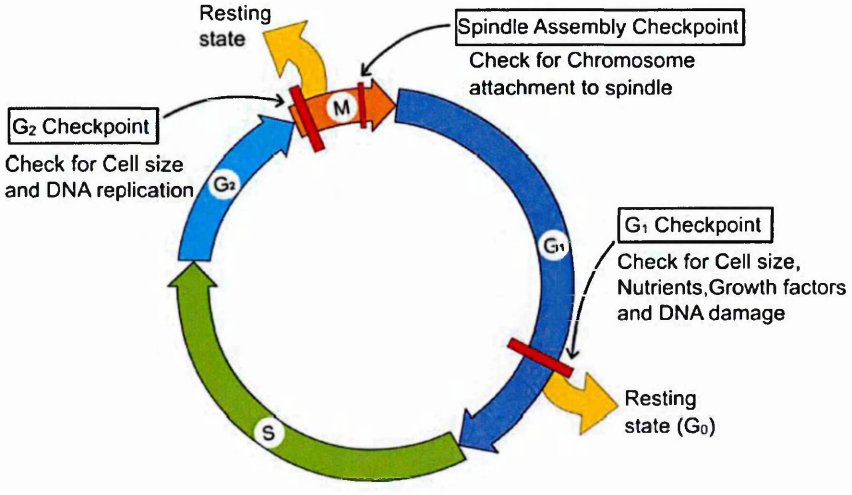

Fig. 9 Cell-cycle. Diagram showing cell-cycle subdivision in G1 (G0), S, G2, M with the related checkpoints: G1, G2 and Spindle Assembly Checkpoint.

3.2 Mitosis

Mitosis is the process that determines the division of a cell into two daughter cells with identical DNA content. Mitosis is divided in six phases: prophase, prometaphase, metaphase, anaphase, telophase and cytokinesis (Alberts B., et al. 1994) (Fig. 10):

- *Prophase*

  During prophase, chromatin starts to condense into chromosomes that were previously duplicated in the S-phase. Each duplicated chromosome consists of a pair of sister chromatids joined at the centromere. During this period, cytoskeletal microtubules disassemble and start to organize into the mitotic spindle. The spindle is a bipolar structure that radiates from the two centrosomes in the cytoplasm. The action of microtubules (polymers of α/β Tubulin that switch phases of polymerization and de-polymerization, a sort of "dynamic instability" [89]), is very important for spindle function. During prophase the nucleolus disappears.

- *Prometaphase*

  This phase starts with nuclear envelope breakdown, spindle entering into the nuclear area and kinetocores that start to form. The function of the kinetocore is to allow the attachment of chromosomes to the spindle microtubules, monitoring the attachment during cell division and activating a signaling pathway (i.e. the Spindle Assembly Checkpoint, described below) to delay cell-cycle if defects are detected. Moreover, it helps to power the movement of chromosomes on the spindle. Kinetocores can be subdivided in two regions: the inner kinetocore, that assembles on a repetitive DNA sequence and it is mainly constituted by CENP proteins and the outer kinetocore, a protein complex that takes contacts with microtubules and is mainly composed by

Ndc80 complex and SAC proteins [78]. Kinetocores attach to the microtubules of the spindle (kinetocore microtubules) and the non-kinetocore microtubules (microtubules not attached to kinetocores) search and attach to non-kinetocore microtubules of the opposite pole; in this way the spindle is completed.

- *Metaphase*

During metaphase, the two centrosomes migrate to the opposite poles of the cell. The kinetocore microtubules align the chromosomes in a plane along the middle of the spindle, equidistant from the two poles (metaphasic plate) and a tension between the chromosomes and the opposite spindle pole is generated by the growing and shrinkage of microtubules. In particular, each chromosome has to be attached to its kinetocore microtubule in order to proceed to the following phase. If there are unattached chromosomes, the respective kinetocore generates a signal that activates the SAC and blocks mitosis progression.

- *Anaphase*

Anaphase begins when the duplicated centromeres of each pair of sister chromatids separate and are pulled toward opposite poles due to the action of the spindle. At the end of anaphase a complete set of chromosomes has assembled at each pole of the cell.

- *Telophase*

When sister chromatids arrive to opposite poles, the kinetocore microtubules disappear and non-kinetocore microtubules increase their length, stretching the cell. At the same time a new nuclear envelope starts to form around each group of chromosomes, chromatin begins to unfold and the nucleoli reassemble.

➢ *Cytokinesis*

The last step consists in the division of the cytoplasm at the level of the previous metaphasic plate. In this region a contractile ring of actin and myosin filaments starts to form that shrinks the cell and breaks it, giving rise to two daughter cells.

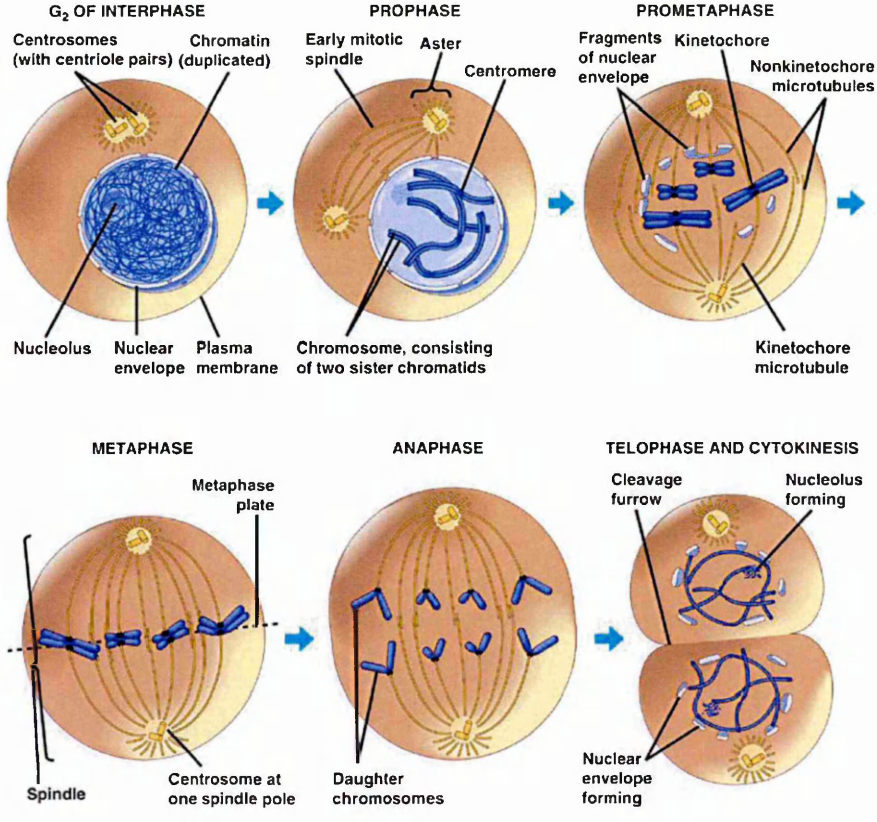

Fig. 10 Mitotic phases. Schematic representation of the mitotic phases with indicated the main components (From: http://kvhs.nbed.nb.ca/gallant/biology/mitosis_phases.html).

3.3 Cell-cycle regulation: the importance of Cyclin-dependent kinases – cyclins complexes

3.3.1 Interphase regulation

Cell-cycle is a very well ordered and controlled process and it is based on the interaction between cyclin-dependent-kinases (CDK) and cyclins. CDK are serine-treonine kinases that phosphorylate specific targets when bound to cyclins. At the onset of the G1-phase, in response to growth factors, the cell determines the expression of fundamental genes for G1/S transition (c-myc, c-fos). These genes are mainly transcription factors that determine the expression of cyclins D. Cyclin D can then associate with and activate CDK4, 6. When the complex CDK4, 6 / cyclin D reaches a critical level, it phosphorylates Rb that releases E2F from its inhibition (Fig. 11). E2F is essential for the G1/S transition; in fact, it determines the expression of genes involved in nucleotides metabolism and DNA synthesis and activates the transcription of cyclins E and A. Cyclin E can then associate with CDK2 in late G1 and helps in maintaining the phosphorylation state of Rb phosphorylated and also phosphorylates p27, a CDK inhibitor, that is subsequently ubiquitinated and degraded. The association of cyclins A and E with CDK2 contributes to the activation of the pre-replication complex. In late G1 cdc25, a phosphatase that removes a phosphate from CDK2 activating it, is also turned on. In this way, cell enter the S-phase and DNA replication begins. Phosphorylation of these initiation factors prevents the reassembly of the pre-replication complex until the cell passes through mitosis, assuring that replication from each origin occurs only once during a cell cycle.

3.3.2 Mitosis regulation

Cyclin B is also produced in the late S-phase and cyclins A and B can then associate with cdc25 activated CDK1. Cyclin A/B – CDK1 functions as a mitosis promoting factor (MPF) that is active until late anaphase when APC/C and Cdh1 determine its polyubiquitination and degradation (Fig. 11). MPF is important in mitosis since it promotes condensins phosphorylation in prophase and can, thus, contribute to chromatin condensation. MPF also phosphorylates regulatory proteins associated to microtubules that are responsible for microtubules dynamics. It then phosphorylates proteins of the nuclear lamina and this determines the nuclear lamina de-polymerization in prometaphase and the breakage of the nuclear envelope. After the attachment of every spindle fiber to the centromere, cdc20 is released and associates with APC/C. APC/C – cdc20, known also as Anaphase Promoting Complex, determines the polyubiquitination and degradation of securin that releases separases. Separases are proteolytic enzymes that cleave the cohesion ring at the centromere. The forces exerted by the mitotic spindle apparatus then pull the released sister chromatids towards opposite spindle poles. Once chromosomes are correctly separated, the cdc14 phosphatase is activated and de-phosphorylates and activates Cdh1 determining the polyubiquitination and degradation of all B cyclins and consequently the inactivation of MPF. Cdh1 de-phosphorylates all the complexes previously activated by phosphorylation and all these proteins go back to their interphase function, leading to de-condensation of chromosomes, formation of interphase microtubules (that can re-constitute the cytoskeleton) and reassembly of the nuclear envelope (Lodish H. et al., 2008).

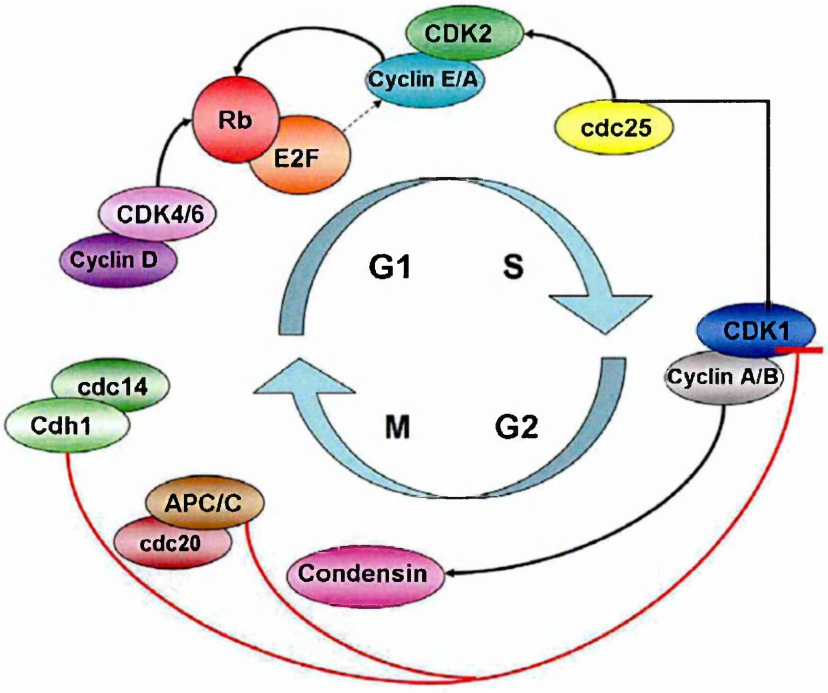

Fig. 11 Cell-Cycle regulation. Schematic representation of the principal components determinant for cell-cycle progression. G1, S, G2 and M indicates the different cell-cycle phases.

3.3.3 Checkpoints

As already mentioned above, cell-cycle is a very well controlled process: each step has to follow a correct order and must be completed before the subsequent steps can be carried out. Checkpoints ensure that chromosomes are intact and that each step has been completed. In case of damage cells undergo cell-cycle arrest until the damage is repaired. In the case it is not repaired, cells induce apoptosis. Checkpoints act by blocking the action of the following CDK – cyclin complex through specific inhibitors. The main CDK inhibitors are p21, p16 and p27 [29,46]. The failure of a checkpoint results in chromosome instability that is at the basis of pre-cancerous and cancerous

lesions. In fact, a defect in DNA replication control can be responsible for chromosomal rearrangements (e.g. deletions, amplifications and traslocations). Moreover, cell transformation or chromosomal disorders may arise from defects in spindle monitoring, leading to mitotic non-disjunction and producing the loss or gain of chromosomes and the consequent change in cell ploidy [45,79].

There are three important checkpoints:

- *interphase checkpoint* (G2 checkpoint), recognizing unreplicated DNA in the S-phase and inhibiting MPF activation; it is mediated by ATR and Chk1;
- *Spindle Assembly Checkpoint* (SAC), prevents the entry into anaphase until every single kinetocore of every chromatid is properly associated with spindle microtubules [92]. It is mainly mediated by MAD2 (Mitotic Arrest Defective 2) that inhibits Cdc20 and, by consequence, its association and activation of APC/C that promotes anaphase entry. The SAC pathway is quite complex: CDK1 and BUB1 phosphorylate cdc20 and induce the recruitment of the SAC complex. The closed form of MAD2 (C-MAD2) dimerizes with MAD1 (CMAD2-MAD1) and is recruited at unattached kinetocores. This dimer activates the binding of the open form of MAD2 (O-MAD2) to cdc20, inhibiting its binding to APC/C. Other proteins, like BUBR1, that contributes to chromosomes alignment, MSP1 that is required for kinetocore localization of MAD proteins and Aurora B that functions as a tension sensor, detecting and destabilizing faulty kinetocore/microtubules attachment (e.g. unreplicated chromosomes), are involved in this pathway.

- *DNA damage checkpoint* (G1 and G2 checkpoint), sensing DNA damage (from chemicals, radiations...) and determining a block in the cell-cycle until the damage is repaired. At the G1/S transition it prevents cells from copying a damaged DNA and at the G2/M transition prevents chromosomes segregation if they are not intact. It is mediated by Chk1/2 and ATM/ATR. After DNA damage, these proteins activate p53 by phosphorylation, that, in turn, induces the expression of p21 [28], GADD45 [60] and MDM2 [133]. In particular p21 has multiple functions: it inhibits CDK/cyclins D, E determining a block in the G1/S transition. It can also inhibit CDK1/cyclin B action, blocking the entry into mitosis and it can also bind PCNA that is part of the DNA polymerase complex involved in DNA replication and, by so doing, determines a block in S-phase.
- *Unreplicated centrosomes*: the lack of centrosomes replication arrests the completion of mitosis [131].

AIM OF THE WORK

The aim of my thesis was to study the interaction between Prepl and its new partner p160 and to elucidate p160 function. The issues that I dealt with were:

a) the interaction between Prepl and p160, trying to elucidate whether this interaction was direct, defining the interacting region and understanding the consequence of this interaction for Prepl function.

b) the mechanism that causes the translocation of p160 from the nucleolus to the nucleoplasm. In fact p160 is localized in the nucleolus while Prepl is found in the nucleus. Among the conditions analyzed that cause translocation of nucleolar proteins to the nucleoplasm was mitosis, a physiological state that causes the disruption of nucleoli and the release of its components in the nucleoplasm.

c) the function of p160 during the cell-cycle through immunofluorescence studies and evaluating the effects of a lower amount of p160 on mitosis progression.

d) a putative role of p160 in neoplastic transformation, since this last aspect is frequently connected with abnormal cell-cycle progression.

e) to connect all the observations made on p160 with its interaction with Prepl, since they share a similar phenotype.

MATERIAL AND METHODS

1. Cell Culture and treatments

1.1 Cell culture

NIH 3T3, HeLa, F9, NT2-D1 and Phoenix cells were grown at 37°C, 5% CO_2 in Dulbecco's modified Eagle's medium (DMEM, Gibco) supplemented with 10% heat-inactivated fetal bovine serum (FBS, Euroclone), 0.2 mg/ml streptomycin (Gibco), 20 U/ml penicillin (Gibco), 2 mM glutamine (Gibco) and 1 mM sodium pyruvate (Gibco). HEK 293T were grown in Iscove's Modified Dulbecco's medium (IMDM, Cambrex) supplemented with 10% FBS, 0.2 mg/ml streptomycin, 20 U/ml penicillin and 2 mM glutamine.

Prep1 non-overexpressing or overexpressing F9 cells clones (A2 and 2A18, respectively) have been described previously [74].

1.2 Treatments

Differentiation of NT2-D1 cells was performed treating the cells with 10 μM Retinoic Acid (RA, Gibco) for 48 hours; treatment with dimethyl sulfoxide (DMSO) was used as control.

To induce stress in the cells the following treatments were done:

- Actinomycin D (ActD, Sigma), 0.2 μM, 1 hour
- Hydroxyurea (Sigma), 10 mM, 4 hours

- α-amanitin (Sigma), 10 μg/ml, 4 hours

- UV irradiation, 20J/m^2 (UVC 254 nm, UV Stratalinker™ 1800 Stratagene)

- Cyclohexemide (Sigma), 10 μg/ml, 4 hours

- Anysomycin (Sigma), 10 μg/ml, 4 hours

- Thapsigargin (Sigma), 2,5 μg/ml, 6 hours

- Tunicamycin (Sigma), 2,5 μg/ml, 6 hours

- Temperature stress: 4°C, 20 minutes; 32°C, 4 hours; 42°C, 4 hours; 45°C, 20 minutes

- Oxidative stress: H_2O_2 (12 volume, Amati) 100 μM, 2 hours or 300 μM, 2 hours; DTT (Boeringer-Mannheim) 100 μM, 2 hours or 300 μM, 2 hours

- Osmotic stress: medium with 60% of H_2O, 2 hours; NaCl (VWR) 150 mM, 4 days

- Low serum stress: 2% FBS, 24 hours; 0,2% FBS, 24 hours

- MG132 (Sigma) 10 μM, 6 hours

To block cells at the G1/S transition I used *double-Thymidine block*. I treated cells (NIH 3T3 or HeLa) with 2 mM Thymidine (Sigma) for 18 hours (first block), followed by a release of 9 hours and a second pulse with 2 mM Thymidine for 17 hours (second block).

2. Plasmids used

The plasmids used are shown in Tab. I.

Tab I. List of the plasmids used

Plasmid	Description
pSG5-Prep1	Plasmid encoding Prep1 [9],[10]
pSG5-Pbx1a/b	Plasmid encoding Pbx1a/b [9],[10]
pSG5-HoxB1	Plasmid encoding HoxB1 [9],[10]
pADML-R3	Plasmid encoding HoxB1 enhancer [9],[10]
pADML-R4	Plasmid encoding HoxB2 enhancer [9],[10]
pact-c-p160 Flag	Plasmid encoding p160-Flag [124] (provided by T.J. Gonda, University of Queensland Diamantina Institute, Australia)
pact-c-p67* Flag	Plasmid encoding p67-Flag [124] (provided by T.J. Gonda)
pGEM3Z-p160	Plasmid encoding p160 (Addgene)
pGEM3Z-p67* and p67 deletion constructs	Plasmid encoding p67 and p67 deleted forms (Addgene)
pRufneo-p160 Flag	Retroviral plasmid encoding p160-Flag [124] (provided by T.J. Gonda)
pGEX2T-Prep1 GST	Bacterial expression vector for Prep1-glutathione-S-transferase (GST) [10].
pBabe-Myc	Retroviral vector for Myc (provided by Bernardi R., Dibit-HSR, Italy)
pBabe-Ras	Retroviral vector for Ras-Val12 (provided by Bernardi R., Dibit-HSR, Italy)

2.1 Preparation of Prep1-GST deletion and point mutants

Bacterial expression vectors for Prep1 deletion mutants were PCR amplified from pSG5-Prep1. Fragments were cloned into pGEX-4T1 (Stratagene). The primers were F1-R4 for HR1, F4-R3 for HR2, F1-R3 for HR1 plus HR2, F1-R2 for HR1 plus HR2* and F5-R1 for HD plus C-terminus. The sequences of the primers used are the following:

- F1 (BamHI): 5'-CCGGGATCCATGATGGCTACACAG-3'

- F2 (XhoI): 5'-CCGCTCGAGATGAACAGTGAAACTCTG-3'
- F4 (BamHI): 5'-CCGGGATCCACAACTTCTGCCAG-3'
- F5 (HindIII): 5'-CCGCTCGAGGGCCAAGTGGTCACACAG-3'
- R1 (NotI): 5'-TCGCGGCCGCTGCAGGGAGTCACTGTTCGC-3'
- R2 (EcoRI): 5'- TCCGAATTCTTGGGGAGTGACGAC-3'
- R3 (EcoRI): 5'-TCCGAATTCTTCTGTTTTCAGACAAGC-3'
- R4 (EcoRI): 5'-TCCGAATTCGCCTTCAGAGCCCTG-3'

The HR1 domain point mutants L63A, L66A and L63/66A were generated using the QuickChange site-directed mutagenesis kit (Stratagene) following the manufacturer instructions. Listed here are the primers used for the mutagenesis:

- L63A(sense):

  CAGGCCATTTATAGGCATCCAGCATTTCCATTATTAGCTTTGT TG
- L63A(antisense):

  CAACAAAGCTAATAATGGAAATGCTGGATGCCTATAAAT GGCCTG
- L66A(sense):

  GCCATTTATAGGCATCCACTATTTCCAGCATTAGCTTTGTTG
- L66A(antisense):

  CAACAAAGCTAATGCTGGAAATAGTGGATGCCTATAAAT GGC
- L63/66A(sense):

  CAAGCAGGCCATTTATAGGCATCCAGCATTTCCAGCATTA

  GCTTTGTTG

- L63/66A(antisense):

  CAACAAAGCTAATGCTGGAAATGCTGGATGCCTATAA

  ATGGCCTGCTTG

All constructs were verified by sequencing.

3. Transient transfection

Cells were plated in 10-cm plates for 24 hours, transfected with 4 μg of plasmid DNA using FuGene 6 (Roche) following the manufacturer protocol.

3.1 Transient p160 silencing in HeLa cells

2 X 10^5 cells/well were plated in triplicate in 6-well plates for 24 hours, transfected with siRNA or control oligonucleotides (High-GC, Medium-GC, Invitrogen) at a concentration of 40 nM, following the manufacturer protocol.

The sequences of the siRNAs are the following:

- siRNA1: CCAGGCTGGTGAATGTGCTGAAGAT
- siRNA2: CCCTGCAGCTAATTCTGGATGTGCT
- siRNA3: GAGGTCCTCAAAGCCGACTTGAATA

4. Generation of retroviruses/lentiviruses and infection of NIH 3T3 cells

4.1 Retroviral infection and selection of stable clones

Phoenix ecotropic packaging cells [64] were transfected with 10 μg of retroviral plasmid using the calcium phosphate protocol [99] and incubated overnight. Two days after the transfection NIH 3T3 cells were infected with the filtered viral supernatant and supplemented with 8 μg/ml of Polybrene (Sigma) for 4 hours at 37°C. 24 hours after the infection the specific antibiotics were added to the DMEM for the selection: Geneticin for pRufneo-p160-Flag (1 mg/ml, Gibco), Puromycin for all pBabe constructs (2 μg/ml, Sigma) and Hygromycin for pBabe-Myc and -Ras (200 μg/ml, Invitrogen).

4.2 Lentiviral infection and selection of stable p160 clones

HEK 293T cells were transfected with 3.5 μg ENV plasmid (VSV-G), 5 μg packaging plasmid (pMDLg/p RRE), 2.5 μg of pRSV-REV and 15 μg of the target plasmid (pLKO.1-puro, containing one of the five different shRNA target sequences, Sigma) following a calcium phosphate transfection protocol. The day after transfection the medium was replaced by fresh medium supplemented with 1 mM Sodium Butyrate (Sigma). After 30 hours, the viral supernatant was collected and used to infect NIH 3T3 cells. The day after the infection 2 μg/ml of Puromycin was added to the medium for selection.

The shRNA target sequences are the following:

- shRNA1:

CCGGCCTGCCCTAGAGACTCCTATTCTCGAGAATAGGAGTCTCTAGGGCA

- shRNA2:

CCGGCCTGATGAAGTCCGTGCAATTCTCGAGAATTGCACGGACTTCATCA

- shRNA3:

CCGGCCGGAGTGTATTTGGTCATATCTCGAGATATGACCAAATACACTCC

- shRNA4:

CCGGCCCAATGATTCGGAGATGAAACTCGAGTTTCATCTCCGAATCATTG

- shRNA5:

CCGGCCAAGCGTAACAGCTCACTTACTCGAGTAAGTGAGCTGTTACGCTT

5. Protein extraction

5.1 Total protein extraction

Cells were washed with PBS 1X and scraped with RIPA buffer (100 µl for a 10 cm dish; buffer composition: Tris-HCl 5 mM pH 8, NaCl 150 mM, SDS 0,1%, NP-40 1%, Na-deoxicolate 0,5%, Protease Inhibitor 1X – Complete, EDTA free, Roche). Cells were incubated on ice for 30 minutes and after centrifugation at 14,000 rpm for 15 minutes at 4°C, protein concentration was detected with the Bradford reagent (Bio-Rad Protein Assay, Bio-Rad) and measured at 595 nm with Ultraspectrophotometer 2100pro.

5.2 Cytoplasmic and Nuclear protein extraction

Cells were detached and washed with cold PBS 1X. Buffer A (300 µl for a 10 cm dish; buffer composition: Hepes-KOH 10 mM pH 7.8, $MgCl_2$ 1.5 mM, KCl 10 mM, DTT 0.5 mM – not added if the extract was for immunoprecipitation, Protease Inhibitor 1X) was added to the cell pellet and incubated on ice for 10 minutes. 10% Triton X-100 (Sigma) was added to the cells as 1/30th of the buffer A volume, and the suspension vortexed for 30 seconds. Samples were centrifuged for 1 minute at 11,000 rpm at 4°C to pellet nuclei. To the supernatant, representing the cytoplasmic fraction, was added 0.11 volume of buffer B (Hepes-KOH 0.3 M pH 7.8, KCl 1.4 M, $MgCl_2$ 30 mM, protease inhibitor 1X). The pellet, representing the nuclear fraction, was washed in buffer A and resuspended in buffer C (1/5 of the original volume; buffer composition: Hepes–KOH 20 mM pH 7.8, glycerol 25%, NaCl 0.42 M, $MgCl_2$ 1.5 mM, EDTA 0.2 mM, DTT 0.5 mM- not added if the extract was for immunoprecipitation, Protease Inhibitor 1X). Protein concentration was detected with the Bradford reagent and measured at 595 nm with Ultraspectrophotometer 2100pro.

6. Western Blot analysis

Protein extracts were resuspended in loading buffer 1X (Buffer 4X composition: Tris 375 mM pH 6.8, glycerol 30%, bromofenol blu 0.5 mg/ml, β-mercaptoethanol 8%, SDS 6%), heated for 5 minutes at 95°C and loaded on a 10% gradient sodium dodecyl sulfate-polyacrylamide gel electrophoresis (SDS-PAGE) [71]. Following SDS-PAGE, proteins were transferred to polyvinylidene difluoride membrane (PVDF, Millipore) as described

[125]. After the transfer, filters were blocked for 16 hours at 4°C with blocking solution (5% w/v non-fat dry milk diluted in PBS 1X supplemented with 0.1% Tween 20 (PBS-T) and incubated with the primary antibodies (Table II) diluted in blocking solution at the indicated concentrations, at room temperature (RT). After 1 hour, filters were washed three times for 10 minutes at RT with PBS-T and incubated for 1 hour with a peroxydase-conjugated secondary anti-mouse (Amersham), anti-rabbit (Amersham) or anti-goat antiserum (Amersham), depending on the primary antibody used, at the final dilution of 1:5,000 in blocking solution. Membranes were washed three times for 10 minutes in PBS-T and developed with Super Signal West Pico chemiluminescence substrate system (Pierce).

7. Immunoprecipitation

Nuclear protein extracts were adjusted to IBB buffer (Tris-HCl 10 mM pH 8, NP-40 0.2%, NaCl 150 mM) and a preclearing was performed with protein G-sepharose beads (Roche) for 1 hour at 4°C. The clarified supernatants were incubated with 5 µg of the indicated antibodies and recovered on protein G-sepharose beads or on M2-anti-Flag affinity resin (Sigma) overnight at 4°C. The beads were rinsed several times with IBB buffer, resuspended twice in loading buffer 1X, heated at 95°C and centrifuged at 10,000 x g. The supernatant was loaded on a 10% gradient SDS-PAGE as described previously.

8. In vitro transcription-translation

Proteins were *in vitro* synthesized using the TNT T7 Quick coupled transcription-translation system (Promega) from 1 μg of plasmid DNA and 2 μl of translation grade [^{35}S] methionine (0.03 mCi, Amersham Bioscences). Protein synthesis was evaluated by SDS-PAGE and the gel was fixed with 10% Methanol, 10% Acetic acid and 5% glycerol, dried and exposed to Amersham films.

9. Pull-down assay

GST fusion proteins were purified from Escherichia Coli BL21 cells grown in Luria-Bertani broth (LB) at 37°C to an optical density at 600 nm of 1. Protein expression was induced with 0.1 mM isopropyl-β-D-thyogalactopyranoside (IPTG, Sigma) for three hours, as described [10]. The pellets were sonicated in PBS 1X with Protease Inhibitor 1X supplemented with 1% Triton X-100, centrifuged at 13,000 rpm for 15 minutes and the supernatants were collected. Lysates containing the GST proteins were incubated with glutathione (GST) -Sepharose beads (Amersham) for 30 minutes at 4°C.

For pull-down assay, 10 μg of *in vitro* translated proteins precleared with 20 μl of glutathione beads in 200 μl of NET-N buffer (Tris-HCl 10 mM pH 8, NaCl 150 mM, NP-40 0.2%, Protease Inhibitor 1X) were incubated for 1 hour at 4°C with 1 to 3 μl of the GST protein previously bound to the beads. Beads were washed five times in NET-N buffer and eluted twice for 15 minutes at RT with 10 mM glutathione. The quantity of eluted GST fusion proteins was evaluated by digital densitometry (ImageQuant 5.2,

Molecular Dynamics) of Coomassie stained gels. Non-specific binding to GST was subtracted and data were normalized to the input.

10. Luciferase assay

4 X 10^4 cells were plated in a 24-well plate and transiently transfected with 25 ng/well of pAMDL-R3Hoxb1, R4-Hoxb2 Luciferase or pSG5-Hoxb1 vector; 50 ng of Pbx1a or Prep1 vector; 20 ng β-galactosidase (β-Gal) plasmid and 50 to 500 ng of pact-c-p160Flag or pact-c-p67Flag vector, using Fugene 6. After 24 hours the cells were lysed with reporter lysis buffer (100X Mg, 1X ONPG reagent and 0.1M Sodium Phosphate, pH 7.5) and the Luciferase activity was determined using the Promega Luciferase Kit (Promega) in a Mithras Luminometer (Berthold Technologies). The Luciferase data were normalized by β-Gal assays as described [13].

11. EMSA

Electrophoretic mobility shift assay (EMSA) with b2-PP2 and Sp1 oligonucleotides were done as described [7,10]. The sequence of oligonucleotide b2-PP2 (5'-GGAGCTGTCAGGGGGCTAAGATTGATCGCCTCA-3') contains both the Prep1-Pbx1 and the Pbx1-HoxB1 binding sites of the Hoxb2 R4 enhancer [34]. The sequence of the Sp1-binding oligonucleotide is 5'-GATCCGATCGGGGCGGGGCGAT-3' [37].

12. RNA extraction

Cells were plated and transfected using lipofectamine (for HeLa experiments) and Fugene (for NIH experiments) as described above. Total RNA was extracted with an RNAeasy minikit (QIAGEN) and quantified by spectrophotometry (Nanodrop, Thermo Scientific).

13. Real-Time PCR

5 μg of total RNA were reverse transcribed using a SuperScript First-Strand kit with random primers (Invitrogen) according to the manufacturer's instructions. For quantitative Real-Time PCR, 5 ng of reverse-transcribed RNA was amplified in a light cycler instrument (Roche) using a Fast Start DNA mix SYBR Green I kit (Roche). The PCR conditions for HoxB2 mRNA were the following: first denaturation and DNA polymerase activation step, 95°C for 10 minutes; second denaturation step, 95°C for 15 seconds; annealing step, 56°C for 6 seconds; extension step, 72°C for 20 seconds. For actin, the conditions were as follow: first denaturation and DNA polymerase activation step, 95°C for 10 minutes; second denaturation step, 95°C for 15 seconds; annealing step, 58°C for 6 seconds; extension step, 72°C for 20 seconds. The amount of HoxB2 mRNA was normalized to actin mRNA. The sequences of the primers used are the following:

- HoxB2 FW: TCCTCCTTTCGAGCAAACCTTCC
- HoxB2 RW: AGTGGAATTCCTTCTCCAGTTCC
- Actin FW: GGCATCCTGACCCTGAAGT

- Actin RW: CGGATGTCAACGTCACACTT

For the microarray validation, 20 ng of the reverse-transcribed RNA was amplified with a Light-Cycler 480 (Roche) using a Universal Probe Library Assay (Roche) and following the manufacturer instructions. The PCR conditions were as follow: pre-incubation at 95°C for 5 minutes, 50 cycles of amplification (denaturation at 95°C for 10 seconds, annealing at 58°C for 15 seconds and extension at 72°C for 1 second), cooling at 40°C for 10 seconds. The amount of the different mRNAs was normalized to GAPDH mRNA.

The sequences of the primers used with the relative probes are the following:

- p160, probe 10

L: AGCACCTTCTGCTCCTCGT

R: ATGCAGGTCTGGATGTCACC

- CDKN1A, probe 32

L: TCACTGTCTTGTACCCTTGTGC

R: GGCGTTTGGAGTGGTAGAAA

- NFKB2, probe 10

L: CACATGGGTGGAGGCTCT

R: ACTGGTAGGGGCTGTAGGC

- GADD45B, probe 10

L: CATTGTCTCCTGGTCACGAA

R: TAGGGGACCCACTGGTTGT

- JUN, probe 19

L: CCAAAGGATAGTGCGATGTTT

R: CTGTCCCTCTCCACTGCAAC

- TOP2B, probe 66

L: TCCAAGAGATTCTTTGCTTAGGA

R: CATCCTCTTCTTCTGAGAAATCAAA

- GAPDH, probe 60

L: AGCCACATCGCTCAGACAC

R: GCCCAATACGACCAAATCC

14. Immunofluorescence and confocal microscopy analysis

Cells were grown on 13 mm glass coverslips (VWR international) for at least 24 hours. Cells were washed three times with PBS 1X, fixed with paraformaldehyde solution (3% paraformaldehyde; 2% sucrose in PBS 1X) for 10 minutes at RT and then washed again three times in PBS 1X. Cells were then permeabilized with a 0.2% PBS-Triton X-100 solution for 5 minutes at RT, washed 3 times in PBS 1X and blocked with 1X PBS-1% BSA for 30 minutes at RT. The primary antibodies were added in blocking solution at the concentrations indicated in Table II for 30 minutes at 37°C. Cells were washed 3 times in PBS and incubated with the secondary antibodies (Alexa-488 and Alexa-546 conjugated anti-mouse or anti-rabbit immunoglobulin, 1:1,000 final dilution) and incubated for 30 minutes at RT protected from light. Cells were washed again 3 times with PBS 1X and incubated with 4'6-diamidino-2-phenylindole dihydrochloride (DAPI) nuclear staining (Fluka) previously resuspended in PBS 1X (1:1,000 final dilution) for 3 minutes at RT or Hoechst 33258 (same conditions, Sigma). Cells were washed 3 times

in PBS 1X and coverslips were mounted with Fluorescent Mounting Medium (Dako Cytomation). Images were obtained with a Leica DMIRE2 (Confocal System Leica TCS SP2) with a 63X objective. Incubations with matched mouse isotype IgGs, irrelevant rabbit IgGs or secondary antibodies were always negative.

14.1 ImmunoFISH

The first part of this technique is a regular immunofluorescence (see above). After the washing step following the incubation with the secondary antibodies, cells were fixed again in 4% paraformaldehyde - 0,1% Triton X-100 at 4°C for 30 minutes. Cells were then incubated for 30 minutes at RT with 100 mM Glycin (VWR) and washed once with PBS 1X. FISH was performed with Telomere PNA FISH kit/Cy3 (DAKO) following the manufacturer instructions; PNA probe was labeled with Cy3.

Table II. List of antibodies used in Western-blot (WB) and Immunofluorescence (IF)

ANTIBODY	Source	WB	IF
Anti-Flag mono/polyclonal	Sigma	1:1,000	1:500
Anti-p160 rabbit polyclonal	Donated by Ishii S. (RIKEN, Japan)		1:100
Anti-p160C rabbit polyclonal	Zymed laboratories	1:250	
Anti-human Prep1 CH12.2 Mouse monoclonal	Homemade [37]	2 μg/ml	
Anti-Prep1 rabbit polyclonal	Homemade [9]	2 μg/ml	
Anti-Prep1 (Meis4) mouse monoclonal	Upstate Biotechnology	1 μg/ml	
Anti-Prep1 mouse monoclonal	Santa Cruz Biotechnology		1:50
Anti-Pbx2 rabbit polyclonal	Santa Cruz Biotechnology	2 μg/ml	
Anti-Pbx1b mouse monoclonal	Donated by Cleary M.L (Stanford University, USA)	2 μg/ml	
Anti-Tubulin mouse monoclonal	Sigma	1:2,000	1:300
Anti-Phospho Histone H3 rabbit polyclonal	Millipore		1 μg/ml
CREST human monoclonal	Homemade		1:50
Anti-Nucleolin mouse monoclonal	Santa Cruz Biotechnology		1:100
Anti-Nucleophosmin mouse monoclonal	Invitrogen		1:50
Anti-active caspase 3 rabbit polyclonal	MBL	1 μg/ml	
Anti-caspase 9 mouse monoclonal	MBL	1 μg/ml	
Anti-β actin goat polyclonal	Santa Cruz Biotechnology	1 μg/ml	

15. Proliferation assay

The measurement of proliferation in HeLa cells was performed plating 2 X 10^5 cells/wells in a 6-well plate and transfecting them with lipofectamine the day after. At 24, 48 and 72 hours after transfection the cells were detached and counted with a cell counter (Coulter Z1, Coulter Diagnostics).

15.1 Crystal Violet assay

3,000 cells/well were plated in a 12-wells plate and fixed at the following time points: T0 (8 hours after plating) and at 2, 4, 6, 8, 10 days after. For fixation, cells were washed in PBS 1X, fixed with 11% glutaraldehyde (Sigma) for 15 minutes at RT and washed again in PBS 1X 3 times and allowed to dry at RT. Cells were stained with Crystal Violet solution (0,1% crystal violet -Sigma- in 20% Methanol, 80% dH_2O) for 20 minutes at RT. Cells were washed with dH_2O and dried at RT. Stained and dried cells were solubilized with a solution of 10% Acetic Acid for 10 minutes at RT and analyzed with a Microplate Reader 680 (Bio-Rad) at 570 nm.

16. Flow-Citometry analysis

16.1 EdU/7AAD staining

For 5'ethynyl-2'-deoxyuridine (EdU) / 7-amino-actinomycin D (7-AAD) double staining, cells were grown and pulsed before the assay with 10 μM EdU for 1 hour, harvested and processed with Click-iT EdU Flow Citometry Assay kit (Invitrogen)

following the manufacturer protocol. Anti-EdU-Fluorescein-isothycyanate (FITC) was used to stain EdU positive cells and 7-AAD was used to stain DNA. Cells were analyzed with FACS CANTO or FACS Calibur (BD Immunocytometry). Results were displayed as bivariate distribution of EdU content versus DNA content. The percent of cells in the S-phase was calculated by gating EdU positive cells (cells with the higher fluorescence intensity in the FITC channel compared to an unstained control) using FCS Express V3 (De Novo Software) or CellQuest program (BD).

16.2 Annexin V staining

Cells were harvested, washed with PBS 1X and the dead and apoptotic cells were detected by Annexin V Phycoerythrin (PE) / 7-AAD staining using PE Annexin V Apoptosis Detection kit I (BD Pharmingen), following the manufacturer's instructions. Cells were analyzed with FACS CANTO or Calibur (BD) and results were displayed as bivariate distribution of Annexin V positive cells versus 7-AAD positive cells. Percentage of early apoptotic cells was calculated by gating Annexin V positive cells using FCS Express V3 or CellQuest programs.

17. Time-Lapse microscopy

Cells were plated in a 6-wells plate (2 X 10^5 cell/well in triplicate), transfected as described above with siRNA or High-GC control and blocked at the G1/S transition using a double thymidine block. Starting 8 hours after the release from the block and up to 24 hours later, the cells were analyzed with Time Lapse Microscope (OKO VISION).

Images were taken in 4 different fields for each sample every 5 minutes with a 5X objective and analyzed with Image J software.

18. Karyotyping

Cytogenetic analysis of HeLa and NIH 3T3 cell lines after siRNA / shRNA treatment was performed according to standard methods: cell lines were incubated overnight with Colcemid (1 μl/ml, Invitrogen), trypsinized and washed with sterile PBS 1X. Cells were then treated for 15 minutes with hypotonic solution (0.075 M KCl) at 37°C and then fixed with three passages in cold Carnoy's fixative (methanol: acetic acid, 3:1). Harvested samples were dropped on wet glass slides and chromosome QFQ banding was carried out using standard procedures. Metaphase spreads were analyzed by a fluorescence microscopy Nikon 90i and the Genikon software (Nikon Instruments Italia). The description of karyotypes and clonality criteria followed the International System for Human Cytogenetic Nomenclature recommendations (ISCN 2009). The karyotype analysis was made by Pecciarini L. at the Pathology Unit (Dibit, HSR, Milan – Italy).

19. Gene Expression Profiling

For gene expression profiling, the RNA from three technical replicates of HeLa cells transfected with High-GC control or siRNA1 was extracted, following the procedure described above. RNAs were analyzed with Affimetrix Human Gene 1.0 ST chip

(Affimetrix). Biotin-labelled cDNA targets were synthesized starting from 100 ng of total RNA. Double stranded cDNA synthesis and related cRNA was obtained with GeneChip WT cDNA Synthesis and Amplification Kit (Ambion). With the same kit the cDNA sense strand was synthesized, then fragmented and labelled with GeneChip WT Teminal Labeling Kit (Ambion). DNA fragmentation was performed with a combination of uracil DNA glycosylase (UDG) and apurinic/apyrimidinic endonuclease 1 (APE 1), while labeling was completed using terminal deoxynucleotidyl transferase (TdT) in the presence of GeneChip® DNA Labeling Reagent. All steps of the labelling protocol were performed as suggested by Affymetrix (http://www.affymetrix.com/support/technical/manual/expression_manual.affx). The size (the range size of the fragmented sample should be approximately 40 to 70 nt) and the accuracy of quantification of targets were checked by agarose gel electrophoresis of 2 µl aliquots of each sample after fragmentation. External controls (spikes) were used; each eukaryotic GeneChip® probe array contains probe sets for several B. subtilis genes that are absent in the samples analyzed (lys, phe, thr, and dap). This Poly-A RNA Control Kit contains *in vitro* synthesized, polyadenylated transcripts for these B. subtilis genes that are pre-mixed at staggered concentrations to assess the overall success of the assay. Samples were then hybridized as indicated by Affymetrix: diluted in hybridization buffer (100 mM MES, 1 M [Na+], 20 mM EDTA, 0.01% Tween 20) at a concentration of 25 ng/µl, denatured at 99 °C for 5 minutes and centrifuged at maximum speed for 1 minute prior to introduction into the GeneChip cartridge. A single GeneChip Human Gene 1.0 ST was then hybridized with each biotin-labelled sense target. Hybridizations were performed for 16 hours at 45 °C in a rotisserie oven. GeneChip

cartridges were washed and stained with GeneChip Hybridization, Wash and Stain Kit in the Affymetrix fluidics station following the FS450_0007 standard protocol. Images were scanned using an Affymetrix GeneChip Scanner3000 7G with default parameters. The resulting images were analysed using GeneChip Operating Software v1.2 (GCOS1.2). Raw data were first normalized using RMA method [12,54,55]. In order to evaluate the variability between samples, Principal Component Analysis (PCA) was performed. After this analysis an ANOVA test and a False Discovery Rate (FDR, [5,107] to exclude false positives) was applied and the resulting gene-list was refined with a p value ≤ 0.05 and a fold change ≥ 1.75. Gene ontology analyses of the differentially expressed genes were performed with the DAVID 6.7 functional annotation tool (Database for Annotation, Visualization and Integration Discovery – NIH, http://david.abcc.ncifcrf.gov/home.jsp) according to Huang et al. [52].

20. Soft-agar assay

Cells were resuspended in DMEM with 0.3% agar in a concentration of 5,000 cells/well and plated over a 0.6 % agar layer in a 6-wells plate. The experiment was performed in triplicate and plates were incubated at 37°C in an humidified incubator for two weeks. Colonies detection was performed staining the cells with 3-(4,5-dimethylthiazol-2-ye)-2,5-diphenyltetrazolium bromide (MTT, 1:10 in PBS 1X) for at least 4 hours. After staining, the plate was scanned and the image obtained was analyzed with Image J Software.

RESULTS

1. Biochemical and functional analysis of the Prep1-p160MBP interaction

1.1 Prep1 co-immunoprecipitates with p160

Tandem Affinity Purification (TAP) followed by a MALDI-TOF/MS analysis was used to identify Prep1 interactors that might be important for its phenotype. From this analysis, few proteins were isolated that specifically interacted with Prep1. Among this interactors p160 myb binding protein 1a (p160) was identified by the sequence of 9 and 8 different peptides in two independent experiments [23]. To demonstrate that the interaction was specific, I performed an immunoprecipitation using nuclear extracts from NIH 3T3 cells infected with p160-Flag or GFP as control. The immunoprecipitation was performed with an M2 anti-Flag affinity resin. As shown in Fig. 12, Prep1 specifically co-immunoprecipitated with p160, but not with GFP, while Pbx1b and Pbx2 did not immunoprecipitate with either p160 or with GFP. As control, I immunoblotted with an anti-p160 antibody: this recognized the protein only in the p160-Flag infected cells (not shown). p160-Flag overexpression did not affect the protein level of Prep1, Pbx1b or Pbx2 (Fig. 12, input panel on the right). This result shows that Prep1 and p160 are part of a stable complex *in vivo* that does not contain Pbx and suggests that p160 might be a specific Prep1 interactor.

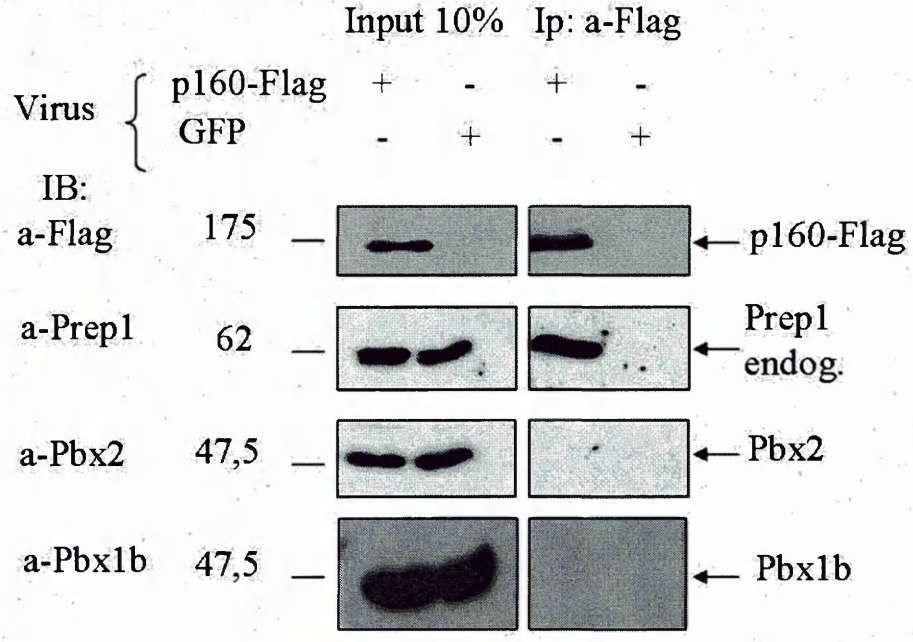

Fig. 12 Prep1 and p160 interact in vivo. Immunoprecipitation using M2 anti-flag resin and immunoblotting with the indicated antibodies of nuclear extracts of NIH 3T3 cells infected with a p160-Flag or GFP (as control) retrovirus. Input and immunoprecipitates (Ip) are compared.

1.2 Prep1 and p160 directly interact *in vitro*

To demonstrate that the interaction between Prep1 and p160 was direct I performed pull-down assays. For this experiment full-length p160 was *in vitro* translated and labeled with ^{35}S. I tested also its shorter forms: p67 (which represents the N-terminal part, aa 1-580) and p160C (the C-terminal of the protein, aa 580-1344) (Fig. 13A). Pbx1b was used as control (since it directly interacts with Prep1, [9]). As shown in Fig. 13B, ^{35}S-p160 binds GST-Prep1 but not GST alone. ^{35}S-p67 also gave a strong signal, while there was no signal with ^{35}S-p160C. As expected, ^{35}S-Pbx1b strongly associated with GST-

Prep1. Therefore this pull-down demonstrates that p160 specifically interacts with Prep1, in particular its N-terminal part.

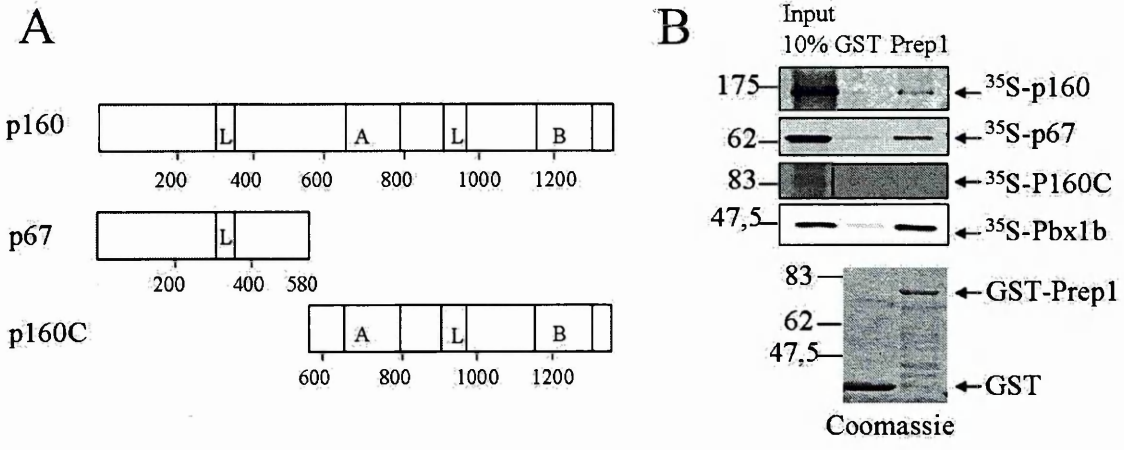

Fig. 13 Prep1 and p160 in vitro interaction. (A) Schematic representation of p160 deletion mutants; the leucine zipper-like motifs (L), the acidic domain (A), and the basic carboxyl-terminal region (B) are indicated. **(B)** Pull-down assay of GST-Prep1 or GST alone as control, with *in vitro* translated ^{35}S-p160, ^{35}S-p67, ^{35}S-p160C and ^{35}S-Pbx1. In the upper part of the figure the different pull-downs are shown and at the bottom, the Coomassie-stained gel of GST and GST-Prep1.

I also wanted to explore which Prep1 domain interacted with p160. I prepared Prep1 deletion mutants as shown in Fig. 14A and performed pull-down assays with ^{35}S-p67 (shown above to interact with Prep1) and ^{35}S-Pbx1b (which interacts with the N-terminal part of Prep1, [9]). As shown in Fig. 14B, ^{35}S-p67 and ^{35}S-Pbx1b strongly bound to HR1, HR2, HR1+HR2 and HR1+HR2* but not to the C-terminal part (HD+CT) of Prep1. Moreover, full length ^{35}S-p160 associated with HR1 (Fig. 14C). The data show that both p160 and Pbx bind the HR1 domain of Prep1. However, ^{35}S-p67 and ^{35}S-Pbx1b have also a low binding activity with HR2.

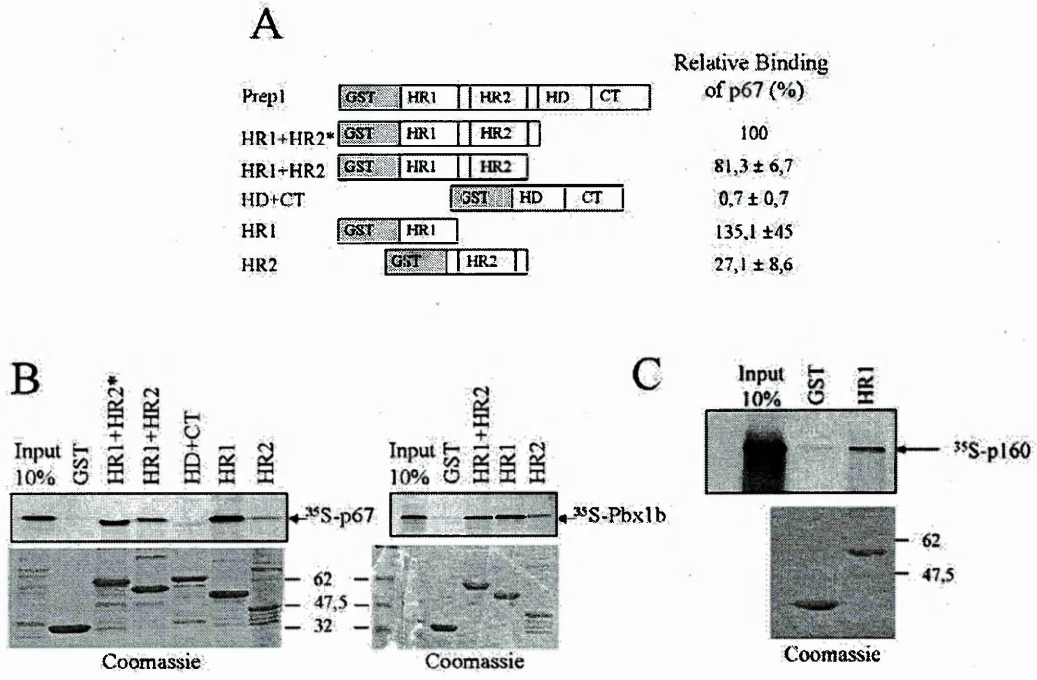

Fig. 14 Identification of the Prep1 domains required for p160 binding. (A) Schematic representation of the Prep1 mutants and quantification of the binding with ^{35}S-p67 (average of three determinations; HR1+HR2* was given the arbitrary value of 100%). **(B)** Representative pull-downs of the *in vitro* translated ^{35}S-p67 (left) and ^{35}S-Pbx1b (right) with the different GST-Prep1 deletion mutants. **(C)** Representative pull-down of ^{35}S-p160 with GST-HR1. On the top are shown the autoradiographies and on the bottom the Coomassie staining of the gels.

1.3 Identification of the p160 binding site on Prep1

To identify the binding site of p160 on Prep1, I analyzed the HR1 sequence and noticed the region 63LFPLLALL70 conserved in all mammalian MEINOX proteins (Fig. 15A). This sequence is composed of 2 overlapping LXXLL motifs. Interestingly, this motif is present also in other p160-binding proteins (e.g. in PGC1α there are 2 LXXLL motifs starting at aa 147 and 210, respectively) [30,124]. I produced HR1 mutants inserting point mutations in L63 and L66 (substituting leucine with alanine) and performed pull-

down assays of the GST-HR1 mutants with the *in vitro* translated ^{35}S-p67 and ^{35}S-Pbx1b. As shown in Fig. 15B and C, the relative binding of ^{35}S-p67 and ^{35}S-Pbx1b to HR1 was decreased in both L63A and L66A mutants and was almost absent when both mutations were present at the same time (HR1 L63/66A). The relative binding of full-length (L63/66A) GST-Prep1 to both ^{35}S-p67 and ^{35}S-Pbx1b was also diminished (Fig. 15D). Therefore p160 and Pbx bind the same region in the HR1 domain of Prep1. Another interesting observation is that L63A mutation alone gives a reduction of the binding of 53% and L66A of 72%, indicating that also the second LXXLL motif is important for the binding.

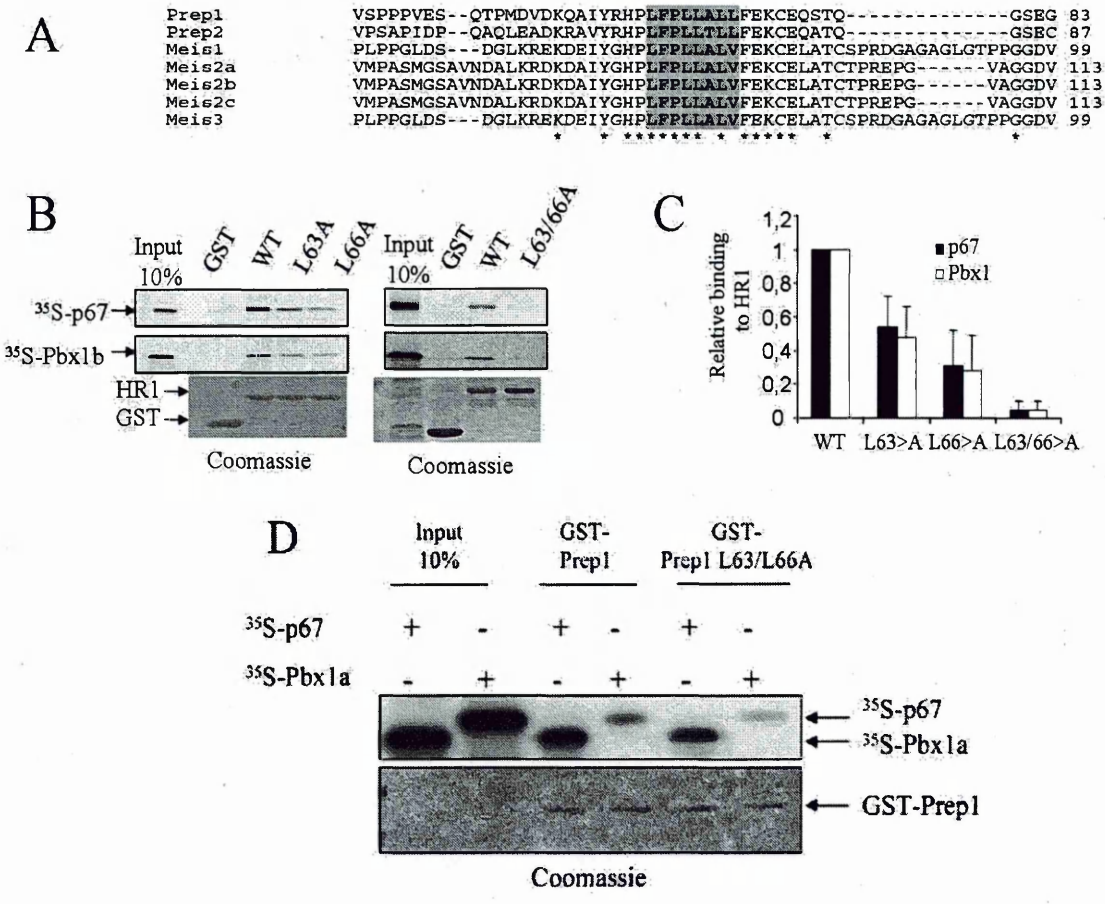

Fig. 15 The LFPLLALL sequence of the HR1 domain is required for the interaction with both p67 and Pbx1. (A) Alignment of murine Prep1 HR1 domains with its murine Meinox homologs, highlighting the conserved leucine-rich region (shaded). The asterisks indicate the conserved amino acids. **(B)** Representative pull-downs of *in vitro* translated ^{35}S-p67 or ^{35}S-Pbx1b with wild-type (WT) and mutant (L63A, L66A, L63/66A) GST-HR1 and GST alone as control. At the top is shown the autoradiography and at the bottom the Coomassie staining of the gel. **(C)** Quantification of the binding after densitometric analysis of the pull-downs autoradiographies (mean of three experiments). The error bars indicate standard deviations. **(D)** Representative pull-down of ^{35}S-p67 and ^{35}S-Pbx1b with GST-Prep1 and GST-Prep1 L63/L66 mutant. On the top is shown the autoradiography and on the bottom the Coomassie staining of the gel.

1.4 Identification of the Prep1 binding region in p160

I also analyzed the p160 region involved in the binding to Prep1 preparing p67 deletion mutants, since this is the region involved in the binding. As described in the

Introduction, p160 contains leucine-rich motifs (one leucine-zipper-like domain and several leucine-charged-domains – LCD) in its N-terminal region, which may be necessary for protein-protein interaction and hence could be important for Prep1 binding (Fig. 16A). Pull-down assays of the *in vitro* translated ^{35}S-p67 deletion mutants and GST-HR1, or GST alone as control, showed that the deletion of the C-terminal part up to residue 228 did not significantly affect the binding (Fig. 16). Therefore the leucine-zipper-like domain located in this region (starting at aa 307) is not important for Prep1 binding: the same was observed for c-Myb [124]. However, further deletion from residue 113 to 228 (p12) almost abolished binding. Moreover, the N-terminal deletion up to residue 51 did not affect the binding. However, the 51-151 deletion greatly decreased the binding. I conclude that the p160 region from amino acid 113 to 151 is extremely relevant for Prep1 binding. As shown in Fig. 4 (Introduction), this region contains LCD motifs and LXXL motifs starting at residues 94, 135, 160 and 245 (Fig. 16A), all sequences that can mediate protein-protein interactions.

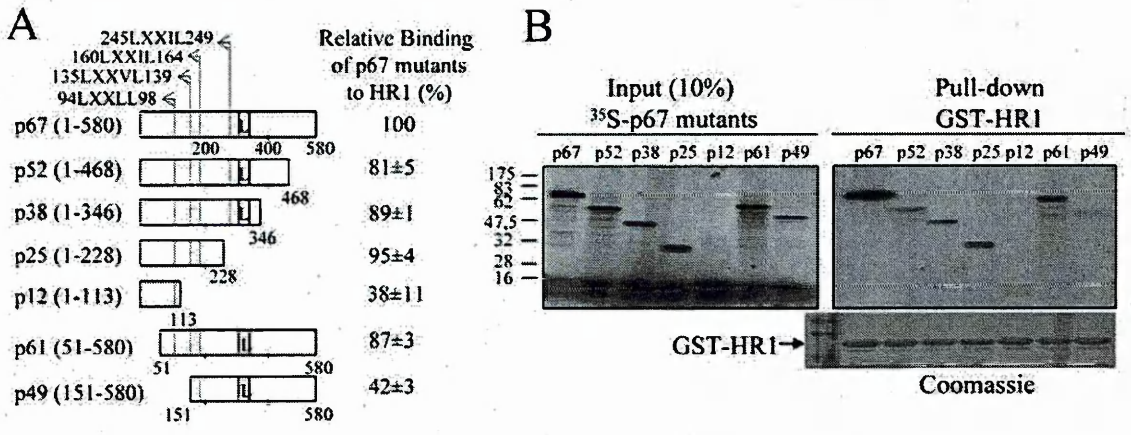

Fig. 16 The region between amino acids 51 and 151 of p160 participates in the binding to Prep1. (A) Schematic representation of the p67 deletion mutants with highlighted the leucine-rich sequences and the leucine zipper domain (L). On the right is shown the quantification by densitometric analysis of the relative binding of each mutant to GST-HR1 (average of three different experiments); wild-type p67 was given the arbitrary value of 100%. **(B)** Representative pull-down of GST-HR1 with the *in vitro* translated ^{35}S-p67 deletion mutants; on the left is shown the input, on the right the pull-down and in the bottom part the Coomassie staining of the gel.

1.5 p160 competes with Pbx for the binding to Prep1 and inhibits its transcriptional activity

Since p160 and Pbx bind the same region on Prep1, they must compete for the binding. Thus, p160 should interfere with Pbx1 transcriptional activity. To test this hypothesis I performed a pull-down assay of GST-Prep1 and GST-HR1 with *in vitro*-translated ^{35}S-p67 and ^{35}S-Pbx1b, separately and together. As shown in Fig. 17A, in the presence of p67, the amount of Pbx1b bound to Prep1 was decreased. This suggests that p160 competes with Pbx for binding Prep1.

I also investigated a possible inhibition of the Pbx1 dependent transcriptional activity. I transiently transfected NIH 3T3 cells, stably expressing p160 or GFP (as control), with a luciferase reporter driven by the HoxB1 enhancer. As already described, a high luciferase activity is induced only in the presence of the three proteins: Prep1, Pbx1 and HoxB1 [9,34,35,56]. However, when p160 was present, the luciferase activity was almost absent (Fig. 17B).

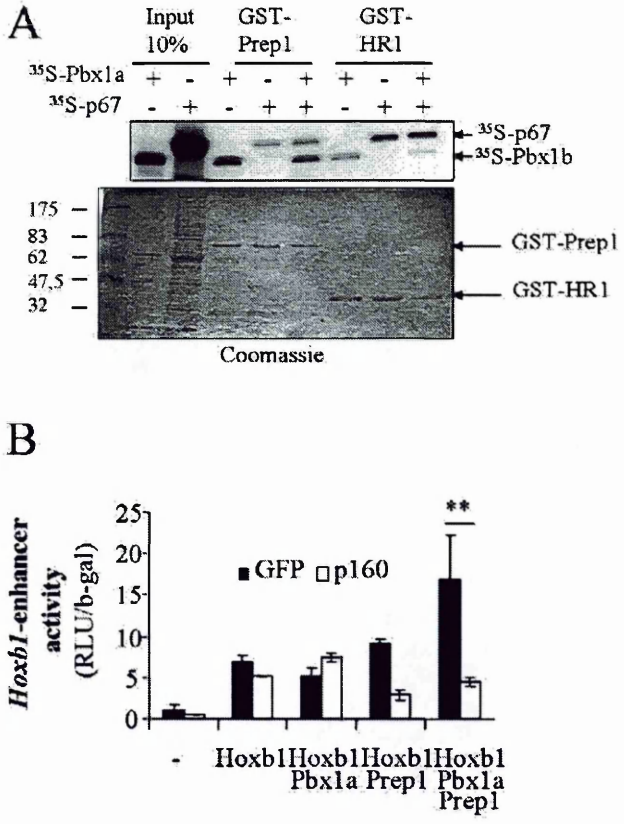

Fig. 17 p160 competes with Pbx in the binding to Prep1 and inhibits its transcriptional activity. (A) Competitive pull-down assay of ^{35}S-p67 and ^{35}S-Pbx1a with GST-Prep1 or GST-HR1 beads. On top is shown the autoradiography, at the bottom the Coomassie staining of the gel. The proteins used in each reaction are indicated on the top of the figure. **(B)** Transient transfection of a Luciferase reporter plasmid (pADML-R3), containing the R3 sequence of the HoxB1 enhancer into NIH 3T3 cells stably expressing p160 (white) or GFP (black) with the indicated expression plasmids. The activity (RLU/β-Gal) was measured 24 h after transfection and the value was divided by the expression of the internal transfection control β-Gal. The histogram represents the average of three independent experiments performed in triplicate; **, $P< 0.001$, t test.

Using EMSA, I also tested the inhibition of Prep1 DNA binding activity by p160. I used NT2-D1 cells, a teracarcinoma cell line that can be induced to differentiate and to transcribe HoxB genes with retinoic acid (RA) [35]. Nuclear extracts of cells stably expressing p160, or empty vector as control, were tested for DNA binding capacity to an oligonucleotide specific for Prep1-Pbx1 dimer and Prep1-Pbx1-HoxB1 trimer [34]. p160 overexpression decreased the intensity of the shifted bands (corresponding to the Prep1/Pbx1 and Prep1/Pbx1/Hoxb1 complexes) in untreated and even more in RA treated cells (Fig. 18A). However p160 did not change the DNA-binding activity of the control transcription factor Sp1.

The significance of this inhibition was checked by Real-Time PCR measuring the level of HoxB2 mRNA in NT2-D1 cells after addition of RA. Induction of HoxB2 mRNA was reduced by 45% in p160 overexpressing compared to control cells (Fig. 18B).

All these experiments demonstrate that p160 competes with Pbx in the binding to Prep1 and this interaction inhibits the transcriptional activity in which Prep1 and Pbx1 are involved.

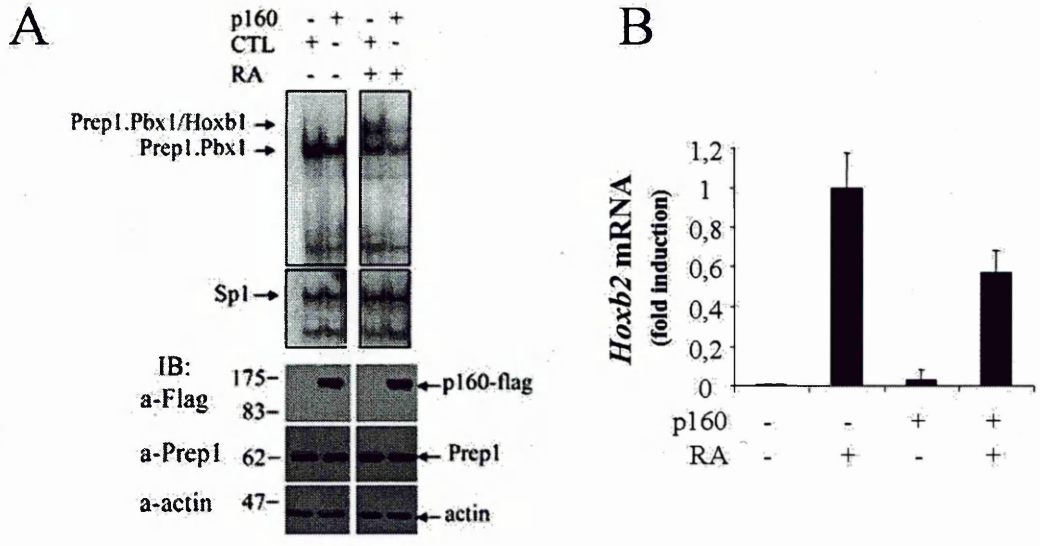

Fig. 18 p160 inhibits Prep1 DNA-binding activity. (A) EMSA assay with nuclear extracts of NT2-D1 control or p160 overexpressing cells, treated/untreated with RA for 48h and incubated with ^{32}P-b2-PP2 oligonucleotide [34]. Below is a control EMSA performed with an oligonucleotide containing the sequence for the Sp1 transcription factor. In the bottom part is shown an immunoblot (IB) with anti-Flag for p160, anti-Prep1 and anti-actin as loading controls. **(B)** Real-Time PCR measurement of Hoxb2 mRNA level in NT2-D1 cells expressing p160 or control vector and treated or not with RA. Data from two independent experiments performed in triplicate.

1.6 p160 interacts with Prep1 in the nucleus

p160 is a nucleolar protein [62,124]. I studied its subcellular localization by confocal microscopy in NIH 3T3 cells. As shown in Fig. 19A, p160 staining indicates that it is localized mainly in the nucleolus and this was confirmed by a co-staining with anti-Nucleolin, a known nucleolar protein antibody (data not shown). I also analyzed the p67 form that was absent in nucleoli, since it lacks the nucleolar localization signal, but mostly present in the nucleoplasm [124] (Fig. 19B). Less than 5% of the cells analyzed

also showed a nuclear staining with the full-length protein, suggesting that it can shuttle between nucleolus and nucleoplasm.

Since Prep1 acts mostly (if not exclusively) at RNA polymerase II-dependent promoters, I expected that a functional interaction between the two proteins would take place in the nucleoplasm. A physiological condition that induces the translocation of nucleolar proteins to nucleoplasm is mitosis. During mitosis, nucleoli disassemble at the stage of prophase (when transcription shuts down) and reassemble around the rDNA genes when cell division is completed [11]. I therefore analyzed p160 and Prep1 localization in NIH 3T3 cells during mitosis by confocal microscopy. As shown in Fig. 19C, immunofluorescence fails to show co-localization between the two proteins in interphase, since Prep1 is present in the nucleus and p160 in the nucleolus. During mitosis, p160 assumed a peculiar localization in a para-chromosomal area (see also later pictures), while Prep1 staining is more diffuse. Therefore there does not seem to be a significant co-localization during mitosis.

Then I tried to induce the translocation of p160 to nucleoplasm with different treatments: drugs that cause the inhibition of RNA-polymerase II transcription (hydroxyurea, α-amanitin, UV, cyclohexemide, anysomycin and actinomycin D), reticulum endoplasmic stress (thapsigargin, tunicamycin), temperature stress (4°C, 32°C, 42°C, 45°C), oxidative stress (H_2O_2, DTT), osmotic stress (H_2O, NaCl), low serum (2%, 0,2%) and proteasome inhibition with MG132 (Fig. 20A). Among these stresses, only Actinomycin D (ActD), an inhibitor of RNA polymerase I and of DNA replication [116,120], determined p160 translocation. After the treatment with 0.2 μM ActD for 1 hour a complete translocation of p160 to the nucleoplasm was visible and the effect was reversible (Fig. 20B). I

performed the same experiment by staining the cells for both Prep1 and p160. In physiological conditions the two proteins did not co-localize, as expected. However, after treatment with ActD there was a significant increase in the nucleoplasmic co-localization (Fig. 20C).

These experiments demonstrate that p160 can shuttle between nucleoli and the nucleoplasm and co-localizes with Prep1 only under conditions that inhibit the nucleolar function.

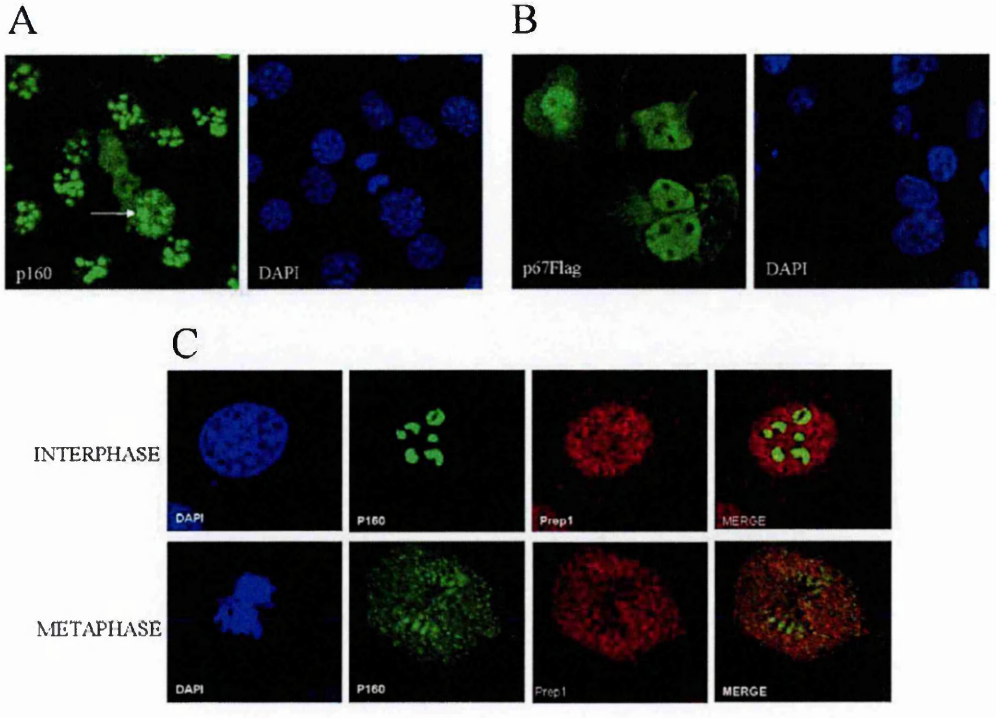

Fig. 19 Immunofluorescence study of p160 and Prep1 localization. (A) Confocal microscopy of NIH 3T3 cells after staining with anti-p160C antibody (left) and Hoechst 33258 for nuclei (right). The arrow shows a cell with both nuclear and nucleolar staining; most cells showed nucleolar staining only. **(B)** Confocal microscopy of NIH 3T3 cells transiently transfected with p67-Flag, after staining with anti-Flag (left) and Hoechst 33258 for nuclei (right); no nucleoli were positive for p67. **(C)** Confocal microscopy of NIH 3T3 cells stably transfected with p160-Flag and stained with anti-Flag (green), anti-Prep1 (red) and DAPI (blue) in interphase (upper part) or metaphase (bottom).

A

Hydroxyurea, 10 mM, 4 h	45°C, 20 min
α-amanitin, 10 µg/ml, 4 h	H2O2 100 µM, 2 h
UV, 20 J/m2	H2O2 300 µM, 2 h
Cyclohexemide, 10 µg/ml, 4 h	DTT 100 µM, 2 h
Anysomycin, 10 µg/ml, 4 h	DTT 300 µM, 2 h
Actinomycin D, 0,2µM, 1 h	Medium with 60% H2O, 2 h
THAPSIGARGIN 2,5 µg/ml, 6 h	NaCl, 150 mM, 4 days
TUNICAMYCIN 2,5 µg/ml, 6 h	2% serum, 24 h
4°C, 20 min	0,2% serum, 24 h
32°C, 4 h	MG132, 10 µM, 6 h
42°C, 4 h	

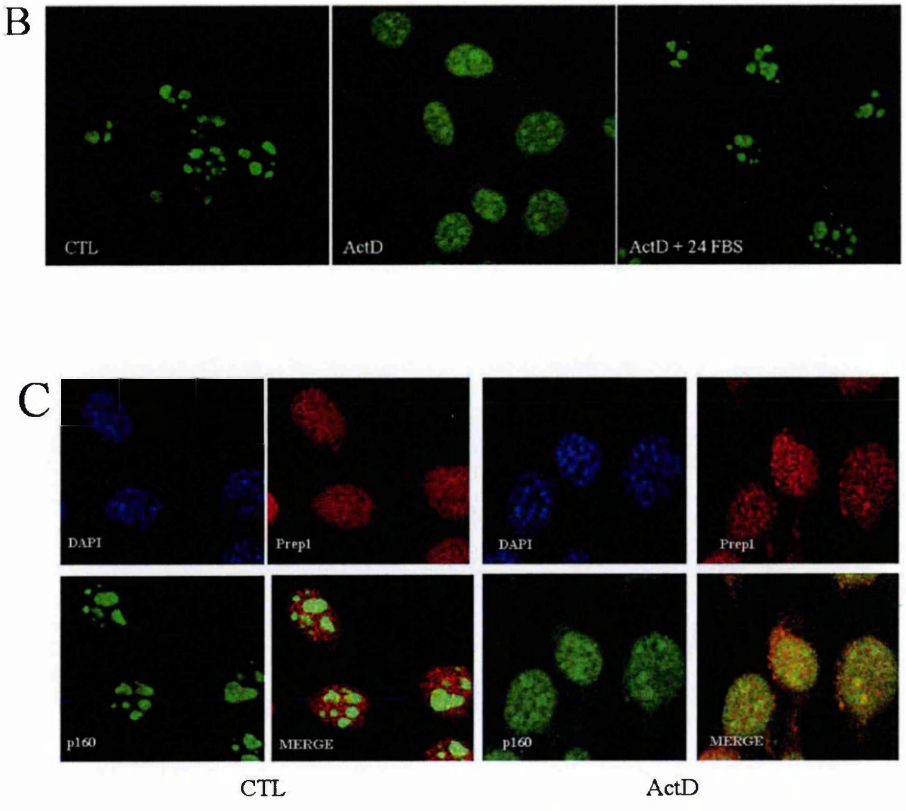

Fig. 20 ActD induces p160 translocation. (A) Summary of the stress stimuli used. **(B)** Confocal microscopy of NIH 3T3 cells, control or treated with 0,2 µM ActD for 1 h. ActD+24 FBS refers to cells treated with ActD as above, washed and left in complete DMEM for 24 h. Staining is with anti-p160C. **(C)** Confocal microscopy of NIH 3T3 cells, control or treated with 0,2 µM ActD for 1 h, stained with anti-p160C, anti-Prep1 and Hoescht 33258 for nuclei.

Since p160 and Prep1 co-localize after ActD treatment, this was the best condition to demonstrate the co-immunoprecipitation of the endogenous proteins. To perform this experiment I used F9 teratocarcinoma cells line since NIH 3T3 cells express very low level of Prep1 while NT2-D1 cells do not contain endogenous p160. F9 cells express good level of both proteins and can be also induced to express HoxB genes with RA [74,98]. After ActD treatment, F9 cells immunofluorescence showed the translocation of p160 in the nucleoplasm where it co-localized with Prep1 (Fig. 21A). ActD treatment induced also the co-immunoprecipitation of the two endogenous proteins (Fig. 21B). Thus, p160 and Prep1 co-localize and co-immunoprecipitate in the nucleoplasm after ActD treatment, while during mitosis it is still not clear. It is very interesting to notice that in untreated F9 cells a certain level of Prep1 is present also in nucleoli, as suggested by co-localization of the two proteins (Fig. 21A).

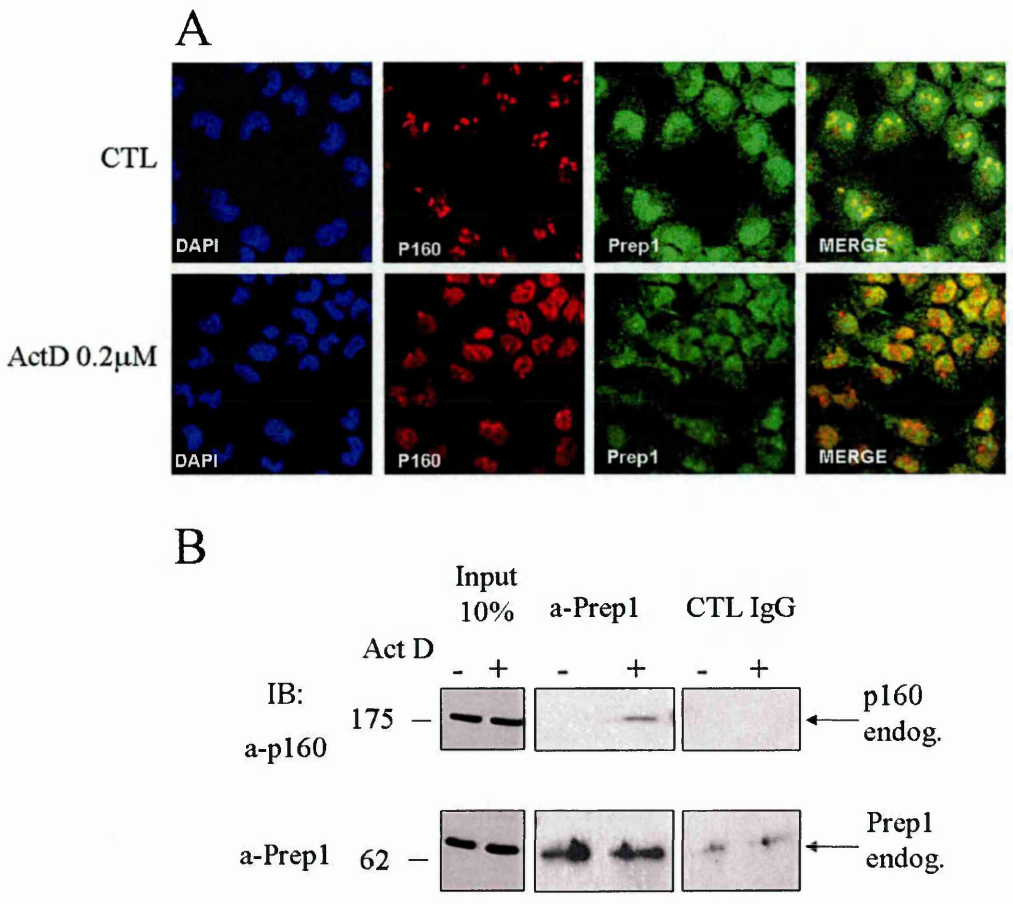

Fig. 21 Endogenous p160 and Prep1 co-localize in the nucleoplasm and co-immunoprecipitate after ActD treatment. (A) Confocal microscopy of F9 cells, control or treated with ActD 0,2 μM for 1 h; the staining was performed with anti-p160C, anti-Prep1 and DAPI for nuclei. **(B)** Co-immunoprecipitation of Prep1 and p160 from nuclear extract of F9 cell treated (+) or not (-) with ActD. The immunoprecipitation was performed with anti-Prep1 monoclonal antibody or control IgG and the immunoblot (IB) with anti-Prep1 and anti-p160C.

Summary of Results 1

In this first section I have shown that p160 is a new direct Prep1 interactor. p160 binds Prep1 at the level of HR1, in a leucine-rich region through its N-terminal part, the same binding region of Pbx. This indicates a competition between the two proteins in the binding to Prep1 and highlights the role of p160 as a Prep1 inhibitor, since, without Pbx, Prep1 cannot exert its transcriptional activity. I demonstrated also that Prep1 and p160 mostly interact in the nucleoplasm, even if the main p160 localization is in the nucleoli. However, the possibility that a minor fraction of Prep1 is localized in the nucleolus and can interact there with p160 or that only the small amount of p160 present in the nucleoplasm mediate this interaction cannot be excluded by my experiments. In fact, in one cell line (F9 cells), immunofluorescence shows that a portion of Prep1 is localized in the nucleolus.

The data presented in this section have been published in: Diaz V.M., Mori S., Longobardi E., Menendez G., Ferrai C., Keough R.A., Bachi A. and Blasi F. "p160 Myb-binding protein interacts with Prep1 and inhibits its transcriptional activity." Mol. Cell. Biol. 27(22), 7981-7990 (2007) [24].

2. Cell-cycle defects in p160-depleted cells

2.1 The nucleolar protein p160 distributes in a para-chromosomal region during mitosis

As already shown by immunofluorescence, p160 is localized in the nucleoli during interphase. Since nucleoli are disrupted at the beginning of mitosis, nucleolar proteins relocate from the nucleolus to other structures [11]. In particular, I observed a peculiar re-localization of p160 around the metaphasic plate (Fig. 22). I studied p160 localization during mitosis in detail by immunofluorescence confocal microscopy on NIH 3T3 cells, stably expressing p160-Flag synchronized by a double Thymidine block to enrich the mitotic population. I used this cell line because of the lack of a good antibody against p160 to use for immunofluorescence. Moreover, in this cell line the level of p160 was not higher than in the wild-type NIH 3T3 cell line (data not shown). As shown in Fig. 22, p160 localization varies within the cell-cycle: in prophase p160 is located on the condensed chromosomes, partly co-localizing with Tubulin, a major constituent of microtubules, essential for the constitution of the mitotic spindle. In metaphase and anaphase, p160 is located at the periphery of the metaphasic plate and, in particular, it accumulates in two regions on the side of the plate, separated from Tubulin. During telophase, p160 starts to re-populate the two daughter cells as pre-nucleolus-like foci and then, as soon as mitosis is completed, p160 redistributes in the newly formed nucleoli.

I then performed a co-staining experiment with anti-phospho-histone-H3 (PH3), a specific mitotic marker of chromosome condensation. As shown in Fig. 23, there is a

partial co-localization of the two proteins both in interphase and mitosis indicating that probably p160 is localized on DNA during mitosis. This confirms the observation made by Gassmann R., that p160 is located on chromosome arms during metaphase [38].

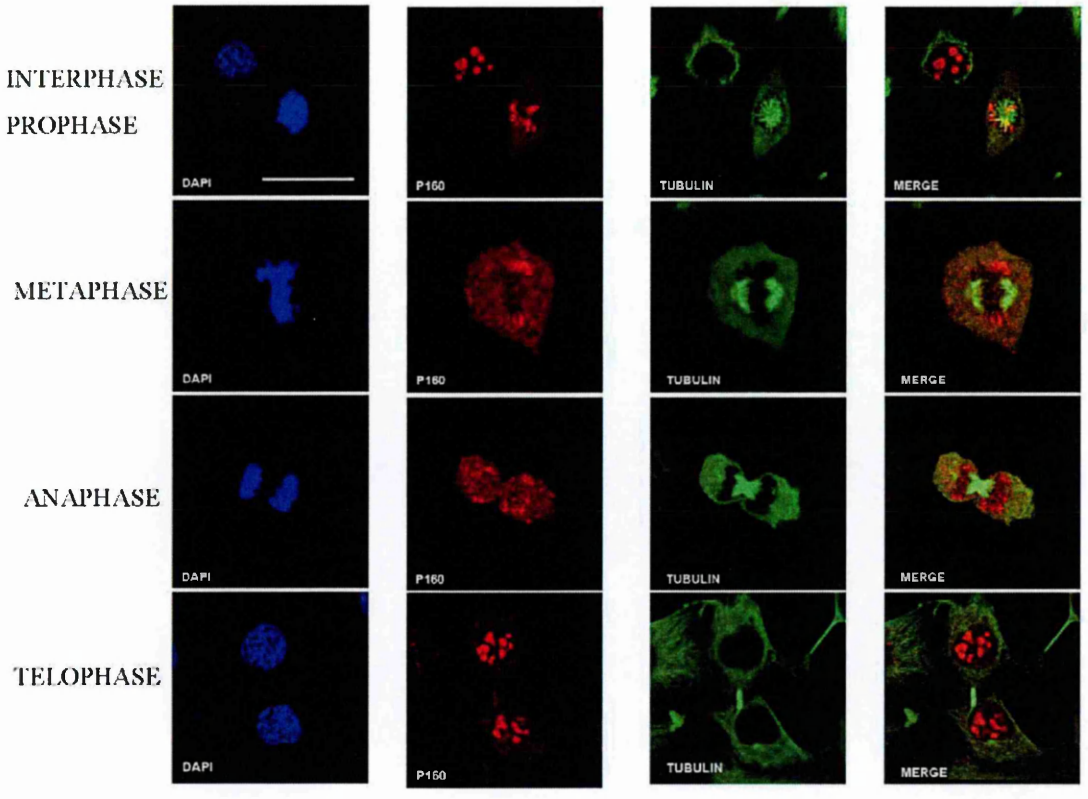

Fig. 22 p160 distribution during cell-cycle. Representative immunofluorescence confocal images of NIH 3T3 cells stably expressing p160-Flag in the mitotic phases indicated on the left. Cells were stained with antibodies against Flag (p160, red), α-Tubulin (green) and DAPI (blue) for DNA. Bar = 10 μm.

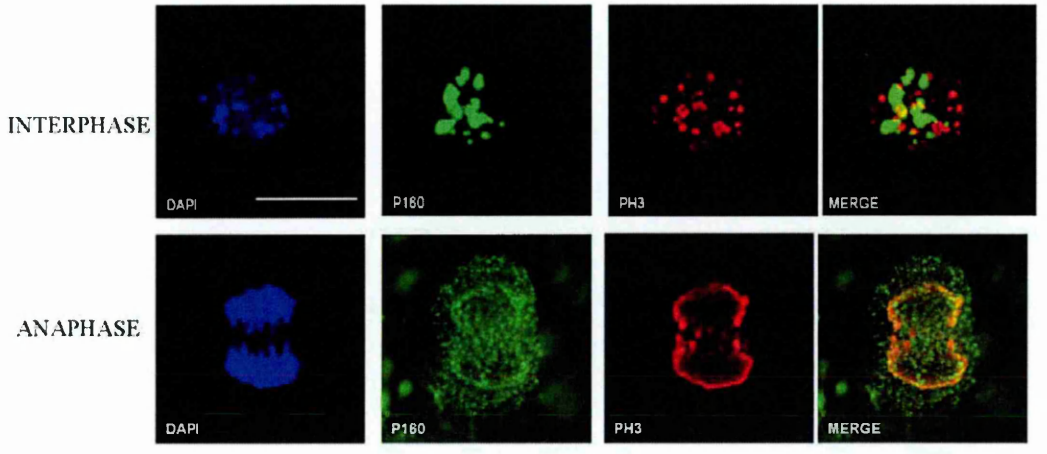

Fig. 23 p160 localizes on DNA during mitosis. Representative confocal images of NIH 3T3 cells expressing p160-Flag in the mitotic phases indicated on the left. The staining was performed with anti-Flag (p160, green), anti-Phospho-Histone-H3 (PH3, red) and DAPI (blue) for DNA. Bar = 5 μm.

From these studies, it was evident that p160 localizes in a para-chromosomal region during mitosis. I then tested the co-localization with other markers that are known to be directly present on DNA. Confocal immunofluorescence staining with CREST, an anti-serum directed against the inner kinetocore region, recognizing three constitutive centromere proteins CENP-A, -B, and –C, showed that p160 does not localize in the kinetocore region either in interphase or in metaphase (Fig. 24A). I also tested a possible localization of p160 on telomeres, the most distal region of chromosomes, performing an immuno-FISH. This particular technique allows to see the localization of proteins on specific DNA regions. I used a FISH probe (PNA) for telomeres and performed immunofluorescence against p160. The staining obtained for p160 with this technique was slightly different from the previous ones, but nevertheless showed the localization of p160 around the metaphasic plate in mitosis and demonstrated that p160 does not localize in the telomeric region (Fig. 24B).

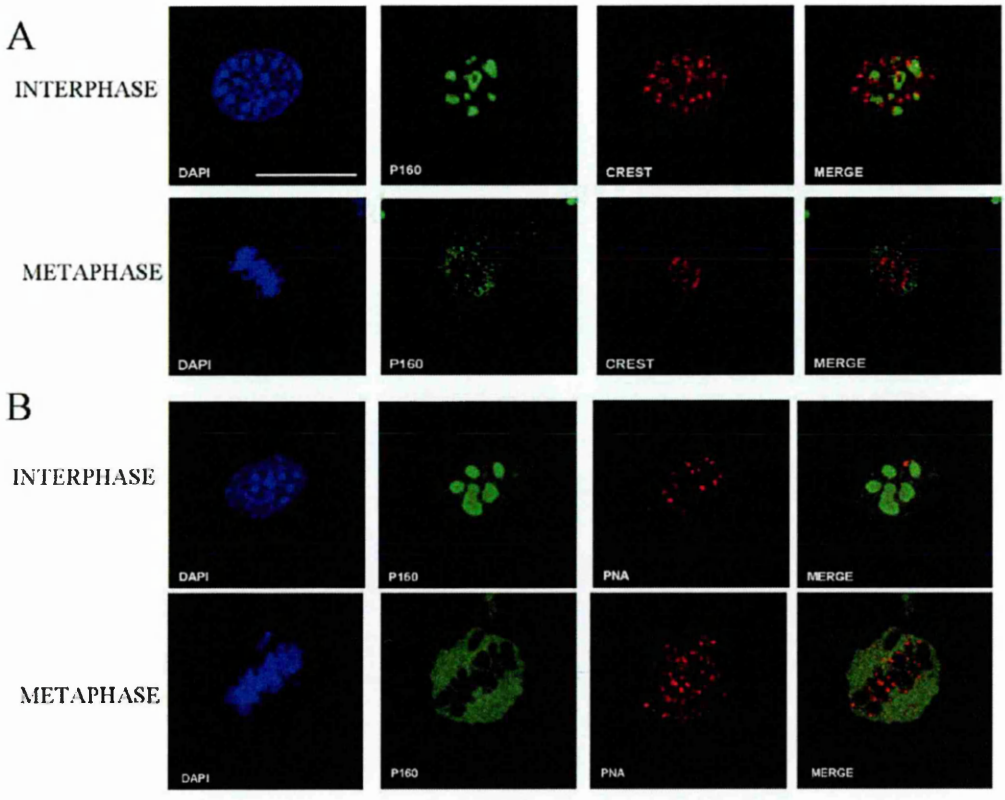

Fig. 24 p160 does not localize at the kinetocore or on telomeres. Representative confocal immunofluorescence of NIH 3T3 cells stably expressing p160-Flag in the mitotic phases indicated on the left. The staining was performed against Flag (p160, green), CREST (red, panel A), PNA (red, panel B) and DAPI (blue) for DNA. Bar = 5μm.

I then compared p160 staining with the localization of other nucleolar proteins which are known to be involved in mitosis. During mitosis, Nucleolin is located both at the chromosome periphery and at spindle pole and is important for correct chromosome alignment, segregation and spindle formation [77]. As shown in Fig. 25A, p160 co-localizes with Nucleolin at interphase, but not at metaphase. I also tested Nucleophosmin (NPM) that is essential for mitosis progression, since it is involved in proper chromosome alignment, spindle formation and centrosome duplication [2]. Also

p160 and NPM co-localize during interphase, but they also partially co-localize during metaphase (Fig. 25B).

In summary, these immunofluorescence studies show that p160 has a para-chromosomal localization during mitosis and is mainly concentrated on DNA. Therefore I investigated the role of p160 in the cell-cycle.

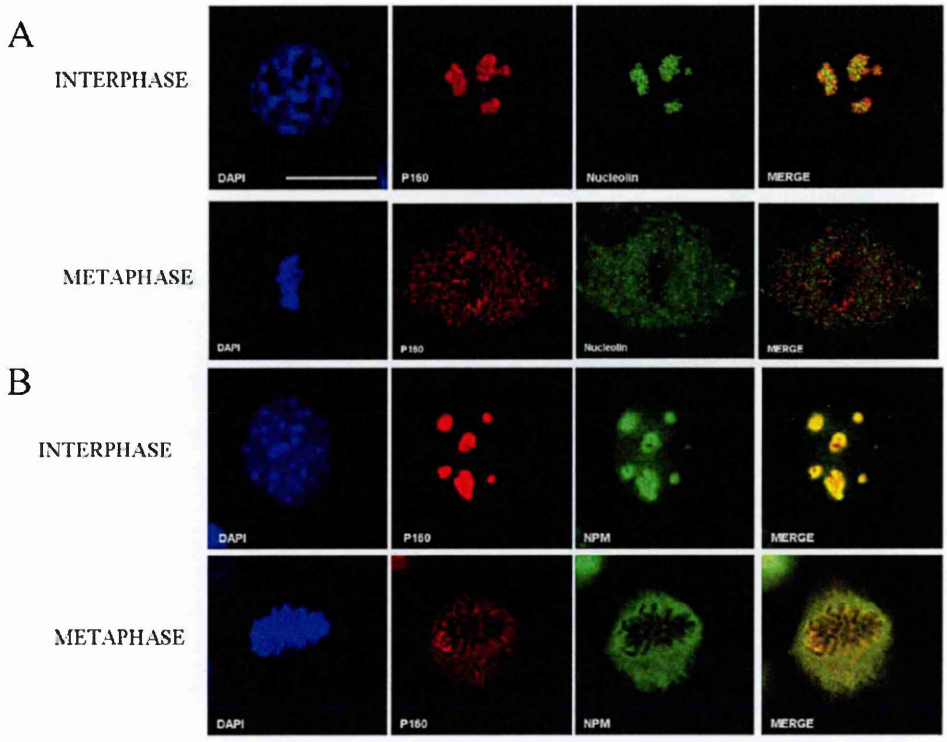

Fig. 25 Nucleolar proteins localization during cell-cycle. Representative confocal microscopy staining of NIH 3T3 cells stably expressing p160 at metaphase and interphase (indicated on the left of the panels). **(A)** Staining with anti-Flag (p160, red), anti-Nucleolin (green) and DAPI (blue) for DNA. **(B)** Staining with anti-Flag (p160, red), anti-Nucleophosmin (NPM, green) and DAPI (blue) for DNA. Bar = 5 μm.

2.2 p160 knock-down determines proliferation defects

To determine the function of p160 in cell-cycle, I inhibited its expression by a transfection with specific siRNA into HeLa cells. I chose HeLa instead of NIH 3T3 cells because I did not obtain good knock-down of the protein (only 50%) in the latter (see Results 3, for a more detailed description). Moreover, HeLa cells are a very good system to study the cell-cycle. I first tested p160 localization to confirm that p160 is nucleolar also in HeLa cells (Fig. 26A). Analyzing the p160 sequence I found three sequences that match all the requirements for siRNA (highlighted in Fig. 26B). I transiently transfected the three siRNAs oligonucleotides and measured the protein level, comparing them with control oligonucleotides (High-GC and Medium-GC, see Material and Methods) after 24, 48, 72 and 96 hours. The silencing was visible already at 24 hours but a major effect was obtained after 48 hours (Fig. 26C).

I checked the morphology of HeLa cells 48 hours after transfection in order to identify a possible phenotype. As shown in Fig. 27A, all the three siRNAs (and in particular siRNA1) induced high level of cell mortality and hence a lower number of cells.

I then measured the proliferation rate by counting the cells at 24, 48 and 72 hours after transfection and observed that with siRNA1 and 2 there was a consistent lower amount of cells at 48 and 72 hours compared to their High-GC control, while siRNA3 had a proliferation rate similar to its Medium-GC control (Fig. 27B). Overall, p160 knock-down decreased the proliferation rate and increased the number of dead cells.

A

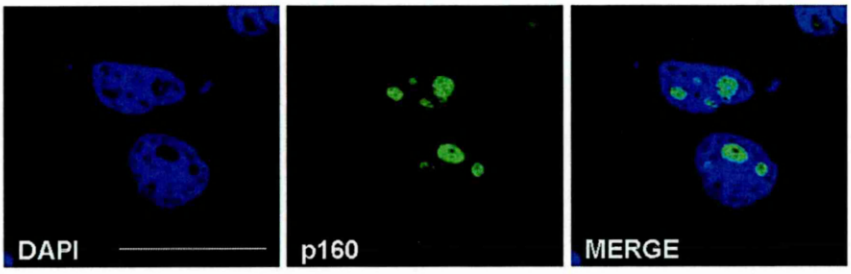

B

```
1     ctgacctgga agcggctggg gccggagcac acgtgtttcg tgtttcggtg agtgtggcgg
61    agatggagag ccgggatccc gcccagccga tgtcgcctgg agaagcgacg cagagtggcg
121   cccggcctgc cgaccgctat ggcctattga agcacagtcg cgagttcttg gacttcttct
181   gggacattgc gaagcctgag caggagacgc gacttgcggc cacggagaag ctgctggagt
241   atctgcgtgg caggccgaag gggtccgaga tgaaatatgc cctgaagcgt ctaatcacgg
301   gactcggggt cgggcgagaa acagcccggc cctgctacag tttggccctg gcacagctgt
361   tacagtcttt tgaagacctc cccttgtgca gcatcctgca gcagatacaa gaaaaatatg
421   acctgcatca ggtgaagaag gcaatgctga gacctgctct ctttgcaaac ctgtttggag
481   tgctcgccct ctttcagtca ggtcggctgg tgaaggacca ggaggcactg atgaagtcgg
541   tgaagctgct gcaggccctg gcccagtacc aaaaccactt gcaggagcag ccccggaagg
601   ccctggtgga catcctctcc gaggtctcga aggccacatt gcaggagatc ctgccggagg
661   tcctcaaagc cgacttgaat ataatactca gctcccctga acagctagag ctcttcctcc
721   tggcccagca gaaggtgccc tccaagctca agaagctggt gggatccgtg aacctattct
781   cagatgagaa tgtccccagg ctggtgaatg tgctgaagat ggccgcctcc tctgtgaaga
841   aggaccgcaa gctgcccgcc attgctctgg acctgctccg cctggcactc aaggaagaca
901   agttcccacg gttctggaag gaggtggtgg aacaagggct gctgaagatg cagttctggc
961   cagccagcta cctgtgtttc cgcctgctgg gcgcggccct gcccctgctg accaaggagc
1021  agctgcacct ggtgatgcag ggagacgtga tccgccatta cggggagcac gtgtgcactg
1081  ctaagctccc aaagcagttc aagtttgccc cagagatgga cgattacgtg ggcaccttcc
1141  tagaggggtg ccaggatgac cctgagcggc agctggccgt gctagtggcc ttctcatctg
1201  tcaccaacca aggcctccct gtcacgccta ctttctggcg ggtcgtgcgg ttcctgagcc
1261  ctccggccct gcagggctat gtggcctggc tgcgggccat gtttctccag ccagacctgg
1321  actccttggt tgacttcagc accaacaacc agaagaaagc ccaggattca tcgctccaca
1381  tgcctgagcg agctgtgttc cggctgagga aatggatcat ctttcgattg gtgagcattg
1441  tggacagcct gcacctggag atggaggagg ccttgactga gcaggtggcc aggttttgtt
1501  tgttccactc gttctttgtc acaaagaagc ccacatccca gatccctgag acaaagcacc
1561  cgttctcctt ccctttggaa aaccaggccc gagaggctgt cagcagtgcc ttcttcagtc
1621  tgttgcagac cctcagcacg cagttcaagc aggcaccggg ccagacccag ggtgggcagc
1681  cctggaccta ccacctggtg cagttcgcag acctcctgtt gaatcacagc cacaacgtga
1741  ccaccgtgac acccttcact gcgcagcagc gccaggcctg ggaccggatg ctgcagactc
1801  tgaaggagct ggaggcccac tccgcagagg ccagggctgc tgccttccag caccttctgc
1861  tcctcgtggg catccacctc ctcaagtccc ctgcagagag ctgtgacctg ctgggtgaca
1921  tccagacctg catcaggaaa agtctgggag agaagccccg ccggagccgc accaagacca
1981  tcgaccccca ggaacccccg tgggtagagg tgctggtgga gatcttgctg gccctgttgg
2041  cccagcccag ccacctcatg cgccaggtgg cccggagcgt gtttggccac atctgctccc
2101  acctgacccc gcgtgccctg cagctaattc tggatgtgct gaaccccgag accagtgagg
2161  atgagaatga ccgtgtggtg gtgacggacg attctgatga gcggcggctg aagggtgcag
…/5022
```

siRNA1, ctl=high GC

siRNA2, ctl=high GC

siRNA3, ctl=medium GC

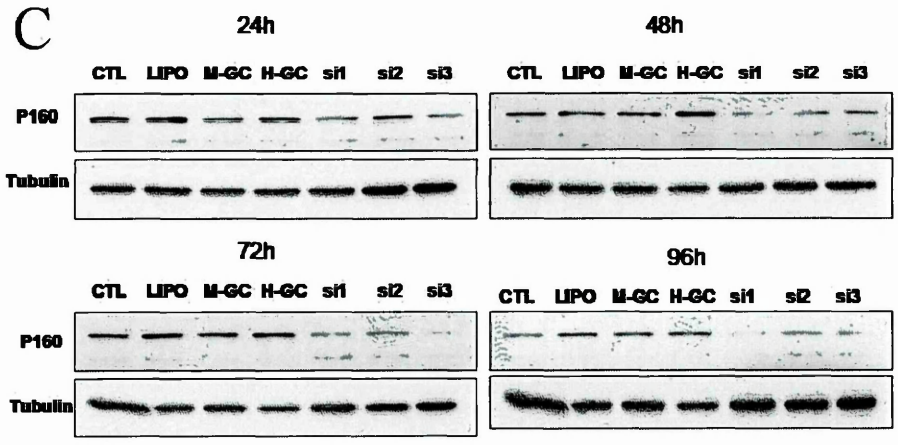

Fig. 26 p160 down-regulation in HeLa cells. (A) Representative confocal microscope image of HeLa cells: anti-p160 was used to stain p160 (green) and DAPI (blue) for DNA. Bar = 12 μm **(B)** Nucleotide sequence of human p160. siRNA sequences are highlighted and the specific controls for each sequence is indicated in the bottom part. **(C)** Western blot analysis of p160 in HeLa cells transiently transfected with siRNA for 24, 48, 72 and 96 hours. CTL, HeLa cells not transfected; LIPO, cells treated with lipofectamine only; M-GC, cells transfected with the control Medium-GC; H-GC, cells transfected with the control High-GC; si1, si2, si3 are HeLa cells transfected with siRNA1, siRNA2 or siRNA3 respectively. Tubulin is shown as loading control.

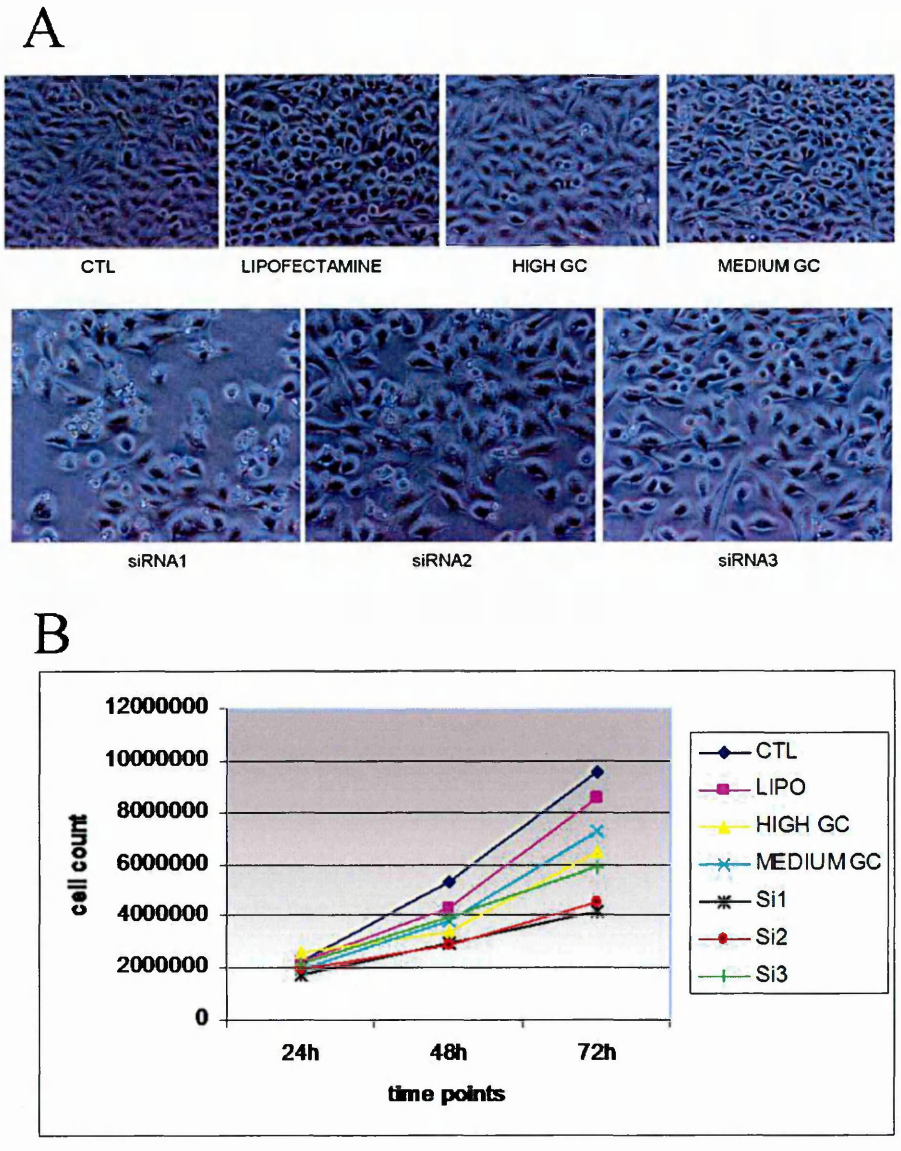

Fig. 27 p160-depleted HeLa cells grow slower than wild-type. (A) Representative images of HeLa cells 48 hours after transfection. Control untreated (CTL), lipofectamine treated, transfected with High-GC or Medium-GC controls and cells transfected with siRNA1, 2 or 3 are shown. **(B)** Measure of the proliferation rate in HeLa cells under the various conditions indicated. Cells were plated in triplicate the day before the transfection at 200000 cells/well (6 well plate) and counted 24, 48 and 72 hours later. The data are the average of three parallel experiments.

2.3 p160-depleted cells have a higher degree of apoptosis

I measured the apoptotic potential of HeLa cells 48 hours after transfection with p160 siRNAs. Annexin V positive cells (measured by Flow Citometry) at 48 and 72 hours were more abundant in HeLa cells treated with siRNAs than their controls. In particular, siRNA1 had three fold more early-apoptotic cells than its High-GC control (Fig. 28A). Similar results were obtained measuring late-apoptotic cells (Annexin V and 7-AAD positive cells, not shown). Since siRNA1 was the siRNA with the strongest phenotype, I used this one for the following experiments.

I also performed an immunoblot analysis to demonstrate apoptosis activation. I used total protein extract from HeLa cells transfected with siRNA1 or High-GC control at 48 hours. As shown in the immunoblot of Fig. 28B, there was an activation of Caspase 3 and Caspase 9 after p160 silencing. Therefore, the results show that p160 depletion induces apoptosis.

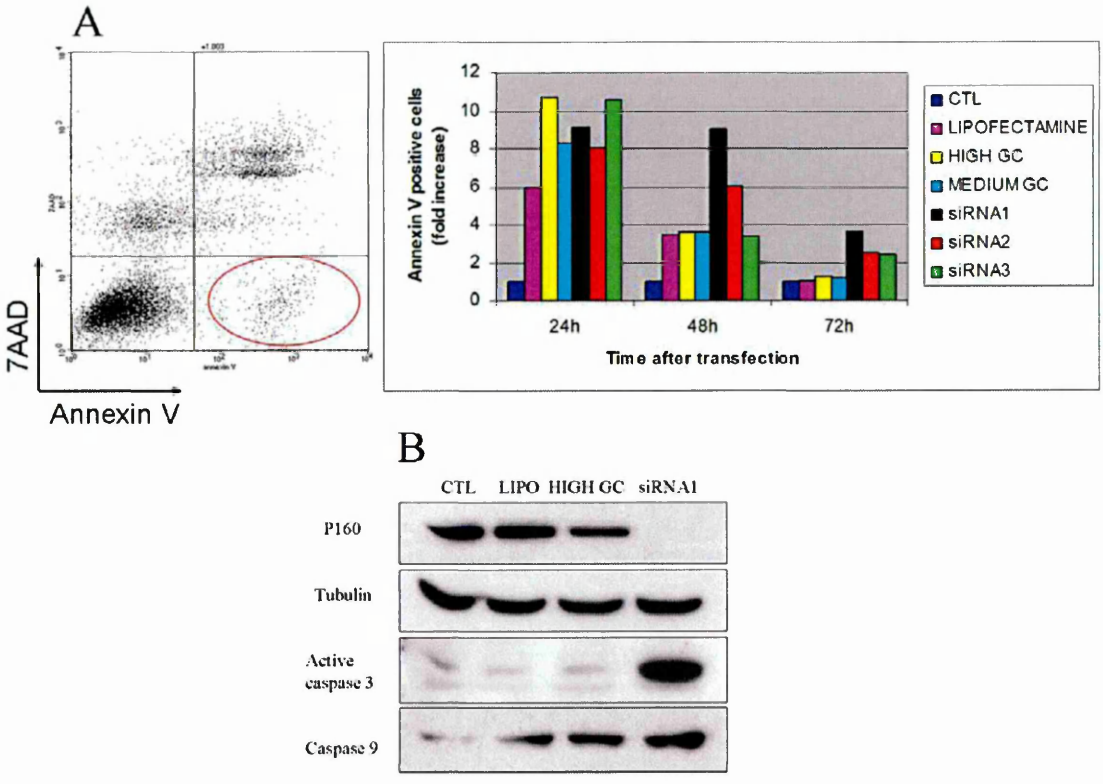

Fig. 28 p160 depletion induces an increase of apoptosis. (A) HeLa cells were transiently transfected for 24, 48 and 72 hours with the oligonucleotides and conditions indicated on the histogram to the right. The number of apoptotic cells was determined by Flow Citometry measuring Annexin V positive cells (early apoptotic cells, left panel, red gate). Control untreated cells were given the arbitrary value of 1. **(B)** Western-blot analysis of HeLa cells transiently transfected for 48 hours as follows: CTL (untreated cells), LIPO (treated with only lipofectamine), HIGH GC (transfected with High-GC control), siRNA1 (transfected with siRNA1). The immunoblot was performed with p160, active Caspase 3 and Caspase 9 antibodies; Tubulin is shown as loading control.

2.4 p160-depleted cells display a variety of the cell-cycle defects

2.4.1 p160-depleted cells accumulate in the G2/M phase of the cell-cycle

From all previous results I concluded that p160 might be important for cell-cycle regulation and/or cell division.

To explore the potential involvement of p160 in cell-cycle progression, I carried out a Flow Citometry analysis by labeling control (High GC treated) or silenced (siRNA1 treated) HeLa cells with 5-Ethynyl-2'deoxyuridine (EdU, a bromodeoxyuridine analog) and 7-amino-actinomycin D (7-AAD). EdU is a thymidine analog, which is incorporated into newly synthesized DNA strands in the S-phase, therefore its detection is useful to estimate the fraction of cells in S-phase; 7-AAD on the other hand detects total DNA. After a pulse with EdU, HeLa cells at 48 hours after transfection were stained with anti-EdU and 7-AAD. HeLa cells treated with siRNA1 showed a decrease of the number of cells in S-phase (22 instead of 27%) and an increase of those in G2/M-phase (13 vs 4%) compared to control cells (Fig. 29). This suggests a block in G2/M, before cell division.

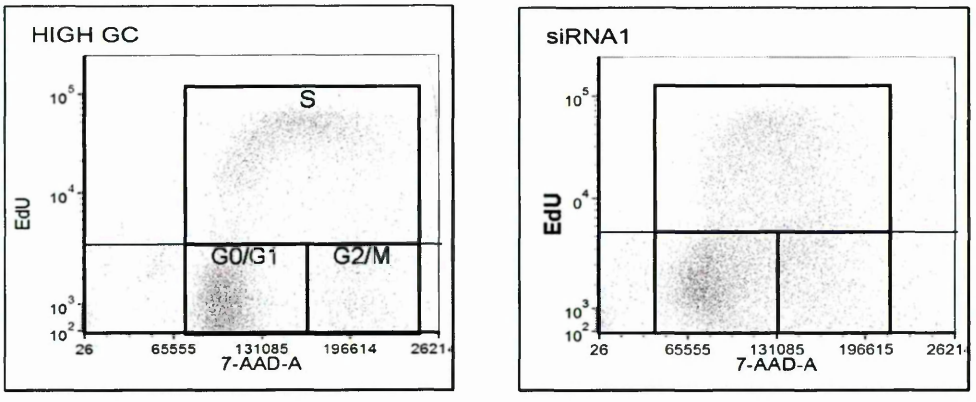

	HIGH GC	siRNA1
% G0/G1	51% ± 4,73	55% ± 4,90
% S	27% ± 4,82	55% ± 4,90
% G2/M	4% ± 1,17	13% ± 0,21

Fig. 29 Alteration in cell-cycle distribution in p160-depleted cells. HeLa cells transfected with control High GC or siRNA1 at 48 hours after transfection were pulse-labeled with EdU and then stained with anti-EdU and 7-AAD and analyzed by Flow Citometry to measure DNA synthesis (EdU-FITC, y axis) and DNA content (7-AAD, x axis). The EdU positive cells (S) and EdU negative (G0/G1 and G2/M) were analyzed by FCS express software (De Novo Software). The percentage of cells in each phase is shown in the table below the plots and is the mean of three independent experiments.

2.4.2 Mitosis structural alterations in p160-depleted cells

To focus on mitosis, I observed by confocal microscopy mitotic HeLa cells transfected with High-GC or siRNA1, after staining with anti-Tubulin antibodies (to identify mitotic spindle) and DAPI (to label DNA). As shown in Fig. 30A, p160-depleted cells have abnormal nuclear shapes, with nuclei smaller than control. Moreover, I measured by confocal microscopy the number of mitotic cells in the two populations: in p160-depleted HeLa cells there were twice as many mitotic figures than in control cells (Fig.

30B). In the same experiment I also counted the number of cells in the different mitotic phases. As shown in Fig. 30C, in p160 down-regulated cells there was a higher number of cells in prophase and metaphase compared to control (~60% vs ~40%), which indicates that there might be a delay in completing the mitotic process. From the above experiments and from the cell-cycle analysis, I conclude that p160 down-regulated cells are blocked or delayed before cell division.

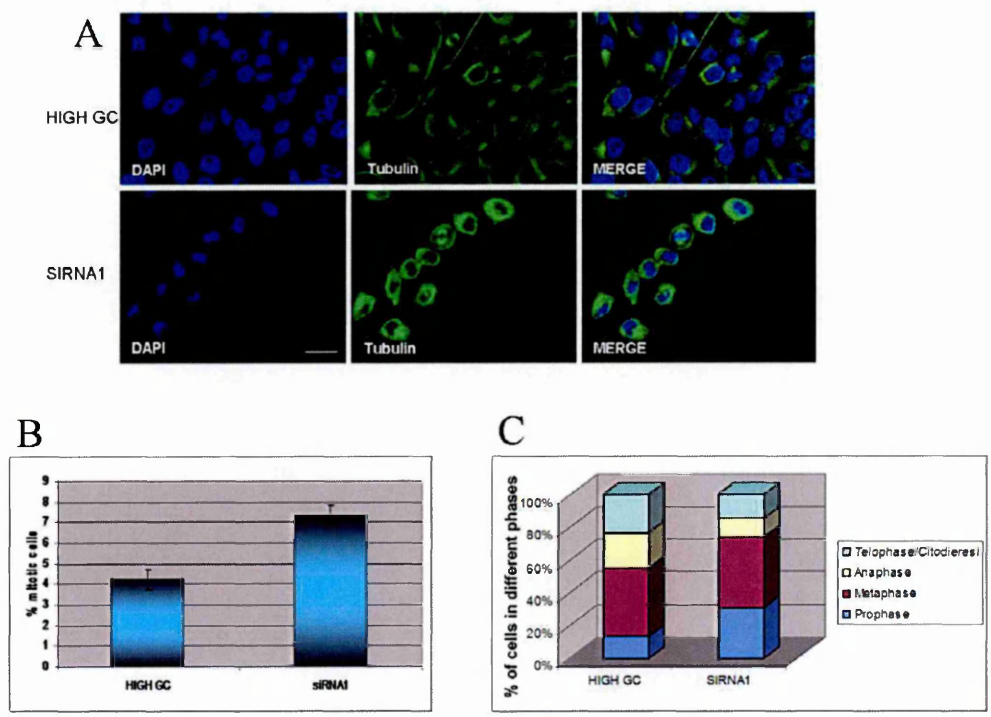

Fig. 30 Mitosis impairment in p160-depleted cells. (A) Representative confocal microscopy of HeLa cells control (High-GC) or silenced with siRNA1, 48 hours post-transfection. The staining was performed with anti-Tubulin (green) and DAPI (blue). Bar = 23,8 μM. **(B)** Count of mitotic cells after confocal microscopy imaging; cell count = 100. Error bars indicate standard deviation. **(C)** Count of cells in different mitotic phases after confocal microscopy imaging. Mitotic phases are indicated on the right; cell count = 100.

I then focused on the analysis of single mitotic figures and observed several alterations: multipolar spindle, incorrect organization of the metaphasic plate, division in three daughter cells, etc. (Fig. 31A). A quantitative analysis (based on the count of altered mitotic cells in control- and siRNA-transfected cells after synchronization by double thymidine block) showed a two fold higher number of altered mitotic cells in p160 depleted cells than in control (Fig. 31B). All these results lead to the conclusion that p160 is important for the mitotic process and that its absence determines impairment in the completion of the cell division process.

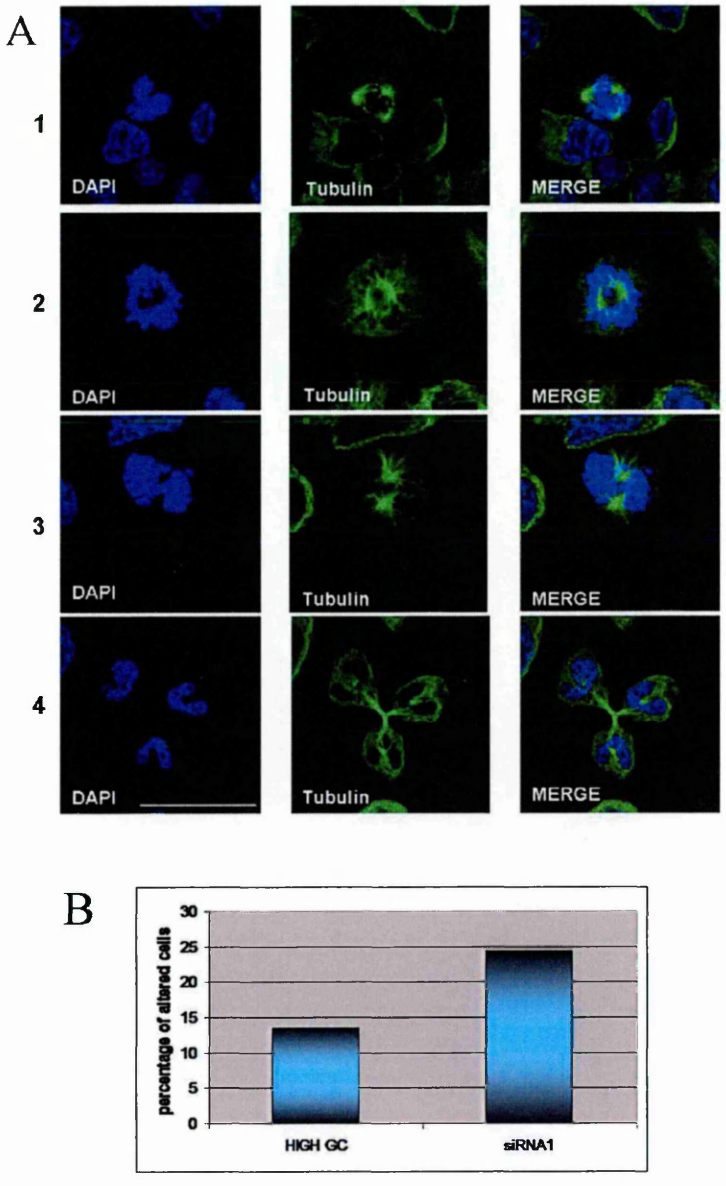

Fig. 31 p160 depletion determines mitotic alterations. (A) Representative confocal microscopy of HeLa cells transfected with siRNA1 for 48 hours. 1) multipolar spindle, 2) and 3) altered metaphasic plate, 4) abnormal cytodieresis. The staining was made against Tubulin (green) for mitotic spindle and DAPI (blue) for DNA. Bar = 12 μm. **(B)** Number of altered mitosis counted in confocal microscopy images. Cell count = 100.

2.5 In p160 silenced cells mitosis is slowed down

I monitored the mitotic process by Time-Lapse microscopy in order to measure the delay in mitosis completion. After transfection of HeLa cells with High-GC control or siRNA, I synchronized the cells with a double thymidine block and, after the release from the block, I examined the cells by Time-Lapse microscopy. Based on the analysis of 60 cells for each condition, the mitosis time in p160-silenced cells was ~90 minutes, while in control cells it was ~70 minutes (Fig. 32A and B). Another interesting observation was that among control cells almost 80% of the cells did divide with respect to only 40% of the silenced cells. Indeed, many cells (~ 30%) died or did not divide during the period analyzed (Fig. 32C). I conclude that p160 down-regulated cells have a longer mitotic time because of abnormalities in cell division and the majority died due to accumulation of mitotic alterations not compatible with life.

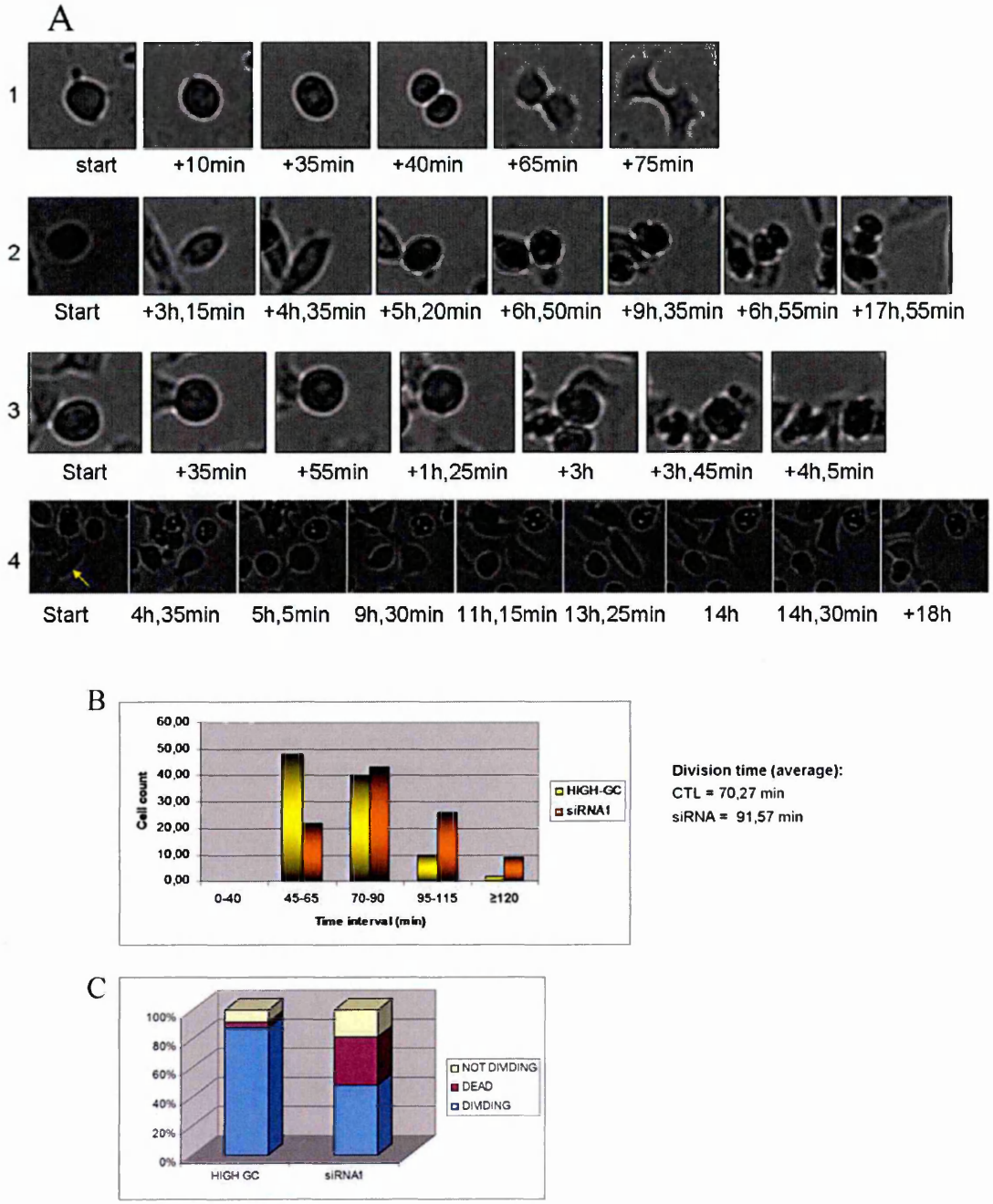

Fig. 32 p160-depleted cells have a longer mitotic time. (A) White-field Time-Lapse video imaging of HeLa cells transfected with siRNA1 for 48 hours and synchronized with a double thymidine block. Images were taken 8 hours after the release from the block (mitosis start) with Oko-Vision Time Lapse microscope for 18 hours; images were taken every 5 minutes. **(B)** Measure of mitotic time with Time-Lapse video imaging. Cell count = 40. **(C)** Percentage of cells dividing, not dividing or died during the period analyzed by Time-Lapse microscopy; cell count = 60.

2.6 No variability in karyotype for p160 down-regulated cells

Twenty-five metaphase spreads were analyzed and 10 karyotypes were elaborated for each cell line. The karyotypes from the HeLa cell line, both control and p160-silenced, had up to 83 chromosomes (ranging from 70 to 83; modal number 73). All samples were similar for chromosomal gains, losses and structural abnormalities. No significant variation in chromosome condensation or increase of chromatids and chromosomes breaks were observed independently of cell treatment, suggesting no effect of p160 silencing on chromosome number and structure (Fig. 33). An interesting point was that HeLa cells silenced and synchronized in mitosis had a five fold reduced number of metaphases (over 50 metaphases counted in the control, only 10 were found in silenced cells), indicating that p160-depleted cells have difficulties to enter in mitosis. This agrees with the above results. I conclude that the alterations induced by p160-depletion are most of the time lethal and therefore they do not apparently affect the karyotype.

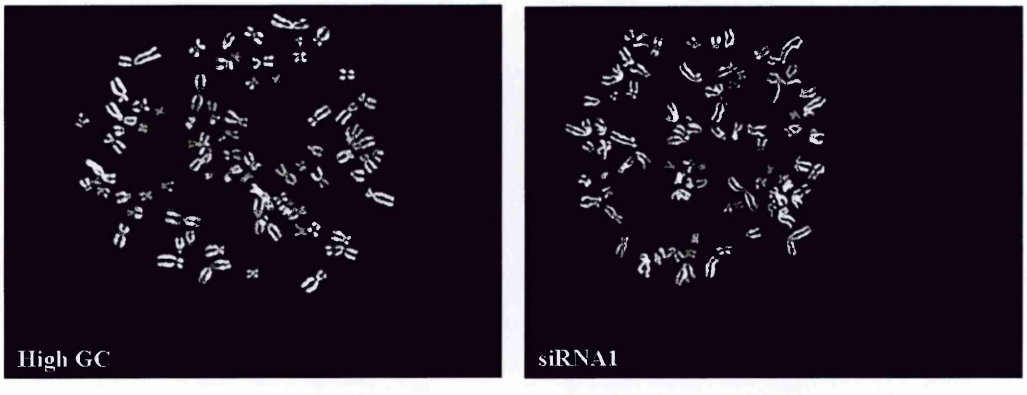

Fig. 33 p160-depleted HeLa cells do not show alterations in karyotype. Metaphasic spread of HeLa cell control (High-GC) and p160-depleted (siRNA1) are compared.

2.7 Gene expression profiling in p160-depleted HeLa cells

2.7.1 Microarray experiment

I performed a gene expression profiling analysis in order to investigate which pathways are altered after p160 silencing. I used Affimetrix microarrays to compare HeLa cells transfected with High-GC control or siRNA1 (three biological replicates for each condition) and I analyzed 28829 genes. After statistical analysis, I found 853 differentially expressed genes: 71,4% were down-regulated and 28,6% were up-regulated (Fig. 34A).

Total number of detected genes = 28829
Differentially expressed genes = 853 (2,96%)
Genes up = 244 (28,6%)
Genes down = 609 (71,4%)

Fig. 34 Statistical analyses of microarray experiment of control vs p160-depleted HeLa cells. In the table are indicated the number of genes analyzed and the differentially expressed genes found.

Once the differentially expressed genes were identified, I wanted to discern which molecular mechanisms and pathways were altered. I used the DAVID software and ran a functional annotation clustering of the differentially expressed genes in p160-depleted HeLa cells. For this analysis I considered only the categories with Benjamini value $\leq 10^{-3}$ statistically significant. Fig. 35A and C shows the main biological processes involved,

while in Fig. 35B and C are shown the main cellular components. The majority of the differentially expressed genes is involved in cell-cycle and mitosis (~56%), but DNA-damage and stress response (~11,5%) and apoptosis (~19,2%) are also highlighted. This result is also confirmed by the main cellular components involved that are: chromatin, nucleus, mitotic structures and microtubules (~49,8%) (Fig. 35 C). What clearly emerges from further analyses is that p160 is involved in the cell-cycle, in particular in the mitotic process. My interpretation is that without p160 cells try to divide and proliferate but are blocked at the stage of metaphase and thus are directed to apoptosis.

A

Category	Term	RT	Genes	Count	%	P-Value	Benjamini
GOTERM_BP_FAT	cell cycle	RT		72	9,3	1,4E-10	3,5E-7
GOTERM_BP_FAT	cell cycle process	RT		57	7,4	8,1E-10	1,0E-6
GOTERM_BP_FAT	cell cycle phase	RT		44	5,7	2,2E-8	1,8E-5
GOTERM_BP_FAT	chromosome organization	RT		48	6,2	4,1E-8	2,6E-5
GOTERM_BP_FAT	mitotic cell cycle	RT		40	5,2	6,8E-8	3,4E-5
GOTERM_BP_FAT	cellular response to stress	RT		52	6,7	1,1E-7	4,7E-5
GOTERM_BP_FAT	chromosome segregation	RT		17	2,2	1,5E-7	5,5E-5
GOTERM_BP_FAT	sister chromatid segregation	RT		12	1,6	1,7E-7	5,3E-5
GOTERM_BP_FAT	organelle fission	RT		28	3,6	8,4E-7	2,3E-4
GOTERM_BP_FAT	mitotic sister chromatid segregation	RT		11	1,4	1,2E-6	3,1E-4
GOTERM_BP_FAT	mitosis	RT		27	3,5	1,3E-6	2,9E-4
GOTERM_BP_FAT	nuclear division	RT		27	3,5	1,3E-6	2,9E-4
GOTERM_BP_FAT	M phase of mitotic cell cycle	RT		27	3,5	1,8E-6	3,8E-4
GOTERM_BP_FAT	response to DNA damage stimulus	RT		37	4,8	1,8E-6	3,5E-4
GOTERM_BP_FAT	cell death	RT		55	7,1	1,3E-5	2,3E-3
GOTERM_BP_FAT	cell division	RT		30	3,9	1,3E-5	2,2E-3
GOTERM_BP_FAT	death	RT		55	7,1	1,5E-5	2,4E-3
GOTERM_BP_FAT	M phase	RT		32	4,2	1,5E-5	2,3E-3
GOTERM_BP_FAT	microtubule-based process	RT		27	3,5	1,7E-5	2,3E-3
GOTERM_BP_FAT	programmed cell death	RT		47	6,1	5,5E-5	7,2E-3
GOTERM_BP_FAT	apoptosis	RT		46	6,0	7,8E-5	9,7E-3
GOTERM_BP_FAT	intracellular transport	RT		49	6,4	7,9E-5	9,4E-3
GOTERM_BP_FAT	cell cycle arrest	RT		15	1,9	8,0E-5	9,1E-3

B

Category	Term	RT	Genes	Count	%	P-Value	Benjamini
GOTERM_CC_FAT	intracellular non-membrane-bounded organelle	RT		155	20,1	5,7E-8	2,6E-5
GOTERM_CC_FAT	non-membrane-bounded organelle	RT		155	20,1	5,7E-8	2,6E-5
GOTERM_CC_FAT	chromosome	RT		44	5,7	1,9E-7	4,4E-5
GOTERM_CC_FAT	membrane-enclosed lumen	RT		114	14,8	1,8E-6	2,8E-4
GOTERM_CC_FAT	microtubule cytoskeleton	RT		46	6,0	3,8E-6	4,3E-4
GOTERM_CC_FAT	organelle lumen	RT		110	14,3	6,5E-6	5,8E-4
GOTERM_CC_FAT	chromosomal part	RT		35	4,5	1,4E-5	1,0E-3
GOTERM_CC_FAT	intracellular organelle lumen	RT		106	13,7	1,9E-5	1,2E-3
GOTERM_CC_FAT	nuclear lumen	RT		90	11,7	2,2E-5	1,3E-3
GOTERM_CC_FAT	microtubule organizing center	RT		25	3,2	8,1E-5	4,1E-3
GOTERM_CC_FAT	centrosome	RT		23	3,0	9,6E-5	4,3E-3
GOTERM_CC_FAT	nucleoplasm	RT		59	7,7	1,2E-4	4,9E-3
GOTERM_CC_FAT	chromatin	RT		21	2,7	1,5E-4	5,8E-3
GOTERM_CC_FAT	condensed chromosome	RT		16	2,1	2,0E-4	6,9E-3
GOTERM_CC_FAT	spindle	RT		17	2,2	2,7E-4	8,5E-3

C

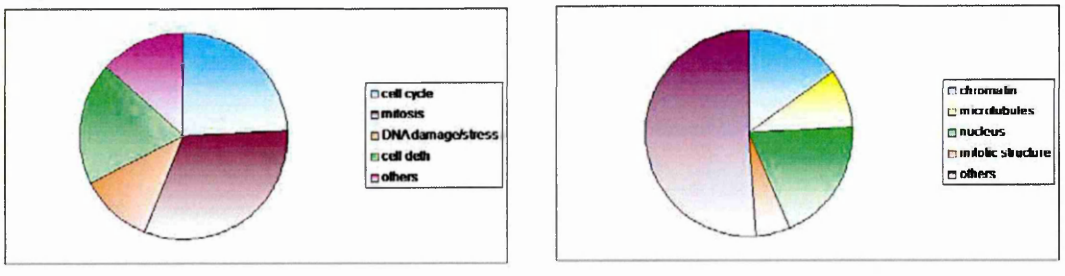

Fig. 35 Functional annotation clustering of the significantly regulated genes in p160-depleted HeLa cells. Functional clustering was performed with DAVID software. To rank their biological significance, the p-value was used. "Counts" is the number of differentially regulated genes within each cluster. **(A)** In this table are listed the main biological processes altered. **(B)** In this table are annotated the main cellular components altered. **(C)** Schematic representation of the biological processes (left) and cellular components (right). These diagrams were obtained grouping the clusters in the categories indicated on the right of each diagram.

2.7.2 Validation of Gene Expression experiment by Real-Time PCR

I focused then on the single genes de-regulated in these categories and validated some of them to confirm the microarray experiment. I tested six genes among either p160 interactors, genes involved in cell-cycle regulation or DNA damage response (Table III).

Table III. Selection of genes differentially expressed in p160-depleted HeLa cells vs control HeLa cells. Genes in bold are the ones selected for Real-Time PCR.

Gene Symbol	Fold Change (silenced vs control)	Molecular function
P160	**-4,13**	
JUN	**3,03**	Repressed by p160; transcription factor; frequently altered in human cancer.
NFKB2	**2,12**	Repressed by p160; transcription factor.
CDKN1A	**4,3**	Cyclin-dependent kinase inhibitor (i.e. cyclin-CDK2 or 4); regulates G1/S transition: in stress condition block cell before S-phase.
RBL2	-2	Involved in G1/S transition regulation.
RBBP8	-2,97	Binds Rb and regulates cell proliferation.
MAPK9	-2,16	Serine/threonine kinase activity; it mediates stress response.
TGFβ2	2,02	Involved in proliferation, differentiation, cell-cycle progression and apoptosis.
AKAP	-2,9	Involved in apoptosis.
VAV3	-2,89	Involved in apoptosis and cytokinesis.
GADD45A	2,13	Induced in response to stress and DNA-damage.
GADD45B	**2,69**	
TOP2A	-2,16	Required for correct chromosome condensation, chromatids separation and thus to prevent DNA-damage.
TOP2B	**-3,4**	
TP53BP2	-2,3	Regulates apoptosis and cell growth.
WRN	-2,5	Nucleolar protein involved in double-strands breaks repair.

With the same RNA preparation used for the microarray experiment I ran a Real-Time PCR for p160 (Fig. 36) and confirmed that it was 80% down-regulated. I also checked JUN and NF-kB2, known to be repressed by p160 [32,97]; these proteins are also important for cell proliferation and indeed are overexpressed in coincidence with p160 silencing. I checked CDKN1A that encodes a cyclin-dependent kinase inhibitor and regulates the G1/S transition; GADD45B was also tested because is an important mediator in DNA damage response and TOP2B, a topoisomerase involved in chromosomes condensation and chromatids separation. Real-Time PCR confirmed that CDKN1A and GADD 45B were increased and TOP2B was decreased in p160-depleted cells. These data overall confirm the down-regulation of p160, the strong decrease in its associated transcriptional activity, the block of the cell-cycle and the induction of DNA or chromosome damage with the activation of the DNA-damage response.

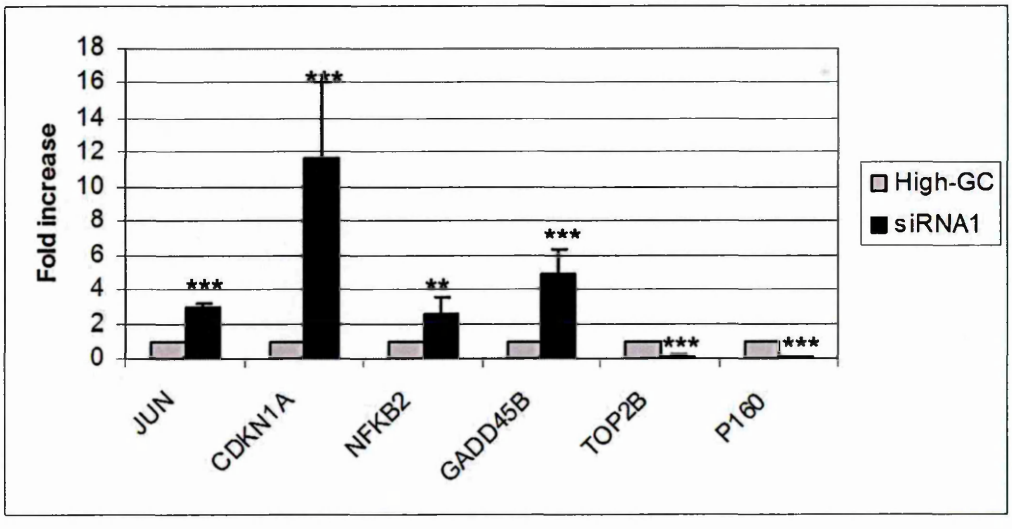

Fig. 36 Gene expression profile by Real-Time PCR. Real-Time PCR was performed on control (High-GC) or p160-depleted HeLa cells (siRNA1) with the same RNA samples used for the microarray experiment. Two biological replicates were used for each condition and the experiment was performed in triplicate; control levels (CTL) were given the arbitrary value of 1. The bars indicate standard deviation and ** means $p \leq 0,01$ while ***, $p \leq 0,001$ (t test).

Summary of results 2

In this second section I have demonstrated that p160 distributes in a para-chromosomal region during mitosis and that is involved in the mitotic process. In fact, after p160 depletion cells showed a lower proliferation rate, a higher degree of apoptosis, accumulation in G2/M phase of cell-cycle with structural alterations in mitosis and a slower mitotic rate. A surprising result was the "apparently" normal karyotype but, since wild-type HeLa cells present an altered number of chromosomes and many alterations, it was also difficult to underline a difference between the samples analyzed. Moreover gene expression profiling demonstrated that without p160 many genes involved in cell-cycle regulation, DNA damage, mitosis and cell death are de-regulated, highlighting an important role of this protein as a late cell-cycle regulator.

The data presented in Fig. 33 were obtained through a collaboration with L. Pecciarini (Pathology Unit of San Raffaele Hospital, Milan, Italy) and Fig. 34 from the Microarray Facility of Cogentech (IFOM, Milan, Italy).

3. Role of p160 in tumorigenesis

3.1 Fifty percent reduction of p160 does not result in changes in the cell-cycle

I demonstrated that a strong down-regulation of p160 impairs the cell-cycle and determines cell death. A condition in which the reduction of p160 was lower, compatible with life, might help to better understand the role of this protein. Since NIH 3T3 cells silenced for p160 with five different shRNAs never gave a reduction of the protein of more than 50%, I used this to model the "heterozygous" condition. Fig. 37A shows the immunoblot against p160 of NIH 3T3 cells stably infected with five different p160 shRNAs. shRNA1 and 3 were performing better, giving more or less fifty percent reduction of the protein (61 – 55% p160 reduction). I tested shRNA1 for cell-cycle distribution and apoptosis in order to compare these cells with p160-depleted HeLa cells. In Fig. 37B it is shown a bivariate FACS analysis using EdU incorporation and 7-AAD staining on NIH 3T3 cells treated with the non-target vector (NT) or with shRNA1. After EdU pulse, NIH 3T3 cells were stained with anti-EdU to detect EdU incorporation, and with 7-AAD to detect total DNA. shRNA1 treated cells showed no differences in cell-cycle distribution compared to their control. I also performed an Annexin V staining on the same population and analyzed by FACS the number of apoptotic cells (Annexin V positive cells). As shown in Fig. 37C, there were no significant differences between non-target control and p160 shRNA. In conclusion, NIH 3T3 cells with a fifty percent reduction of p160 level show no differences in cell-cycle.

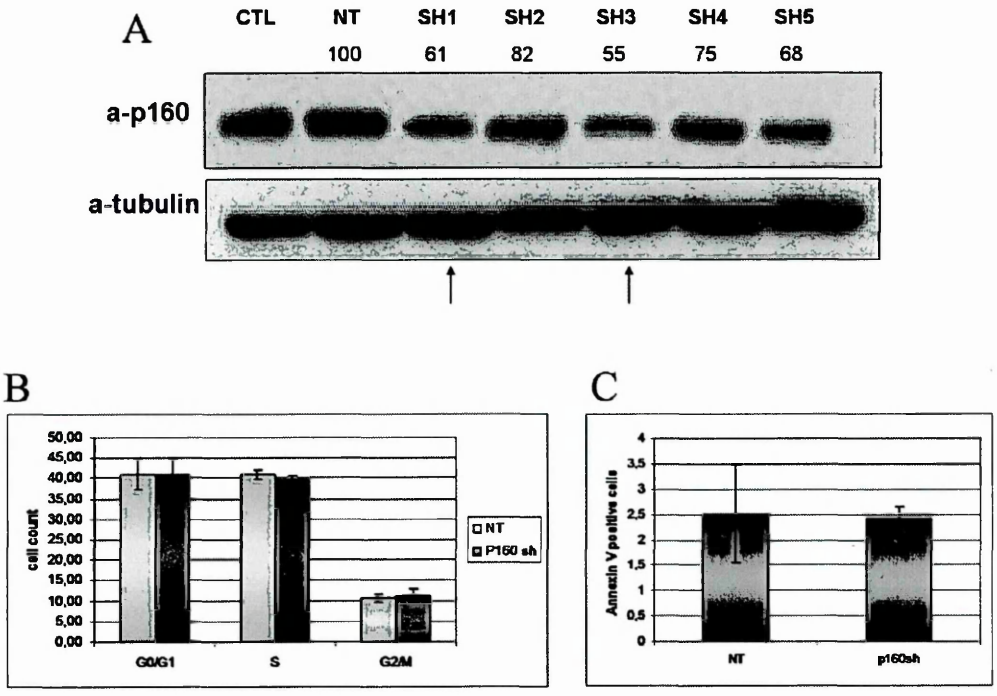

Fig. 37 p160 down-regulated NIH 3T3 cells show no changes in cell-cycle. (A) Immunoblot analysis of NIH 3T3 cells not infected (CTL), infected with non-target (NT), or with shRNA1,2,3,4,5 lentiviral vectors (SH1,2,3,4,5 respectively). Total protein extracts were immunoblotted against p160 and tubulin as loading control. The numbers on the top of the immunoblot indicate the amount of the protein quantified after densitometric analysis; values were compared to NT, non-target control (100%). **(B)** Cell-cycle distribution in NIH 3T3 cells infected with non-target vector (NT) or shRNA1 (p160sh) measured with EdU and 7-AAD incorporation by FACS analysis. **(C)** Measure of the number of apoptotic cells (Annexin V positive cells) by Flow Citometry in NIH 3T3 cells control (NT) or silenced with shRNA1 (p160sh). Error bars indicate standard deviation.

3.2 A small reduction in p160 level favors cell transformation

It is already published for other nucleolar proteins that a fifty-percent reduction of their level induces accumulation of genetic alterations (chromosomal rearrangements, deletions, etc.) that favor cell transformation. This was well demonstrated for Nucleophosmin (NPM) where in the heterozygous $NPM^{+/-}$ mice there is genomic

instability (for incorrect centrosome duplication) that favors cell transformation. Moreover, all human tumors with rearrangements/deletions in the NPM1 locus express half the amount of NPM [43]. I performed a literature search for tumors associated with p160. Using the Mitelman database (http://cgap.nci.nih.gov/Chromosomes/Mitelman) I found that the p160 locus was translocated in 406 human tumors and that the most recurrent type of tumors were leukemias (148) and lymphomas (82). The locus for p160, 17p13.3, is also frequently deleted in solid tumors [61]. I thought that also in NIH 3T3 cells with fifty-percent less p160 there might be genomic instability favoring cell transformation. I first performed a karyotype analysis on control or p160 down-regulated (shRNA1) NIH 3T3 cells but also in this experiment (like for the HeLa karyotype) I did not detect any significant difference between the two populations (data not shown), probably due to an already altered karyotype.

I decided anyway to study tumorigenesis in this "heterozygous" cell line. NIH 3T3 cells are a good system to study oncogene-induced tumorigenesis and can be transformed by active Ras alone (while non-immortalized cells require the action of two oncogenes). If p53 is diminished (and this happens when an oncosuppressor is absent), the transformation induced by Ras is even stronger. I studied proliferation in NIH 3T3 cells infected with control non-target and shRNA1 and 3 (the two constructs performing better) with and without the Ras-Val12 oncogene. I measured cell proliferation with a crystal violet assay counting the cells every 2 days for 10 days. As shown in Fig. 38, in the absence of Ras, shRNA1 and 3 treated cells proliferated faster than control, especially shRNA3 ($p < 0,001$ at 10 days). Upon infection of the cells with Ras-Val12, shRNA3 induced a significant increase in cell proliferation ($p < 0,001$).

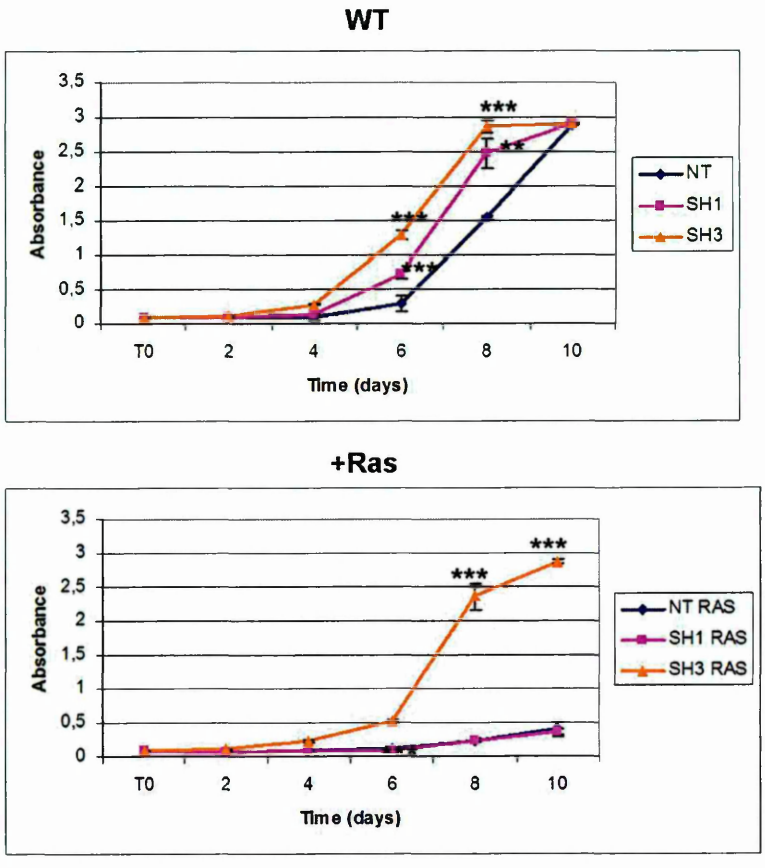

Fig. 38 p160 down-regulated NIH 3T3 cells proliferate more than wild-type. Growth curve of control NIH 3T3 cells infected with non-target (NT), shRNA1,3 (SH1,3) and Ras-Val12 infected cells (bottom panel). Crystal violet assay performed for 10 days counting the cells in triplicate every 2 days. **, $p \leq 0,01$; ***, $p \leq 0,001$ (t test).

I performed also a soft agar assay to test whether p160 also favors the formation of colonies in agar. I analyzed non-target shRNA (NT), shRNA1 and shRNA3 infected or Ras-Val12 and shRNA double-infected NIH 3T3 cells. In the first experiment, plating 50,000 cells in each well in triplicate (Fig. 39A), Ras induced colony formation both in NT and shRNA treated cells already at 9 days after plating. However, the number of colonies was significantly higher in NIH 3T3 cells with a lower level of p160 (shRNA1

and 3). I repeated the experiment plating a lower number of cells: 5,000 cells in each well, using the same cell lines, and in parallel I also infected NIH 3T3 cell with Myc. As shown in the histogram in Fig. 39B, 15 days after plating there were almost no colonies in the untreated samples while in Ras and even more in Myc infected cells there was a significant number of colonies, especially in the shRNA samples.

All these data confirm that a lower amount of p160 in the cells favors cell transformation and that this effect is generalized and not only linked to Ras over-expression. Overall, the data could indicate that p160 has a tumor suppressor function.

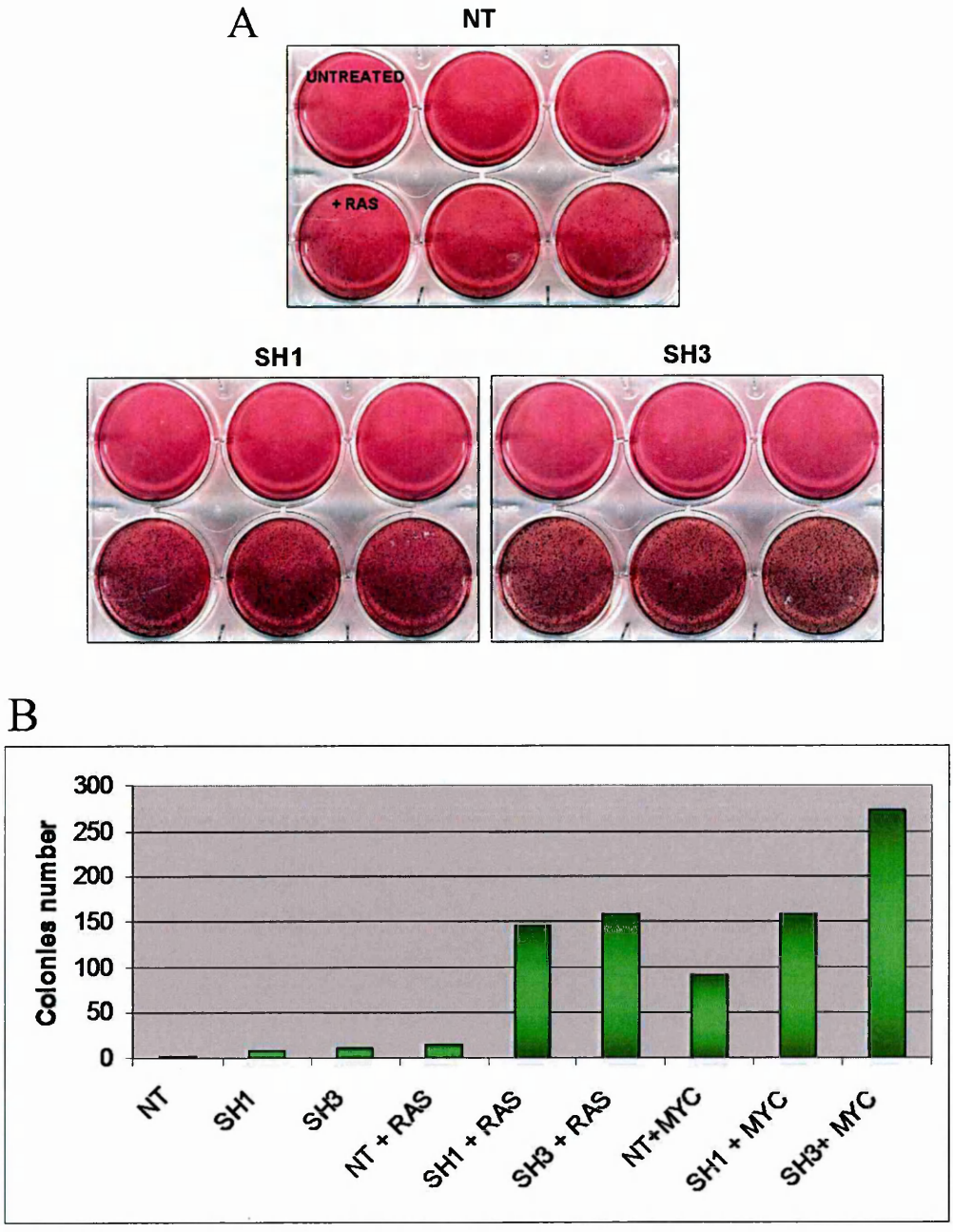

Fig. 39 A reduction in p160 level favors cell transformation. (A) Soft agar colony assay with NIH 3T3 cells infected with NT, shRNA1 or shRNA3 vectors with or without a co-infection with Ras-Val12. 50,000 cells were plated in triplicate and the images were taken 9 days after plating. **(B)** Histogram that summarizes the soft agar colony assay performed with NIH 3T3 cells infected with NT, shRNA1 or shRNA3 with or without a co-infection with Ras-Val12 and Myc. 5,000 cells were plated in triplicate and colonies were counted after 15 days using Image J software.

Summary of Results 3

In this last section I showed that a fifty percent reduction in p160 level favors NIH 3T3 cell proliferation and transformation. In fact, this condition increases the proliferation in association with Ras, and results in the formation of a large number of colonies in soft agar when there is an overexpression of Ras or Myc oncogenes. This highlights a possible role of p160 as a tumor suppressor. It is very interesting to notice that p160 is an interactor of Prep1, which is also a tumor suppressor [75]. It will be important, therefore, to verify the cell-cycle dependence of the Prep1-p160 interaction.

The data presented in this section are unpublished.

DISCUSSION

p160 myb binding protein 1a is a nucleolar protein, the function of which is largely unknown. The presence in its structure of many leucine-charged domains and leucine-zipper-like domains, involved in protein-protein interaction, justifies the finding that transcription factors (e.g. c-myb) are among its interactors [124]. p160 is a ubiquitous protein, highly conserved among species, that shares a high degree of similarity with yeast POL5, a nucleolar protein involved in rRNA synthesis [119]. Another interesting feature of p160 is its localization on human chromosome 17p13.3, a region frequently involved in loss of heterozygosity observed in many tumors [61]. In this thesis work I demonstrated an involvement of p160 in the cell-cycle and a putative role of this protein as a tumor suppressor.

I also studied Prep1, an homeodomain transcription factor essential for embryonic development. In particular it influences hematopoiesis, angiogenesis and oculogenesis [37]. It is also involved in apoptosis [86,87] and in tumorigenesis as a tumor suppressor [75]. Prep1 functions as a transcription factor when it is translocated to the nucleoplasm through its binding to Pbx. Here it can interact with Hox (or other) proteins and increases their affinity for DNA and their transcriptional activation. By Tandem Affinity Purification (TAP) [23] we found that p160 is a specific Prep1 interactor capable of inhibiting Prep1 transcriptional activity by preventing Pbx binding [24].

1. p160 is a direct Prepl interactor that inhibits its transcriptional activity

p160 binds through its N-terminal region to the HR1 domain of Prepl. This domain is essential for Prepl function since it is the region that makes contact with Pbx and increases the binding of the Pbx/Hox heterodimer and its transcriptional activity. In particular p160 binds a leucine-rich region in the HR1 domain, a LXXLL motif (Fig. 14 and 15), i.e. the same protein sequence that p160 uses to bind Myb and PGC1α [30,94]. I also showed, by a Luciferase assay, EMSA and Real-Time PCR (Fig. 17 and 18) that Prepl activity was significantly decreased by p160. In particular, p160 competes with Pbx in the binding to Prepl hence inhibiting the interaction with Pbx and the resulting transcriptional activation. This demonstrates that p160 is a Prepl regulator.

Prepl lacks a nuclear localization signal, but translocates to the nucleoplasm through its binding to Pbx. On the other hand, p160 is mainly located in nucleoli and only 5% was found in the nucleoplasm. I showed that Actinomycin D treatment, that causes the inhibition of RNA polymerase I, determines the shuttling of p160 from nucleoli to nucleoplasm and allows the visualization of the co-immunoprecipitation and co-localization of the two proteins (Fig. 20 and 21). However, at least in the untreated F9 cell line, Prepl is observed also in nucleoli in co-localization with p160. I also studied the co-localization of p160 and Prepl during mitosis, since it is a physiological condition that causes disruption of nucleoli at the onset of prophase and the release of nucleolar proteins in the nucleoplasm [73]. However, in these conditions co-localization of the two proteins was not detected: p160 has a peculiar para-chromosomal localization, typical of many nucleolar components, while Prepl is more dispersed (Fig. 19). It is

possible, although unlikely, that minor amounts of Prep1 are present in the nucleolus and that some interactions, functionally relevant, but not visible with this technique, indeed take place in both nucleoli and chromosomal areas.

The relation between Prep1 and p160 is also important for glucose metabolism. p160 is an inhibitor of the transcription factor PGC1α that regulates glucose uptake by promoting the synthesis of GLUT4 glucose receptors. At low levels of p160, PGC1α increases and induces GLUT4 expression [1,88]. In fact $Prep1^{i/i}$ mice show an increased sensitivity to insulin due to increased GLUT4 and are resistant to diabetes [96]. Moreover, p160 seems to be protected from degradation by Prep1: at low levels of Prep1 (like in the $Prep1^{i/i}$ mice) there is also a low level of p160 and this is restored by proteasome inhibition.

In summary, I identified p160 myb binding protein 1a as a new Prep1 inhibitor that modulates its transcriptional activity. How the two proteins interact and the importance of Prep1 in p160 function at mitosis is, however, still not clear.

2. p160 is involved in cell-cycle regulation

p160 is a nucleolar protein that interacts with many transcription factors: c-Myb, c-Jun, PGC1α, AhR and NF-kB [30,57,97,124], but its function is still not clear. The fact that it interacts with many transcription factors suggested that p160 might be a co-regulator of transcription by both polymerase I and II [124]. Another hypothesis is that p160 is part of a large complex that regulates ribosome biogenesis in the nucleolus. Inhibition of ribosomal biogenesis determines the proteolytic cleavage of p160 into p67 or p140 that

translocate to the nucleoplasm and form a complex with many transcription factors (Myb, PGC1α, NF-kB, etc.) affecting cell-cycle arrest and apoptosis [134].

Here I demonstrated that p160 is involved in the cell-cycle. p160 has a para-chromosomal localization during mitosis: it distributes around the metaphasic plate and concentrates in two regions on the side of the plate, in agreement with p160 localization on chromosomes arm during mitosis [38] (Fig. 22). Due to its particular localization, I studied the role of this protein in cell division. After p160 silencing, as shown in Figures 27 and 28, cells grow slower and die mainly of apoptosis. Interestingly this agrees with the observation that p160 KO embryos die at the stage of blastocyst (Keough R., personal communication).

By studying cell-cycle distribution, it was evident that, after p160 depletion, HeLa cells accumulate in the G2/M phase and display an increased mitotic index (Fig. 29 and 30). In particular, I noticed an increase number of cells in prophase and metaphase with respect to anaphase and telophase. This indicates that cells can start proliferating, replicate their DNA content but are then blocked at the stage of chromosomes segregation. Chromosome segregation is well controlled by the Spindle Assembly Checkpoint (SAC), a protein complex located at the level of kinetocores that ensures the fidelity of chromosome segregation in mitosis. If chromosomes are not properly attached to the spindle or not aligned to the metaphasic plate the SAC complex (in particular MAD2) binds cdc20 that can no longer bind and activate APC/C and hence determines a delay of the subsequent anaphase. If the problem is solved, the cell can proceed with chromosomes segregation, otherwise apoptosis is induced [92]. In my model, p160-depleted HeLa cells might not divide because SAC is activated. Checking several

metaphasic plates by immunofluorescence, I noticed structural alterations (Fig. 31) and found that division was blocked or, at best, delayed (Fig. 32). These data confirm that the cells try to divide but often they are unable to do so. Consequently they die of apoptosis or, in a few cases, they proceed through division accumulating alterations. This was not visible with karyotype analysis probably because the cell system used (HeLa and NIH 3T3 cell line) has already a very altered karyotype. However, the sensitivity of p160 down-regulated NIH 3T3 cells to oncogene-induced transformation, shown in the last part of my Results, might be interpreted in this way: without p160, cells accumulate genetic alterations that favor tumorigenesis (see later). Thus, p160 is involved in controlling cell-cycle progression and, in particular, it seems to be important for chromosome segregation and cell division.

Very recently a paper was published that supports this idea. Perrera et al. (2010), claimed that p160 is a novel substrate of Aurora B. Aurora B is a serine-threonine kinase involved in centrosomes segregation and maturation, spindle assembly and stability, chromosomes condensation, congression and segregation, cytokinesis [68,127]. p160 is phosphorylated by Aurora B in serine 1303 (C-terminal part) and indeed it is phosphorylated *in vivo* during mitosis. For this reason they studied also the cell-cycle and obtained results in line with ours: a decrease in p160 level led to a decreased proliferation rate, longer mitosis time and mitotic spindle defects [101].

A further confirmation of this idea has also been obtained by the gene expression studies. The microarray experiment suggested that silencing of p160 determines mainly alterations in transcription of the cell-cycle, mitosis, DNA damage response and cell death pathways (Fig. 35). These results were confirmed by Real-Time PCR and were

consistent: p160 was down-regulated in treated samples versus control, as expected, as HeLa cells were treated with a siRNA for p160. JUN and NF-kB, known to be repressed by p160, were up-regulated in treated samples. I confirmed also the expression data of CDKN1A, GADD45B and TOP2B. The alteration of their expression and of the genes listed in Tab. III, implies that there is a de-regulation of cell-cycle and apoptosis. These data emphasize that, in response to p160 depletion, there is an activation of the genes involved in cell-cycle control and mitosis probably in response to an alteration of this process. This determines the activation of the apoptotic pathway in cells that cannot repair the damage. Thus, p160 is a transcription factor binding protein involved in cell-cycle progression. Its peculiar phenotype led me to investigate also a possible involvement in neoplastic transformation.

3. p160 is a putative tumor suppressor

The NPM KO determines mitotic alterations, proliferation defects and apoptosis, while an heterozygous condition determines genomic instability that leads to cell transformation [43]. Given this similarity and the fact that the p160 gene is frequently translocated in human cancers (as analyzed from the Mitelman database), I studied the consequences of a 50% reduction of the protein. NIH 3T3 cells infected with lentiviral vectors expressing p160 shRNA show 50% of the protein, no alteration in the cell-cycle distribution and apoptosis, but grow slightly faster than the parental counterparts (Fig. 37 and 38).

A striking result was obtained when the oncogenes Ras or Myc were co-infected with the shRNA lentivectors. p160 down-regulated NIH 3T3 cells grew faster than control and formed more colonies in a soft agar assay (Fig. 39). These data led me to think that p160 might have a role in tumorigenesis, because the accumulation of genetic alterations during cell division may accelerate the onset of the mutations required for tumorigenesis. This can be indicative of a p160 role as tumor suppressor. This phenotype may also be due to a clonal selection and hence unrelated to p160 decrease, as I did not analyze this point directly. Preliminary data on nude mice subcutaneous injection of NT or p160 down-regulated NIH 3T3 cells again demonstrate that under conditions of p160 down-regulation, cells become more tumorigenic, giving rise to the formation of bigger tumors.

Concluding remarks and future perspectives

In summary, in this thesis I have demonstrated that p160 is a Prep1 interactor and inhibitor and it is involved in cell-cycle regulation.

I showed that p160 and Prep1 directly interact and that this binding (demonstrated by co-immunoprecipitation and co-localization) is visible only in overexpression of one of the two partners or in stress conditions. This indicates that probably the two proteins physiologically interact but just a minor fraction of them is involved in this binding. However this interaction seems to be functionally relevant since p160 can inhibit Prep1 transcriptional activity. Overall I think that there are few aspects in this first part of my results that need to be further investigated. First of all, even if strong evidence suggests that Prep1 and p160 directly interact, another experiment, to finally prove this binding can be performed. In fact p160 was in-vitro synthesized with a TNT T7 Quick coupled transcription-translation system (Promega) that employs the rabbit reticulocyte lysate containing the eukaryotic protein machinery required for translation. This technique is very convenient because it allows to obtain a good amount of radio-labeled protein but the mix contains eukaryotic proteins that can interfere or facilitate the binding of two proteins. A pull-down made with proteins prepared in prokaryotic organism, such as yeast, could be useful in order to exclude that the interaction is not direct but part of a complex. Another key point that needs to be further investigated is p160 localization. p160 is mainly located in the nucleoli but probably has a dynamic localization and can shuttle between different compartments, demonstrated also by the fact that it was also found in the nucleoplasm. Therefore a more accurate analysis of p160 localization can

be performed using FLIP (Fluorescence Loss In Photobleaching) or FRAP (Fluorescence Recovery After Photobleaching), techniques that allow to monitor the movement of proteins inside cells. In this way it will be possible to elucidate p160 shuttling and maybe understand also where it co-localizes with Prep1 or find other cellular compartments where the protein might concentrate and exert a function. For example p160 staining suggests that it can localize in Cajal bodies, subnuclear structures important for snRNPs biogenesis [95]. A co-staining with coilin will uncover this point.

With this thesis work I also discovered that p160 functions as a cell-cycle regulator, since p160 is essential for a proper cell division. A major reduction in p160 level determines cell-cycle alterations, apoptosis and hence a lower proliferation rate. A small reduction, however, determines accumulation of alterations and favors cell transformation. Therefore my hypothesis is that in the absence of p160, DNA damage may occur due to problems in DNA replication or cell division. Cells slow down their cell-cycle and accumulate in metaphase to repair the damage. However, in the absence of p160, DNA repair is not achieved: hence growth arrests and cells die for apoptosis. A fifty percent reduction in p160 levels is however compatible with cell division, despite the accumulation of genetic alterations by cells. These mutations may favor cell transformation and uncontrolled proliferation that are at the basis of tumor formation. Hence my data have uncovered a new function for p160 as a cell-cycle regulator and possibly as tumor suppressor. To validate this hypothesis I think it will be useful to perform the rescue of the phenotype, reintroducing p160 into silenced Hela cells. In fact my experiments were done with a transformed cell line with transiently transfected

siRNAs that can interfere with the final result. Finally it will be helpful to perform p160 silencing in a primary cell line to monitor genetic instability (probably responsible of the cell transformation) not visible in Hela and NIH 3T3 cell lines.

APPENDIX

I. Study of p160MBP sumoylation

The Sumoylation process

Sumoylation is a process similar to ubiquitination but instead of inducing the target protein to degradation, it modifies the substrate activity or function. This process is mediated by SUMO (Small Ubiquitin-like Modifier). The sumoylation process consists of three steps (Fig. A1):

- ATP-dependent activation of SUMO by the E1 enzyme
- conjugation by the E2 enzyme
- binding to the substrate with the help of the E3 ligase.

Sumoylation is a reversible process; SUMO can be deconjugated from the substrate by the action of desumoylases (SENP) [136].

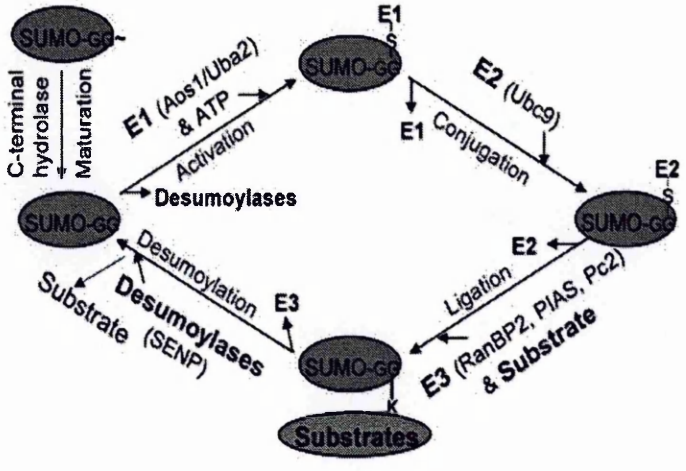

Fig. A1 Sumoylation process. Schematic representation of the sumoylation process; the enzymes involved are indicated [136].

The primary function of sumoylation is in the nucleus: it regulates transcription, modulates nuclear trafficking, genomic stability and chromosomal integrity. Sumoylation can also regulate protein-protein interaction and protein localization.

Aim of the work

I decided to study sumoylation because p160 was found between the endogenous sumoylated proteins upon proteasome inhibition [85]. After proteasome inhibition the SUMO-1 conjugates accumulates in the nucleoli and this allowed the identification of several putative SUMO substrates by quantitative proteomics; among them, p160. Sumoylation can be the process that determines p160 translocation from nucleoli to nucleoplasm where it interacts with Prep1; I decided then to study this process in details.

Materials & Methods

- *Cell culture and treatments*

NIH 3T3 cells were cultured as described in Material and Methods. Cells were infected with pRufneo-p160-Flag as described previously.

- *In vitro sumoylation reaction*

NIH 3T3 cells nuclear extracts were prepared as described previously and incubated for 30 minutes at 25°C with HIS-SUMO 40 ng (SUMO conjugated with Histidine tag), Aos1/Uba2 20 ng (E1 activating enzyme), Ubc9 10 ng (E2 enzyme), inorganic pyrophosphatase 0.6Units, ATP 10 mM, Tris-HCl 50 mM pH 7.6, MgCl2 10 mM. The reaction was then loaded on a polyacrylamide gel and SDS-PAGE was performed as described previously.

- *Co-immunoprecipitation and in-vitro translation of proteins* was performed as described previously.

Results

1. P160 is sumoylated *in vitro* and *in vivo*

In order to validate p160 sumoylation an *in vitro* sumoylation reaction was performed. As shown in Fig. A2 A, after adding SUMO to the nuclear extract of NIH 3T3 cells stably expressing p160-flag, there was an upward shift of the band representing p160, indicating that p160 was sumoylated. We tested this hypothesis also *in vivo*, performing p160 immunoprecipitation in NIH 3T3 cells overexpressing p160-flag, followed by a blot with anti-SUMO antibody. As shown in Fig. A2 B, p160 was sumoylated also *in vivo* because the immunoprecipitated band was detected with SUMO antibodies.

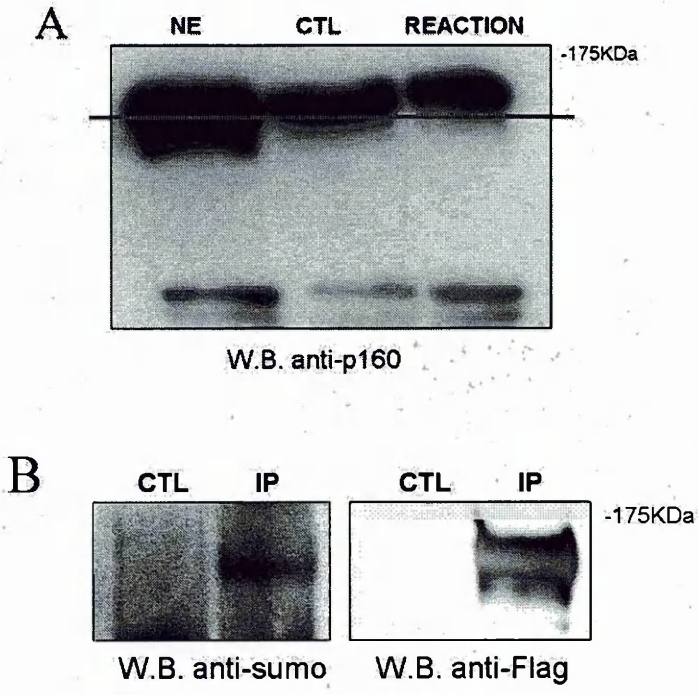

Fig. A2 p160 sumoylation. (A) *In vitro* sumoylation reaction of NIH 3T3 cells nuclear extracts (NE): NE is untreated nuclear extract; CTL is NE incubated with sumoylation mix but without SUMO and REACTION is NE incubated with the whole sumoylation mix. **(B)** Co-immunoprecipitation of p160 and SUMO in NIH 3T3 cells overexpressing p160-flag. The reaction was performed with M2 anti-Flag beads and the immunoblot was performed with anti-SUMO and anti-Flag antibodies as control. CTL are NIH 3T3 cells not infected with p160.

2. Detection of the SUMO binding site

We wanted to find the SUMO binding site in order to create p160 mutants that cannot bind SUMO, useful to discover the function of this post-translational modification in p160. We used SUMOplot Analysis Program (Abgent), a software that calculates the most likely SUMO binding sites. The majority of the sites found were in the N-terminal part of the protein and in particular we chose an AKPD motif (position 41-44, score 0,79). We mutated the lysine (K) to arginine but apparently there was no change in the

sumoylation state. This experiment needs to be repeated, possibly trying to mutate another SUMO binding site.

We prepared also p160 deletion mutants on which an *in-vitro* sumoylation reaction was performed after *in-vitro* translation. Since the most likely binding site was in the N-terminal region we used only the p160 fragments 1-200, 200-400 and p67 (1-580). After the reaction we tested p160 sumoylation. The result showed sumoylation only in the 1-200 fragment and in p67, suggesting that the 1-200 region contained the sumoylation site (Fig. A3).

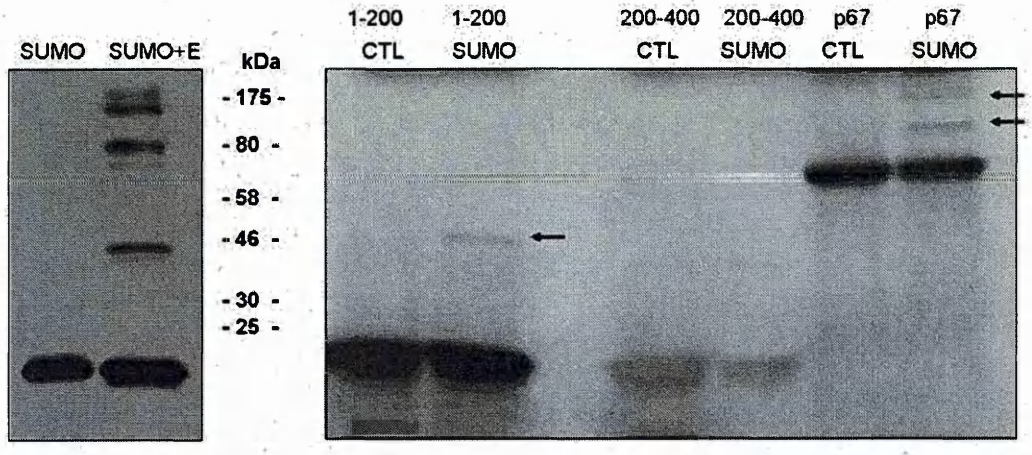

Fig. A3 The SUMO binding site is located in the N-terminal region of p160. *In vitro* sumoylation reaction of *in vitro*-translated p160 fragments: 1-200, 200-400 and p67. In the left panel is shown the coomassie staining of the gel showing that sumoylation happens only when sumoylation enzymes are added to the reaction: SUMO indicates that only SUMO was added to the proteins and SUMO+E indicates that also the sumoylation enzymes were added. On the right is shown the autoradiography of the different reactions where CTL indicates the control reaction without SUMO and SUMO the reaction with it.

Summary

In conclusion we can say that p160 is sumoylated. After finding the protein among the nucleolar endogenous sumoylated proteins after proteasome inhibition, we demonstrated this post-translational modification both *in vitro* and *in vivo*. We also demonstrated that SUMO binds the N-terminal part of p160, i.e. the same region involved in Prep1 binding. We need now to understand which is the function of this modification. One hypothesis is that p160 sumoylation takes place in the nucleoli and this allows the protein to translocate in the nucleoplasm where it is de-sumoylated and can interact with Prep1 or other transcription factors. P160 then returns again into nucleoli.

This work contains unpublished data and was done in collaboration with A. Bachi's group (DIBIT2, San Raffaele Hospital, Milan, Italy).

II. List of figures / tables

III. List of abbreviations

P160, MYBBP1a, p160 myb binding protein1

HTH, Helix Turn Helix

HLH, Helix-Loop-Helix

HD, Homeodomain

C-terminal, Carboxil-terminus

N-terminal, Amino-terminus

TALE, Three Amino acid Loop Extension

Pbx, Pre-B cell lymphoma

Prep, Pbx regulating protein

Meis, Myeloid ecotropic viral integration site

HR, Holomogy Region

NLS, Nuclear Localization Signal

NES, Nuclear Export Signal

LCD, Leucine Charged Domain

KO, Knock-down

$Prep^{i/i}$, Prep hypomorphic

d.p.c., days post coitum

E, embryonic day

P, days post partum

MEF, Mouse Embryonic Fibroblast

TAP, Tandem Affinity Purification

ActD, Actinomycin D

NPM, Nucleophosmin

PGC1α, PPAR gamma co-activator 1α

FC, Fibrillar Center

DFC, Dense Fibrillar Component

GC, Granular Component

NOR, Nucleolar Organizing Region

CDK, Cyclin Dependent Kinase

PR, Perichromosomal Region

NDF, Nucleolar Derived Foci

G1, G2, gap1,2

S-phase, Synthesis phase

SAC, Spindle Assembly Checkpoint

APC/C, Anaphase Promoting Complex

MPF, Mitosis Promoting Factor

DMEM, Dulbecco's Modified Eagle's Medium

FBS, Fetal Bovine Serum

SDS, Sodium Dodecyl Phosphate

PBS, Phosphate Buffered Saline

RT, Room Temperature

β-Gal, β-Galactosidase

EMSA, Electrophoretic mobility shift assay

DAPI, 4'6-diamidino-2-phenylindole dihydrochloride

EdU, 5'ethynyl-2'-deoxyuridine

7-AAD, 7-amino-actinomycin D

FITC, Fluorescein Isothyocynate

PE, Phycoeruthrin

aa, amino acids

RA, retinoic acid

PH3, Phospho-Histone H3

FACS, Flow Cytometer

NT, Non-target

wt, wild-type

REFERENCES

1 Al-Khalili, L., Forsgren, M., Kannisto, K., Zierath, J.R., Lonnqvist, F., & Krook, A., Enhanced insulin-stimulated glycogen synthesis in response to insulin, metformin or rosiglitazone is associated with increased mRNA expression of GLUT4 and peroxisomal proliferator activator receptor gamma co-activator 1. *Diabetologia* 48 (6), 1173-1179 (2005).

2 Amin, M.A., Matsunaga, S., Uchiyama, S., & Fukui, K., Nucleophosmin is required for chromosome congression, proper mitotic spindle formation, and kinetochore-microtubule attachment in HeLa cells. *FEBS Lett* 582 (27), 3839-3844 (2008).

3 Azcoitia, V., Aracil, M., Martinez, A.C., & Torres, M., The homeodomain protein Meis1 is essential for definitive hematopoiesis and vascular patterning in the mouse embryo. *Dev Biol* 280 (2), 307-320 (2005).

4 Bailey, J.S., Rave-Harel, N., McGillivray, S.M., Coss, D., & Mellon, P.L., Activin regulation of the follicle-stimulating hormone beta-subunit gene involves Smads and the TALE homeodomain proteins Pbx1 and Prep1. *Mol Endocrinol* 18 (5), 1158-1170 (2004).

5 Benjamini, Y., Drai, D., Elmer, G., Kafkafi, N., & Golani, I., Controlling the false discovery rate in behavior genetics research. *Behav Brain Res* 125 (1-2), 279-284 (2001).

6 Berthelsen, J., Kilstrup-Nielsen, C., Blasi, F., Mavilio, F., & Zappavigna, V., The subcellular localization of PBX1 and EXD proteins depends on nuclear import and export signals and is modulated by association with PREP1 and HTH. *Genes Dev* 13 (8), 946-953 (1999).

7 Berthelsen, J., Vandekerkhove, J., & Blasi, F., Purification and characterization of UEF3, a novel factor involved in the regulation of the urokinase and other AP-1 controlled promoters. *J Biol Chem* 271 (7), 3822-3830 (1996).

8 Berthelsen, J., Viggiano, L., Schulz, H., Ferretti, E., Consalez, G.G., Rocchi, M., & Blasi, F., PKNOX1, a gene encoding PREP1, a new regulator of Pbx activity,

maps on human chromosome 21q22.3 and murine chromosome 17B/C. *Genomics* 47 (2), 323-324 (1998).

9 Berthelsen, J., Zappavigna, V., Ferretti, E., Mavilio, F., & Blasi, F., The novel homeoprotein Prep1 modulates Pbx-Hox protein cooperativity. *EMBO J* 17 (5), 1434-1445 (1998).

10 Berthelsen, J., Zappavigna, V., Mavilio, F., & Blasi, F., Prep1, a novel functional partner of Pbx proteins. *EMBO J* 17 (5), 1423-1433 (1998).

11 Boisvert, F.M., van Koningsbruggen, S., Navascues, J., & Lamond, A.I., The multifunctional nucleolus. *Nat Rev Mol Cell Biol* 8 (7), 574-585 (2007).

12 Bolstad, B.M., Irizarry, R.A., Astrand, M., & Speed, T.P., A comparison of normalization methods for high density oligonucleotide array data based on variance and bias. *Bioinformatics* 19 (2), 185-193 (2003).

13 Brendolan, A., Ferretti, E., Salsi, V., Moses, K., Quaggin, S., Blasi, F., Cleary, M.L., & Selleri, L., A Pbx1-dependent genetic and transcriptional network regulates spleen ontogeny. *Development* 132 (13), 3113-3126 (2005).

14 Burglin, T.R., Analysis of TALE superclass homeobox genes (MEIS, PBC, KNOX, Iroquois, TGIF) reveals a novel domain conserved between plants and animals. *Nucleic Acids Res* 25 (21), 4173-4180 (1997).

15 Burglin, T.R., The PBC domain contains a MEINOX domain: coevolution of Hox and TALE homeobox genes? *Dev Genes Evol* 208 (2), 113-116 (1998).

16 Chang, C.P., Brocchieri, L., Shen, W.F., Largman, C., & Cleary, M.L., Pbx modulation of Hox homeodomain amino-terminal arms establishes different DNA-binding specificities across the Hox locus. *Mol Cell Biol* 16 (4), 1734-1745 (1996).

17 Chang, C.P., Jacobs, Y., Nakamura, T., Jenkins, N.A., Copeland, N.G., & Cleary, M.L., Meis proteins are major in vivo DNA binding partners for wild-type but not chimeric Pbx proteins. *Mol Cell Biol* 17 (10), 5679-5687 (1997).

18 Chang, C.P., Shen, W.F., Rozenfeld, S., Lawrence, H.J., Largman, C., & Cleary, M.L., Pbx proteins display hexapeptide-dependent cooperative DNA binding with a subset of Hox proteins. *Genes Dev* 9 (6), 663-674 (1995).

19 Choesmel, V., Bacqueville, D., Rouquette, J., Noaillac-Depeyre, J., Fribourg, S., Cretien, A., Leblanc, T., Tchernia, G., Da Costa, L., & Gleizes, P.E., Impaired ribosome biogenesis in Diamond-Blackfan anemia. *Blood* 109 (3), 1275-1283 (2007).

20 Derenzini, M., Montanaro, L., & Trere, D., What the nucleolus says to a tumour pathologist. *Histopathology* 54 (6), 753-762 (2009).

21 Di Bacco, A., Ouyang, J., Lee, H.Y., Catic, A., Ploegh, H., & Gill, G., The SUMO-specific protease SENP5 is required for cell division. *Mol Cell Biol* 26 (12), 4489-4498 (2006).

22 Di Rocco, G., Mavilio, F., & Zappavigna, V., Functional dissection of a transcriptionally active, target-specific Hox-Pbx complex. *EMBO J* 16 (12), 3644-3654 (1997).

23 Diaz, V.M., Bachi, A., & Blasi, F., Purification of the Prep1 interactome identifies novel pathways regulated by Prep1. *Proteomics* 7 (15), 2617-2623 (2007).

24 Diaz, V.M., Mori, S., Longobardi, E., Menendez, G., Ferrai, C., Keough, R.A., Bachi, A., & Blasi, F., p160 Myb-binding protein interacts with Prep1 and inhibits its transcriptional activity. *Mol Cell Biol* 27 (22), 7981-7990 (2007).

25 Dimario, P.J., Cell and molecular biology of nucleolar assembly and disassembly. *Int Rev Cytol* 239, 99-178 (2004).

26 DiMartino, J.F., Selleri, L., Traver, D., Firpo, M.T., Rhee, J., Warnke, R., O'Gorman, S., Weissman, I.L., & Cleary, M.L., The Hox cofactor and proto-oncogene Pbx1 is required for maintenance of definitive hematopoiesis in the fetal liver. *Blood* 98 (3), 618-626 (2001).

27 Dubendorff, J.W., Whittaker, L.J., Eltman, J.T., & Lipsick, J.S., Carboxy-terminal elements of c-Myb negatively regulate transcriptional activation in cis and in trans. *Genes Dev* 6 (12B), 2524-2535 (1992).

[28] el-Deiry, W.S., Tokino, T., Velculescu, V.E., Levy, D.B., Parsons, R., Trent, J.M., Lin, D., Mercer, W.E., Kinzler, K.W., & Vogelstein, B., WAF1, a potential mediator of p53 tumor suppression. *Cell* 75 (4), 817-825 (1993).

[29] Elledge, S.J., Cell cycle checkpoints: preventing an identity crisis. *Science* 274 (5293), 1664-1672 (1996).

[30] Fan, M., Rhee, J., St-Pierre, J., Handschin, C., Puigserver, P., Lin, J., Jaeger, S., Erdjument-Bromage, H., Tempst, P., & Spiegelman, B.M., Suppression of mitochondrial respiration through recruitment of p160 myb binding protein to PGC-1alpha: modulation by p38 MAPK. *Genes Dev* 18 (3), 278-289 (2004).

[31] Fatica, A. & Tollervey, D., Making ribosomes. *Curr Opin Cell Biol* 14 (3), 313-318 (2002).

[32] Favier, D. & Gonda, T.J., Detection of proteins that bind to the leucine zipper motif of c-Myb. *Oncogene* 9 (1), 305-311 (1994).

[33] Fernandez-Diaz, L.C., Laurent, A., Girasoli, S., Turco, M., Longobardi, E., Iotti, G., Jenkins, N.A., Fiorenza, M.T., Copeland, N.G., & Blasi, F., The absence of Prep1 causes p53-dependent apoptosis of mouse pluripotent epiblast cells. *Development.*

[34] Ferretti, E., Cambronero, F., Tumpel, S., Longobardi, E., Wiedemann, L.M., Blasi, F., & Krumlauf, R., Hoxb1 enhancer and control of rhombomere 4 expression: complex interplay between PREP1-PBX1-HOXB1 binding sites. *Mol Cell Biol* 25 (19), 8541-8552 (2005).

[35] Ferretti, E., Marshall, H., Popperl, H., Maconochie, M., Krumlauf, R., & Blasi, F., Segmental expression of Hoxb2 in r4 requires two separate sites that integrate cooperative interactions between Prep1, Pbx and Hox proteins. *Development* 127 (1), 155-166 (2000).

[36] Ferretti, E., Schulz, H., Talarico, D., Blasi, F., & Berthelsen, J., The PBX-regulating protein PREP1 is present in different PBX-complexed forms in mouse. *Mech Dev* 83 (1-2), 53-64 (1999).

[37] Ferretti, E., Villaescusa, J.C., Di Rosa, P., Fernandez-Diaz, L.C., Longobardi, E., Mazzieri, R., Miccio, A., Micali, N., Selleri, L., Ferrari, G., & Blasi, F., Hypomorphic mutation of the TALE gene Prep1 (pKnox1) causes a major

reduction of Pbx and Meis proteins and a pleiotropic embryonic phenotype. *Mol Cell Biol* 26 (15), 5650-5662 (2006).

38 Gassmann, R., Henzing, A.J., & Earnshaw, W.C., Novel components of human mitotic chromosomes identified by proteomic analysis of the chromosome scaffold fraction. *Chromosoma* 113 (7), 385-397 (2005).

39 Gautier, T., Robert-Nicoud, M., Guilly, M.N., & Hernandez-Verdun, D., Relocation of nucleolar proteins around chromosomes at mitosis. A study by confocal laser scanning microscopy. *J Cell Sci* 102 (Pt 4), 729-737 (1992).

40 Gehring, W.J., Affolter, M., & Burglin, T., Homeodomain proteins. *Annu Rev Biochem* 63, 487-526 (1994).

41 Gehring, W.J., Qian, Y.Q., Billeter, M., Furukubo-Tokunaga, K., Schier, A.F., Resendez-Perez, D., Affolter, M., Otting, G., & Wuthrich, K., Homeodomain-DNA recognition. *Cell* 78 (2), 211-223 (1994).

42 Goudet, G., Delhalle, S., Biemar, F., Martial, J.A., & Peers, B., Functional and cooperative interactions between the homeodomain PDX1, Pbx, and Prep1 factors on the somatostatin promoter. *J Biol Chem* 274 (7), 4067-4073 (1999).

43 Grisendi, S., Bernardi, R., Rossi, M., Cheng, K., Khandker, L., Manova, K., & Pandolfi, P.P., Role of nucleophosmin in embryonic development and tumorigenesis. *Nature* 437 (7055), 147-153 (2005).

44 Grisendi, S., Mecucci, C., Falini, B., & Pandolfi, P.P., Nucleophosmin and cancer. *Nat Rev Cancer* 6 (7), 493-505 (2006).

45 Hartwell, L.H. & Kastan, M.B., Cell cycle control and cancer. *Science* 266 (5192), 1821-1828 (1994).

46 Hartwell, L.H. & Weinert, T.A., Checkpoints: controls that ensure the order of cell cycle events. *Science* 246 (4930), 629-634 (1989).

47 Heiss, N.S., Knight, S.W., Vulliamy, T.J., Klauck, S.M., Wiemann, S., Mason, P.J., Poustka, A., & Dokal, I., X-linked dyskeratosis congenita is caused by mutations in a highly conserved gene with putative nucleolar functions. *Nat Genet* 19 (1), 32-38 (1998).

48 Hernandez-Verdun, D. & Gautier, T., The chromosome periphery during mitosis. *Bioessays* 16 (3), 179-185 (1994).

49 Herzig, S., Fuzesi, L., & Knepel, W., Heterodimeric Pbx-Prep1 homeodomain protein binding to the glucagon gene restricting transcription in a cell type-dependent manner. *J Biol Chem* 275 (36), 27989-27999 (2000).

50 Hisa, T., Spence, S.E., Rachel, R.A., Fujita, M., Nakamura, T., Ward, J.M., Devor-Henneman, D.E., Saiki, Y., Kutsuna, H., Tessarollo, L., Jenkins, N.A., & Copeland, N.G., Hematopoietic, angiogenic and eye defects in Meis1 mutant animals. *EMBO J* 23 (2), 450-459 (2004).

51 Hu, Y.L., Ramsay, R.G., Kanei-Ishii, C., Ishii, S., & Gonda, T.J., Transformation by carboxyl-deleted Myb reflects increased transactivating capacity and disruption of a negative regulatory domain. *Oncogene* 6 (9), 1549-1553 (1991).

52 Huang da, W., Sherman, B.T., & Lempicki, R.A., Bioinformatics enrichment tools: paths toward the comprehensive functional analysis of large gene lists. *Nucleic Acids Res* 37 (1), 1-13 (2009).

53 Hussain, S., Benavente, S.B., Nascimento, E., Dragoni, I., Kurowski, A., Gillich, A., Humphreys, P., & Frye, M., The nucleolar RNA methyltransferase Misu (NSun2) is required for mitotic spindle stability. *J Cell Biol* 186 (1), 27-40 (2009).

54 Irizarry, R.A., Bolstad, B.M., Collin, F., Cope, L.M., Hobbs, B., & Speed, T.P., Summaries of Affymetrix GeneChip probe level data. *Nucleic Acids Res* 31 (4), e15 (2003).

55 Irizarry, R.A., Hobbs, B., Collin, F., Beazer-Barclay, Y.D., Antonellis, K.J., Scherf, U., & Speed, T.P., Exploration, normalization, and summaries of high density oligonucleotide array probe level data. *Biostatistics* 4 (2), 249-264 (2003).

56 Jacobs, Y., Schnabel, C.A., & Cleary, M.L., Trimeric association of Hox and TALE homeodomain proteins mediates Hoxb2 hindbrain enhancer activity. *Mol Cell Biol* 19 (7), 5134-5142 (1999).

[57] Jones, L.C., Okino, S.T., Gonda, T.J., & Whitlock, J.P., Jr., Myb-binding protein 1a augments AhR-dependent gene expression. *J Biol Chem* 277 (25), 22515-22519 (2002).

[58] Kadrmas, J.L. & Beckerle, M.C., The LIM domain: from the cytoskeleton to the nucleus. *Nat Rev Mol Cell Biol* 5 (11), 920-931 (2004).

[59] Kanei-Ishii, C., MacMillan, E.M., Nomura, T., Sarai, A., Ramsay, R.G., Aimoto, S., Ishii, S., & Gonda, T.J., Transactivation and transformation by Myb are negatively regulated by a leucine-zipper structure. *Proc Natl Acad Sci U S A* 89 (7), 3088-3092 (1992).

[60] Kastan, M.B., Zhan, Q., el-Deiry, W.S., Carrier, F., Jacks, T., Walsh, W.V., Plunkett, B.S., Vogelstein, B., & Fornace, A.J., Jr., A mammalian cell cycle checkpoint pathway utilizing p53 and GADD45 is defective in ataxia-telangiectasia. *Cell* 71 (4), 587-597 (1992).

[61] Keough, R., Woollatt, E., Crawford, J., Sutherland, G.R., Plummer, S., Casey, G., & Gonda, T.J., Molecular cloning and chromosomal mapping of the human homologue of MYB binding protein (P160) 1A (MYBBP1A) to 17p13.3. *Genomics* 62 (3), 483-489 (1999).

[62] Keough, R.A., Macmillan, E.M., Lutwyche, J.K., Gardner, J.M., Tavner, F.J., Jans, D.A., Henderson, B.R., & Gonda, T.J., Myb-binding protein 1a is a nucleocytoplasmic shuttling protein that utilizes CRM1-dependent and independent nuclear export pathways. *Exp Cell Res* 289 (1), 108-123 (2003).

[63] Kim, S.K., Selleri, L., Lee, J.S., Zhang, A.Y., Gu, X., Jacobs, Y., & Cleary, M.L., Pbx1 inactivation disrupts pancreas development and in Ipf1-deficient mice promotes diabetes mellitus. *Nat Genet* 30 (4), 430-435 (2002).

[64] Kinsella, T.M. & Nolan, G.P., Episomal vectors rapidly and stably produce high-titer recombinant retrovirus. *Hum Gene Ther* 7 (12), 1405-1413 (1996).

[65] Knoepfler, P.S., Bergstrom, D.A., Uetsuki, T., Dac-Korytko, I., Sun, Y.H., Wright, W.E., Tapscott, S.J., & Kamps, M.P., A conserved motif N-terminal to the DNA-binding domains of myogenic bHLH transcription factors mediates cooperative DNA binding with pbx-Meis1/Prep1. *Nucleic Acids Res* 27 (18), 3752-3761 (1999).

66 Knoepfler, P.S. & Kamps, M.P., The pentapeptide motif of Hox proteins is required for cooperative DNA binding with Pbx1, physically contacts Pbx1, and enhances DNA binding by Pbx1. *Mol Cell Biol* 15 (10), 5811-5819 (1995).

67 Knoepfler, P.S. & Kamps, M.P., The highest affinity DNA element bound by Pbx complexes in t(1;19) leukemic cells fails to mediate cooperative DNA-binding or cooperative transactivation by E2a-Pbx1 and class I Hox proteins - evidence for selective targetting of E2a-Pbx1 to a subset of Pbx-recognition elements. *Oncogene* 14 (21), 2521-2531 (1997).

68 Kollareddy, M., Dzubak, P., Zheleva, D., & Hajduch, M., Aurora kinases: structure, functions and their association with cancer. *Biomed Pap Med Fac Univ Palacky Olomouc Czech Repub* 152 (1), 27-33 (2008).

69 Krumlauf, R., Hox genes in vertebrate development. *Cell* 78 (2), 191-201 (1994).

70 Kurant, E., Eytan, D., & Salzberg, A., Mutational analysis of the Drosophila homothorax gene. *Genetics* 157 (2), 689-698 (2001).

71 Laemmli, U.K., Cleavage of structural proteins during the assembly of the head of bacteriophage T4. *Nature* 227 (5259), 680-685 (1970).

72 Latchman, D.S., Transcription factors: an overview. *Int J Biochem Cell Biol* 29 (12), 1305-1312 (1997).

73 Leung, A.K., Gerlich, D., Miller, G., Lyon, C., Lam, Y.W., Lleres, D., Daigle, N., Zomerdijk, J., Ellenberg, J., & Lamond, A.I., Quantitative kinetic analysis of nucleolar breakdown and reassembly during mitosis in live human cells. *J Cell Biol* 166 (6), 787-800 (2004).

74 Longobardi, E. & Blasi, F., Overexpression of PREP-1 in F9 teratocarcinoma cells leads to a functionally relevant increase of PBX-2 by preventing its degradation. *J Biol Chem* 278 (40), 39235-39241 (2003).

75 Longobardi, E., Iotti, G., Di Rosa, P., Mejetta, S., Bianchi, F., Fernandez-Diaz, L.C., Micali, N., Nuciforo, P., Lenti, E., Ponzoni, M., Doglioni, C., Caniatti, M., Di Fiore, P.P., & Blasi, F., Prep1 (pKnox1)-deficiency leads to spontaneous tumor development in mice and accelerates EmuMyc lymphomagenesis: a tumor suppressor role for Prep1. *Mol Oncol* 4 (2), 126-134.

[76] Lumsden, A. & Krumlauf, R., Patterning the vertebrate neuraxis. *Science* 274 (5290), 1109-1115 (1996).

[77] Ma, N., Matsunaga, S., Takata, H., Ono-Maniwa, R., Uchiyama, S., & Fukui, K., Nucleolin functions in nucleolus formation and chromosome congression. *J Cell Sci* 120 (Pt 12), 2091-2105 (2007).

[78] Maiato, H., DeLuca, J., Salmon, E.D., & Earnshaw, W.C., The dynamic kinetochore-microtubule interface. *J Cell Sci* 117 (Pt 23), 5461-5477 (2004).

[79] Malumbres, M. & Barbacid, M., Cell cycle, CDKs and cancer: a changing paradigm. *Nat Rev Cancer* 9 (3), 153-166 (2009).

[80] Manley, N.R., Selleri, L., Brendolan, A., Gordon, J., & Cleary, M.L., Abnormalities of caudal pharyngeal pouch development in Pbx1 knockout mice mimic loss of Hox3 paralogs. *Dev Biol* 276 (2), 301-312 (2004).

[81] Mann, R.S., The specificity of homeotic gene function. *Bioessays* 17 (10), 855-863 (1995).

[82] Mann, R.S. & Affolter, M., Hox proteins meet more partners. *Curr Opin Genet Dev* 8 (4), 423-429 (1998).

[83] Mann, R.S. & Chan, S.K., Extra specificity from extradenticle: the partnership between HOX and PBX/EXD homeodomain proteins. *Trends Genet* 12 (7), 258-262 (1996).

[84] Marciniak, R.A., Lombard, D.B., Johnson, F.B., & Guarente, L., Nucleolar localization of the Werner syndrome protein in human cells. *Proc Natl Acad Sci U S A* 95 (12), 6887-6892 (1998).

[85] Matafora, V., D'Amato, A., Mori, S., Blasi, F., & Bachi, A., Proteomics analysis of nucleolar SUMO-1 target proteins upon proteasome inhibition. *Mol Cell Proteomics* 8 (10), 2243-2255 (2009).

[86] Micali, N., Ferrai, C., Fernandez-Diaz, L.C., Blasi, F., & Crippa, M.P., Prep1 directly regulates the intrinsic apoptotic pathway by controlling Bcl-XL levels. *Mol Cell Biol* 29 (5), 1143-1151 (2009).

87 Micali, N., Longobardi, E., Iotti, G., Ferrai, C., Castagnaro, L., Ricciardi, M., Blasi, F., & Crippa, M.P., Down syndrome fibroblasts and mouse Prep1-overexpressing cells display increased sensitivity to genotoxic stress. *Nucleic Acids Res* 38 (11), 3595-3604.

88 Michael, L.F., Wu, Z., Cheatham, R.B., Puigserver, P., Adelmant, G., Lehman, J.J., Kelly, D.P., & Spiegelman, B.M., Restoration of insulin-sensitive glucose transporter (GLUT4) gene expression in muscle cells by the transcriptional coactivator PGC-1. *Proc Natl Acad Sci U S A* 98 (7), 3820-3825 (2001).

89 Mitchison, T. & Kirschner, M., Dynamic instability of microtubule growth. *Nature* 312 (5991), 237-242 (1984).

90 Moens, C.B. & Selleri, L., Hox cofactors in vertebrate development. *Dev Biol* 291 (2), 193-206 (2006).

91 Mongelard, F. & Bouvet, P., Nucleolin: a multiFACeTed protein. *Trends Cell Biol* 17 (2), 80-86 (2007).

92 Musacchio, A. & Salmon, E.D., The spindle-assembly checkpoint in space and time. *Nat Rev Mol Cell Biol* 8 (5), 379-393 (2007).

93 Nelson, D.M., Ye, X., Hall, C., Santos, H., Ma, T., Kao, G.D., Yen, T.J., Harper, J.W., & Adams, P.D., Coupling of DNA synthesis and histone synthesis in S phase independent of cyclin/cdk2 activity. *Mol Cell Biol* 22 (21), 7459-7472 (2002).

94 Nomura, T., Tanikawa, J., Akimaru, H., Kanei-Ishii, C., Ichikawa-Iwata, E., Khan, M.M., Ito, H., & Ishii, S., Oncogenic activation of c-Myb correlates with a loss of negative regulation by TIF1beta and Ski. *J Biol Chem* 279 (16), 16715-16726 (2004).

95 Ogg, S.C. & Lamond, A.I., Cajal bodies and coilin--moving towards function. *J Cell Biol* 159 (1), 17-21 (2002).

96 Oriente, F., Fernandez Diaz, L.C., Miele, C., Iovino, S., Mori, S., Diaz, V.M., Troncone, G., Cassese, A., Formisano, P., Blasi, F., & Beguinot, F., Prep1 deficiency induces protection from diabetes and increased insulin sensitivity through a p160-mediated mechanism. *Mol Cell Biol* 28 (18), 5634-5645 (2008).

97 Owen, H.R., Elser, M., Cheung, E., Gersbach, M., Kraus, W.L., & Hottiger, M.O., MYBBP1a is a novel repressor of NF-kappaB. *J Mol Biol* 366 (3), 725-736 (2007).

98 Papalopulu, N., Lovell-Badge, R., & Krumlauf, R., The expression of murine Hox-2 genes is dependent on the differentiation pathway and displays a collinear sensitivity to retinoic acid in F9 cells and Xenopus embryos. *Nucleic Acids Res* 19 (20), 5497-5506 (1991).

99 Pear, W.S., Nolan, G.P., Scott, M.L., & Baltimore, D., Production of high-titer helper-free retroviruses by transient transfection. *Proc Natl Acad Sci U S A* 90 (18), 8392-8396 (1993).

100 Penkov, D., Di Rosa, P., Fernandez Diaz, L., Basso, V., Ferretti, E., Grassi, F., Mondino, A., & Blasi, F., Involvement of Prep1 in the alphabeta T-cell receptor T-lymphocytic potential of hematopoietic precursors. *Mol Cell Biol* 25 (24), 10768-10781 (2005).

101 Perrera, C., Colombo, R., Valsasina, B., Carpinelli, P., Troiani, S., Modugno, M., Gianellini, L., Cappella, P., Isacchi, A., Moll, J., & Rusconi, L., Identification of Myb-binding protein 1A (MYBBP1A) as a novel substrate for aurora B kinase. *J Biol Chem* 285 (16), 11775-11785.

102 Phelan, M.L., Rambaldi, I., & Featherstone, M.S., Cooperative interactions between HOX and PBX proteins mediated by a conserved peptide motif. *Mol Cell Biol* 15 (8), 3989-3997 (1995).

103 Phillips, N.J., Ziegler, M.R., Radford, D.M., Fair, K.L., Steinbrueck, T., Xynos, F.P., & Donis-Keller, H., Allelic deletion on chromosome 17p13.3 in early ovarian cancer. *Cancer Res* 56 (3), 606-611 (1996).

104 Piper, D.E., Batchelor, A.H., Chang, C.P., Cleary, M.L., & Wolberger, C., Structure of a HoxB1-Pbx1 heterodimer bound to DNA: role of the hexapeptide and a fourth homeodomain helix in complex formation. *Cell* 96 (4), 587-597 (1999).

105 Popperl, H., Bienz, M., Studer, M., Chan, S.K., Aparicio, S., Brenner, S., Mann, R.S., & Krumlauf, R., Segmental expression of Hoxb-1 is controlled by a highly conserved autoregulatory loop dependent upon exd/pbx. *Cell* 81 (7), 1031-1042 (1995).

106 Puig, O., Caspary, F., Rigaut, G., Rutz, B., Bouveret, E., Bragado-Nilsson, E., Wilm, M., & Seraphin, B., The tandem affinity purification (TAP) method: a general procedure of protein complex purification. *Methods* 24 (3), 218-229 (2001).

107 Qian, H.R. & Huang, S., Comparison of false discovery rate methods in identifying genes with differential expression. *Genomics* 86 (4), 495-503 (2005).

108 Ramsay, R.G., Ishii, S., & Gonda, T.J., Increase in specific DNA binding by carboxyl truncation suggests a mechanism for activation of Myb. *Oncogene* 6 (10), 1875-1879 (1991).

109 Rave-Harel, N., Givens, M.L., Nelson, S.B., Duong, H.A., Coss, D., Clark, M.E., Hall, S.B., Kamps, M.P., & Mellon, P.L., TALE homeodomain proteins regulate gonadotropin-releasing hormone gene expression independently and via interactions with Oct-1. *J Biol Chem* 279 (29), 30287-30297 (2004).

110 Rieder, C.L., Faruki, S., & Khodjakov, A., The centrosome in vertebrates: more than a microtubule-organizing center. *Trends Cell Biol* 11 (10), 413-419 (2001).

111 Rigaut, G., Shevchenko, A., Rutz, B., Wilm, M., Mann, M., & Seraphin, B., A generic protein purification method for protein complex characterization and proteome exploration. *Nat Biotechnol* 17 (10), 1030-1032 (1999).

112 Ryoo, H.D., Marty, T., Casares, F., Affolter, M., & Mann, R.S., Regulation of Hox target genes by a DNA bound Homothorax/Hox/Extradenticle complex. *Development* 126 (22), 5137-5148 (1999).

113 Sakita-Suto, S., Kanda, A., Suzuki, F., Sato, S., Takata, T., & Tatsuka, M., Aurora-B regulates RNA methyltransferase NSUN2. *Mol Biol Cell* 18 (3), 1107-1117 (2007).

114 Sankar, M., Tanaka, K., Kumaravel, T.S., Arif, M., Shintani, T., Yagi, S., Kyo, T., Dohy, H., & Kamada, N., Identification of a commonly deleted region at 17p13.3 in leukemia and lymphoma associated with 17p abnormality. *Leukemia* 12 (4), 510-516 (1998).

115 Savino, T.M., Gebrane-Younes, J., De Mey, J., Sibarita, J.B., & Hernandez-Verdun, D., Nucleolar assembly of the rRNA processing machinery in living cells. *J Cell Biol* 153 (5), 1097-1110 (2001).

[116] Scheer, U. & Weisenberger, D., The nucleolus. *Curr Opin Cell Biol* 6 (3), 354-359 (1994).

[117] Schonemann, M.D., Ryan, A.K., Erkman, L., McEvilly, R.J., Bermingham, J., & Rosenfeld, M.G., POU domain factors in neural development. *Adv Exp Med Biol* 449, 39-53 (1998).

[118] Selleri, L., Depew, M.J., Jacobs, Y., Chanda, S.K., Tsang, K.Y., Cheah, K.S., Rubenstein, J.L., O'Gorman, S., & Cleary, M.L., Requirement for Pbx1 in skeletal patterning and programming chondrocyte proliferation and differentiation. *Development* 128 (18), 3543-3557 (2001).

[119] Shimizu, K., Kawasaki, Y., Hiraga, S., Tawaramoto, M., Nakashima, N., & Sugino, A., The fifth essential DNA polymerase phi in Saccharomyces cerevisiae is localized to the nucleolus and plays an important role in synthesis of rRNA. *Proc Natl Acad Sci U S A* 99 (14), 9133-9138 (2002).

[120] Sollner-Webb, B. & Tower, J., Transcription of cloned eukaryotic ribosomal RNA genes. *Annu Rev Biochem* 55, 801-830 (1986).

[121] Stack, M., Jones, D., White, G., Liscia, D.S., Venesio, T., Casey, G., Crichton, D., Varley, J., Mitchell, E., Heighway, J., & et al., Detailed mapping and loss of heterozygosity analysis suggests a suppressor locus involved in sporadic breast cancer within a distal region of chromosome band 17p13.3. *Hum Mol Genet* 4 (11), 2047-2055 (1995).

[122] Stearns, T., Centrosome duplication. a centriolar pas de deux. *Cell* 105 (4), 417-420 (2001).

[123] Steichen-Gersdorf, E., Baumgartner, M., Kreczy, A., Maier, H., & Fink, F.M., Deletion mapping on chromosome 17p in medulloblastoma. *Br J Cancer* 76 (10), 1284-1287 (1997).

[124] Tavner, F.J., Simpson, R., Tashiro, S., Favier, D., Jenkins, N.A., Gilbert, D.J., Copeland, N.G., Macmillan, E.M., Lutwyche, J., Keough, R.A., Ishii, S., & Gonda, T.J., Molecular cloning reveals that the p160 Myb-binding protein is a novel, predominantly nucleolar protein which may play a role in transactivation by Myb. *Mol Cell Biol* 18 (2), 989-1002 (1998).

125 Towbin, H., Staehelin, T., & Gordon, J., Electrophoretic transfer of proteins from polyacrylamide gels to nitrocellulose sheets: procedure and some applications. *Proc Natl Acad Sci U S A* 76 (9), 4350-4354 (1979).

126 Tschochner, H. & Hurt, E., Pre-ribosomes on the road from the nucleolus to the cytoplasm. *Trends Cell Biol* 13 (5), 255-263 (2003).

127 Vader, G. & Lens, S.M., The Aurora kinase family in cell division and cancer. *Biochim Biophys Acta* 1786 (1), 60-72 (2008).

128 Villaescusa, J.C., Buratti, C., Penkov, D., Mathiasen, L., Planaguma, J., Ferretti, E., & Blasi, F., Cytoplasmic Prep1 interacts with 4EHP inhibiting Hoxb4 translation. *PLoS One* 4 (4), e5213 (2009).

129 Waskiewicz, A.J., Rikhof, H.A., Hernandez, R.E., & Moens, C.B., Zebrafish Meis functions to stabilize Pbx proteins and regulate hindbrain patterning. *Development* 128 (21), 4139-4151 (2001).

130 Williams, T.M., Williams, M.E., & Innis, J.W., Range of HOX/TALE superclass associations and protein domain requirements for HOXA13:MEIS interaction. *Dev Biol* 277 (2), 457-471 (2005).

131 Winey, M. & Byers, B., Assembly and functions of the spindle pole body in budding yeast. *Trends Genet* 9 (9), 300-304 (1993).

132 Wsierska-Gadek, J. & Horky, M., How the nucleolar sequestration of p53 protein or its interplayers contributes to its (re)-activation. *Ann N Y Acad Sci* 1010, 266-272 (2003).

133 Wu, X., Bayle, J.H., Olson, D., & Levine, A.J., The p53-mdm-2 autoregulatory feedback loop. *Genes Dev* 7 (7A), 1126-1132 (1993).

134 Yamauchi, T., Keough, R.A., Gonda, T.J., & Ishii, S., Ribosomal stress induces processing of Mybbp1a and its translocation from the nucleolus to the nucleoplasm. *Genes Cells* 13 (1), 27-39 (2008).

135 Yang, W., Rogozin, I.B., & Koonin, E.V., Yeast POL5 is an evolutionarily conserved regulator of rDNA transcription unrelated to any known DNA polymerases. *Cell Cycle* 2 (2), 120-122 (2003).

[136] Zhao, J., Sumoylation regulates diverse biological processes. *Cell Mol Life Sci* 64 (23), 3017-3033 (2007).

* Alberts B., Bray D., Lewis J., Raff M., Roberts K. & Watson J.D., Molecular Biology of the Cell. Garland Publishing Inc., New York & London, third edition, 1994.

*Lodish H., Berk A., Kaiser C.A., Krieger M., Scott M.P., Bretscher A., Ploegh H. & Matsudaira P., Molecular Cell Biology. W.H. Freeman Publishing Group, sixth edition, 2008.

ACKNOWLEDGMENTS

I want to thank many persons that help me during these years, allowing me to grow scientifically and professionally.

First of all I want to thank my Director of Studies Francesco Blasi who gave me the opportunity to work at this project. I want to thank also my external supervisor Jesper Svejstrup and my tutor Alessandra Boletta for their support.

Thank you to our collaborators, for the Sumoylation experiments, in Angela Bachi's group here at DIBIT; to the persons working at the Confocal Microscopy and Cytometry Facility for their help in the setting of my experiments. Thank you also to Lorenza Pecciarini of the Pathology Unit and the Cogentech Facility at IFOM.

Many thanks to the Blasi's lab members present and past, in particular Elena Longobardi, who helped me a lot with many experiments and gave me always good advices. Thanks also to the Brendolan's lab, especially Elisa and Laura, and Giorgia that during these years became good friends and made this experience more fun. Thank you also to Daniela Talarico that was always available, giving to me good advices and helping with all the paper work related to Open University and to Jose just because he knows everything. Thank you also to Massimo Crippa for its help in the last months.

A big thank you to my family that always supported me and encouraged me during difficult moments.

Thanks to all the friends and the persons that soon or later I met here in Milan during these last 4 years.

The last but most important thank you is for Daniele, just thanks to be there for me.

Silvia